1980

Petrology of the Eocene volcanic sequence Nez Perce and Blue Joint Creeks southern Bitterroot Mountains Montana

Carleen D. Holloway
The University of Montana

PETROLOGY OF THE EOCENE VOLCANIC SEQUENCE, NEZ PERCE AND BLUE JOINT CREEKS, SOUTHERN BITTERROOT MOUNTAINS, MONTANA

by

Carleen D. Holloway

B.S., University of California, Santa Barbara, 1975

Presented in partial fulfillment of the
requirements for the degree of

Master of Science

UNIVERSITY OF MONTANA

1980

Approved by:

Donald W. Hyndman
Chairman, Board of Examiners

Dean, Graduate School

June 10, 1980
Date

ABSTRACT

Holloway, Carleen D., M.S., Spring, 1980 Geology

Petrology of the Eocene Volcanic Sequence, Nez Perce and Blue Joint Creeks, Southern Bitterroot Mountains, Montana

Director: Donald W. Hyndman

This study describes the petrography, whole-rock chemistry, and structural relationships of a 48 km^2 area of coeval Eocene rhyolitic volcanic rocks, epiclastic deposits, and associated epizonal granites located in the southern Bitterroot Mountains, Montana. The volcanic and epiclastic rocks comprise a 600 m-thick sequence of lava flows, vitrophyres, ash-flow tuffs, porphyritic dikes and plugs, airfall tuff, and lahar deposits. Lava flows greatly predominate over pyroclastic and epiclastic material. The granitic rocks consist of coarse-grained and porphyritic phases of a shallow-level, zoned granitic pluton which extends beyond the boundaries of the study area for several kilometers on all sides. The extrusive and intrusive rocks are coeval, have a similar mineralogy, and show linear trends in major-element variation diagrams; the two suites are interpreted as being comagmatic. Contact relationships show the granitic rocks to be intrusive into the volcanic and epiclastic rocks and the surrounding Precambrian quartzite country rocks. Intrusion appears to have been accomplished by stoping large blocks of the volcanic and quartzite roof of the pluton. The general configuration, of an epizonal granitic pluton forcibly intruding its coeval and comagmatic volcanic cover, has been interpreted as a characteristic feature of caldera environments in many areas. Two models may be proposed to interpret the volcano-plutonic assemblage within the study area in terms of such an environment. The first interprets the volcanic rocks as a caldera-margin "facies" developed on the western boundary of a large collapse structure whose intra-caldera facies is represented by welded ash-flow tuffs and breccias east of the study area. The second model interprets the study area itself as representing a small "trapdoor-style" caldera-collapse structure within the "caldera" of the first model.

ACKNOWLEDGMENTS

I wish to thank the members of my committee: my advisor, Don Hyndman, for many valuable discussions during the research and writing stages of this study, and my committee members, Gray Thompson, Bill Greenwood, and R. Keith Osterheld, for their careful editing of the manuscript. Karen Lund, Warren Rehn, Felix Mutschler, Patty Billings, Robert Bruce, and Steve Azadian of the Blue Joint and Magruder projects provided many hours of geologic brainstorming. Peter Hooper and Ivan Herrick of Washington State University supplied the whole-rock chemical analyses. The aid of my colleagues is much appreciated: Fess Foster and Steve Luthy provided enlightened discussions of calderas and high-level plutons; Jon Achuff contributed on drafting matters; George Kendrick made available the CIPW computer program. Jim Harrington proved throughout that as both petrologist and friend, he is indeed a Pro. Toward the end, Mt. St. Helens provided a somewhat excessively pyroclastic example of why volcanic rocks are worth studying. Lastly, I would like to thank the late Norman L. Bowen for some valuable words of advice and encouragement:

> "This documentation of our ignorance of magmas could be expanded manyfold. Should we be discouraged? Certainly not. It has been well said, 'Better the high road than the inn'".

CDH--May, 1980

TABLE OF CONTENTS

CHAPTER Page

LIST OF TABLES

List of Figures

LIST OF PLATES

CHAPTER I

INTRODUCTION

The objectives of this study were primarily to describe the petrography and field relations of a sequence of Eocene rhyolitic volcanic rocks in the southern Bitterroot Mountains, Montana and to use this information to reconstruct the volcanic history of the area. In addition, whole-rock chemical analyses and radiometric dates provide substantiation for the spatial and temporal relationships suggested by field work and thin-section petrography. The intent of this report is to present the field, petrographic, and chemical data, and to propose an origin for the volcanic rocks in terms of a possible caldera environment.

The Eocene volcanic rocks of the study area comprise a 600 m-thick sequence of lava flows, ash-flow tuffs, airfall tuffs, vitrophyres, shallow-level porphyritic intrusive rocks and associated epiclastic deposits. This assemblage of lithologies is here given the informal designation "Castle Rock volcanics", after a prominent landmark within the study area. Other lithologies present in the area include Pre-cambrian "Y" group quartzites, foliated biotite granodiorite of the Cretaceous Idaho batholith, epizonal granitic rocks of presumed Eocene age, and unconsolidated Quaternary deposits.

Location of Study Area

The study area is located in the Bitterroot National Forest, approximately 135 km south of Missoula, Montana, and approximately 70 km northwest of Salmon, Idaho (Figure 1). Nez Perce Pass lies on its western border. Access to the area's edge is gained via the Nez Perce Fork-Magruder Corridor road (Forest Service route 468) and three other Forest Service roads. Four Forest Service-maintained pack trails provide hiking access from the roads. The area is bounded on the west by the Montana-Idaho divide and an unnamed creek, on the north by the Nez Perce Fork of the Bitterroot River, on the south by Blue Joint Creek, and on the east by an arbitrary northeast-trending line east of Bare Cone Mountain. These boundaries encompass some 48 km^2 of rugged, mostly wooded terrain.

Previous Work

The Castle Rock volcanics have received only cursory examination in previous reconnaissance geologic mapping of the area. The geologic map of Montana (Ross and others, 1955) shows only two small patches of Tertiary volcanic rocks slightly east of the study area, along with several dikes, also of Tertiary age. The country rocks are shown as intrusive rocks of the Cretaceous Idaho batholith and Precambrian metasedimentary rocks. Berg and Goldberg (1973) published a preliminary geologic map having boundaries which are substantially the same as those in this report. They described the Castle Rock volcanics only as

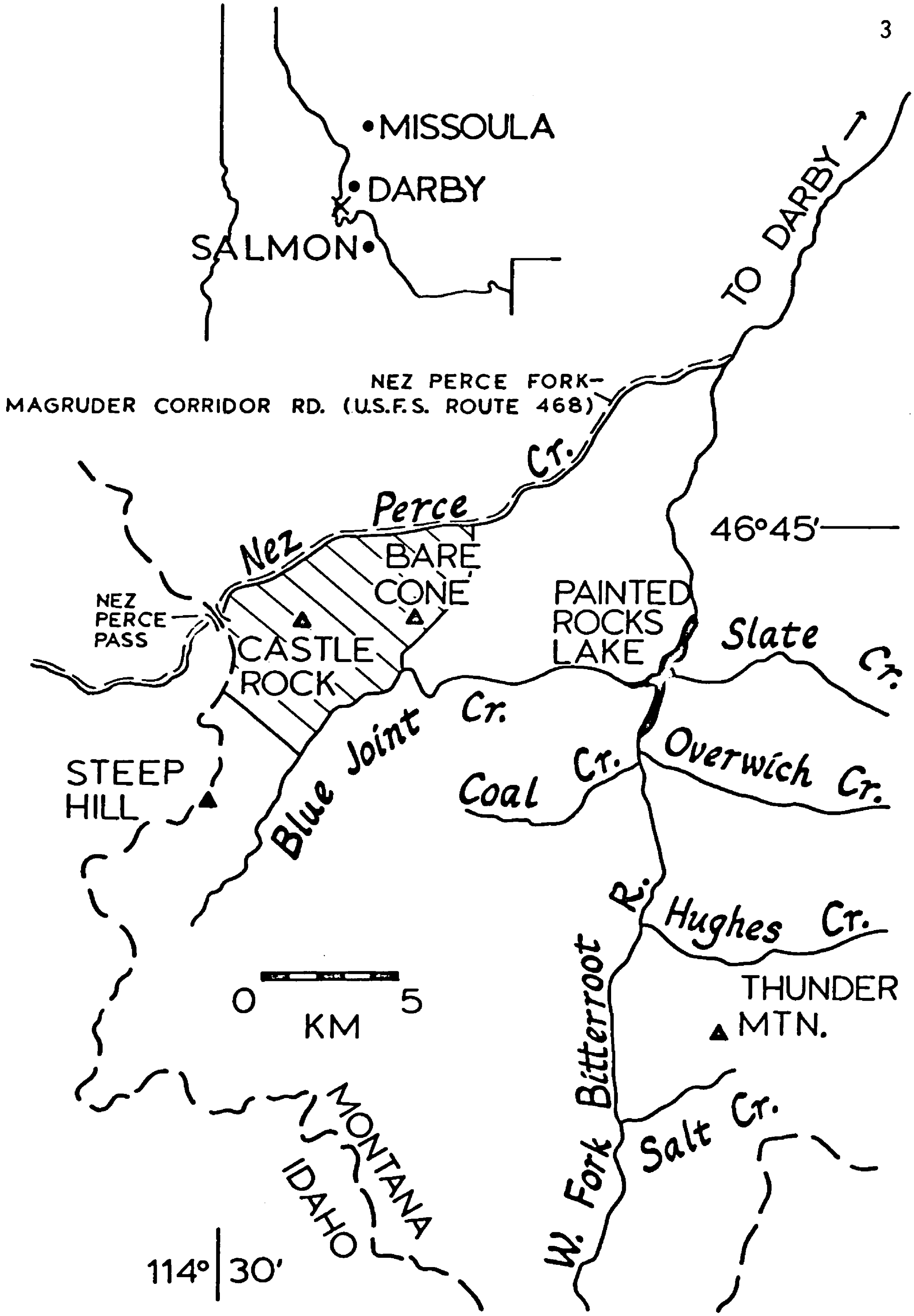

Figure 1. Location of study area.

"Tertiary volcanic rocks". Many unit contacts on their map differ substantially from those of the present study, reflecting in part their different interpretation of certain outcrops. Winegar (1974) shows many of the same contacts as Berg and Goldberg on his map for the Forest Service Bitterroot II geologic survey. Williams (1977) described the Tertiary granitic rocks along the road on the northern boundary of the study area. Noting the complex field relationships between coarse-grained and porphyritic phases of the granite, he suggested that these rocks may have been situated near a volcanic vent.

More-detailed mapping has been done in compositionally-similar volcanic rocks which crop out not far from the study area, along the West Fork of the Bitterroot River near Painted Rocks Lake. Fisk (1969) described porphyritic rhyolite dikes, obsidian or pitchstone flows, tuff, tuff breccia, lahars, and a possible extinct fumarole in the area around Painted Rocks Lake. Winegar (1973) outlined the geology of a larger area in reports for the Forest Service, wherein he mentioned a range of volcanic lithologies, including ash, tuff, agglomerate, rhyolite, lahars, obsidian, vitrophyres, and intrusive quartz latite. Badley (1978) studied a series of rhyodacite to andesite dikes on the East Fork of the Bitterroot River; she suggested that these may have formed as outliers of a magma source in the vicinity of the West Fork. In two reports on the geology of southernmost Ravalli County, Montana, Berg (1973, 1977) described outcrops of welded tuff, bedded tuff, and lava flows, as well as dikes ranging in composition from rhyolite to basalt. Based on outcrop characteristics and structural data, he inferred that the volcanic rocks had been deposited on a topographic surface similar to that of the present.

In a reconnaissance study covering some 7,600 km^2 of the Selway-Bitterroot wilderness area to the north and west, Greenwood and Morrison (1973) mapped dikes and batholith-sized bodies of pink Tertiary epizonal granite and dikes of porphyritic rhyolite, quartz latite, and dacite; no extrusive volcanic rocks are noted from this area. Recent mapping south of the study area (Lund and others,ms) has likewise delineated no outcrops of volcanic rocks south of Blue Joint Creek. Dike rocks of silicic, intermediate, and basaltic composition, are however, prevalent.

The Castle Rock volcanics thus appear to be the westernmost of several discontinuous outcrops of rhyolitic volcanic and hypabyssal rocks and related epiclastic deposits, which extend from approximately the Montana-Idaho divide to at least the East Fork of the Bitterroot River, a distance of 55 km. Interpretation of this distribution is hampered by the paucity of fossil or radiometric dates on the volcanic rocks. However, the overall uniformity of the lithologies permits speculation that these isolated outcrops represent erosional remnants of a once-continuous volcanic field.

This Study

The present study was undertaken in support of a U.S. Geological

Survey investigation of the mineral resource potential of the Blue Joint wilderness study area (Figure 2). Financial aid and logistical support were provided by the U.S. Geological Survey. Field work was carried out during the period June-September, 1979, with mapping on a scale of 1:24,000. The area of this study is wholly contained on the U.S. Geological Survey Thunder Mtn. NW 7½' advance sheet.

Ten major bedrock lithologic units were mapped within the study area (Plate 1). All of the units were originally delineated in the field, on the basis of hand specimen and outcrop characteristics. In a few cases, later thin-section examination resulted in the reclassification of particular outcrops. Because of the abundant vegetative cover, "binocular geology" was largely impossible, and very few unit contacts could be seen. Outcrops of most lithologic units are scarce, and structural data is in many places unreliable or unobtainable. Many units were mapped primarily on the basis of "rubble"--loose, unconsolidated material presumed to be locally-derived on the basis of lithologic continuity or situation on a topographic high. Because of this, an outcrop-mapping approach was utilized. Sample locations are shown on Plate 1. Several traverses were also made in regions surrounding the study area; the geology along these traverses was mapped in reconnaissance fashion and is shown on Plate 2.

Age of the Castle Rock Volcanics

K/Ar age determinations on two samples of the Castle Rock volcanics--

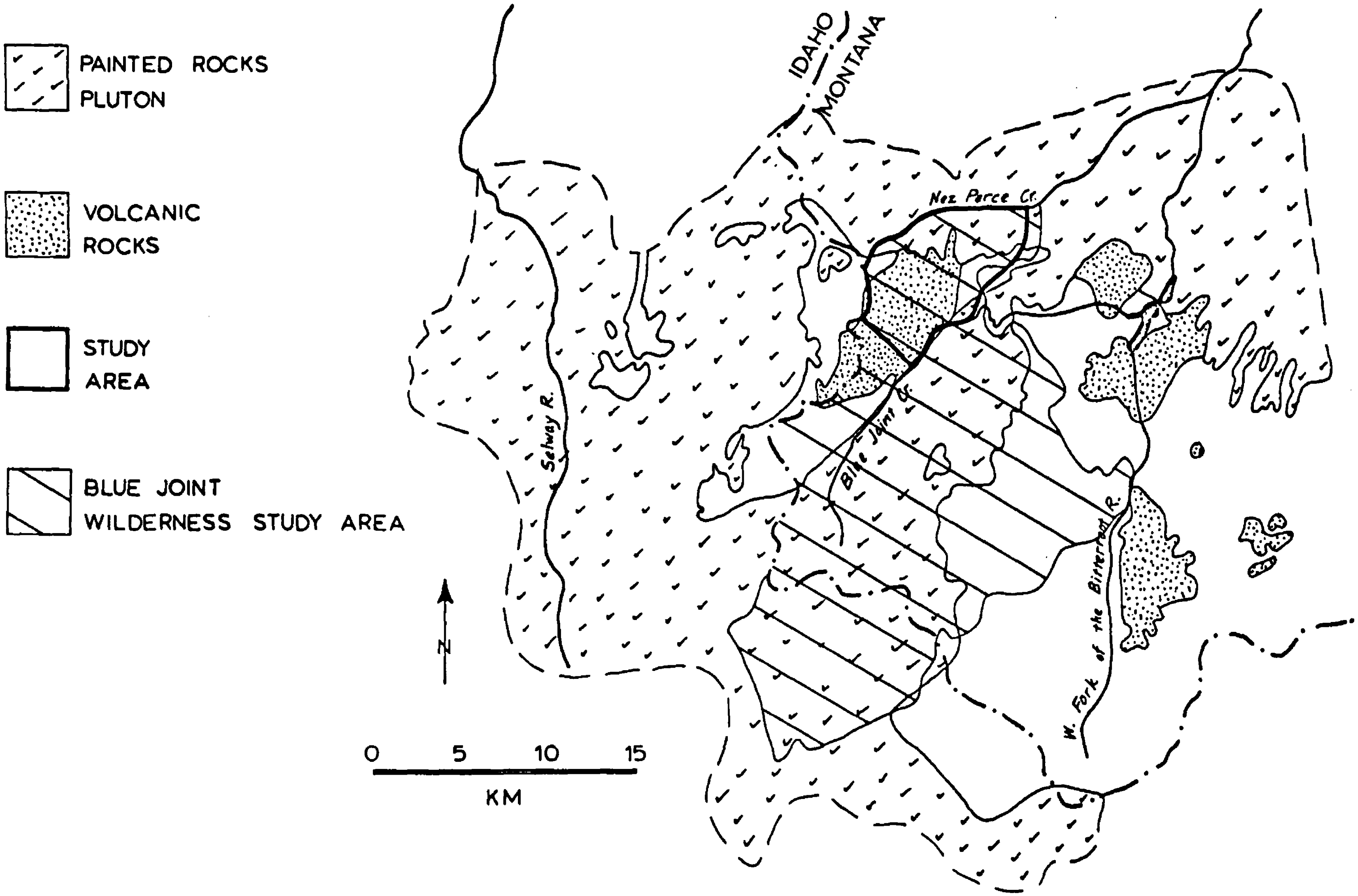

Figure 2. Location map showing Blue Joint wilderness study area, area of this study, and approximate extent of Painted Rocks pluton.

an airfall tuff and an intrusive porphyritic rhyolite plug--are currently underway by Dr. Robert J. Fleck of the U.S. Geological Survey. Initial results are as follows (Robert Fleck, pers. comm., 1980):

airfall tuff (sample 70A*):	biotite, 1st run:	46.8 m.y.
rhyolite plug (sample 176B):	sanidine, 1st run:	47.2 m.y.
	sanidine, 2nd run:	45.4 m.y.
	biotite, 1st run:	45.2 m.y.

These preliminary dates document the eruption of the Castle Rock volcanics during Middle Eocene time.

Regional Geology

The Challis Volcanics. On the basis of age, mineralogy, chemistry, lithologies, and proximity, the Castle Rock volcanics are comparable to rocks of the dominantly Middle Eocene Challis volcanic field of central Idaho. The Challis field is discontinuously exposed over an area of at least 1250 km^2 (Figure 3). Present outcrops comprise only the erosional remnant of a once far larger field. Maximum preserved thicknesses of the volcanics and related sedimentary rocks commonly reach several thousand meters (Ross and Forrester, 1958; Cater and others, 1973; Armstrong, 1974).

---

*Field numbers are preceeded by "79CH"

Figure 3. Regional geology. Cretaceous rocks of the Idaho batholith shown in crystalline pattern, Tertiary plutons in stippled pattern, and Challis Volcanics in ruled pattern. Volcanic rocks from this study shown in black.

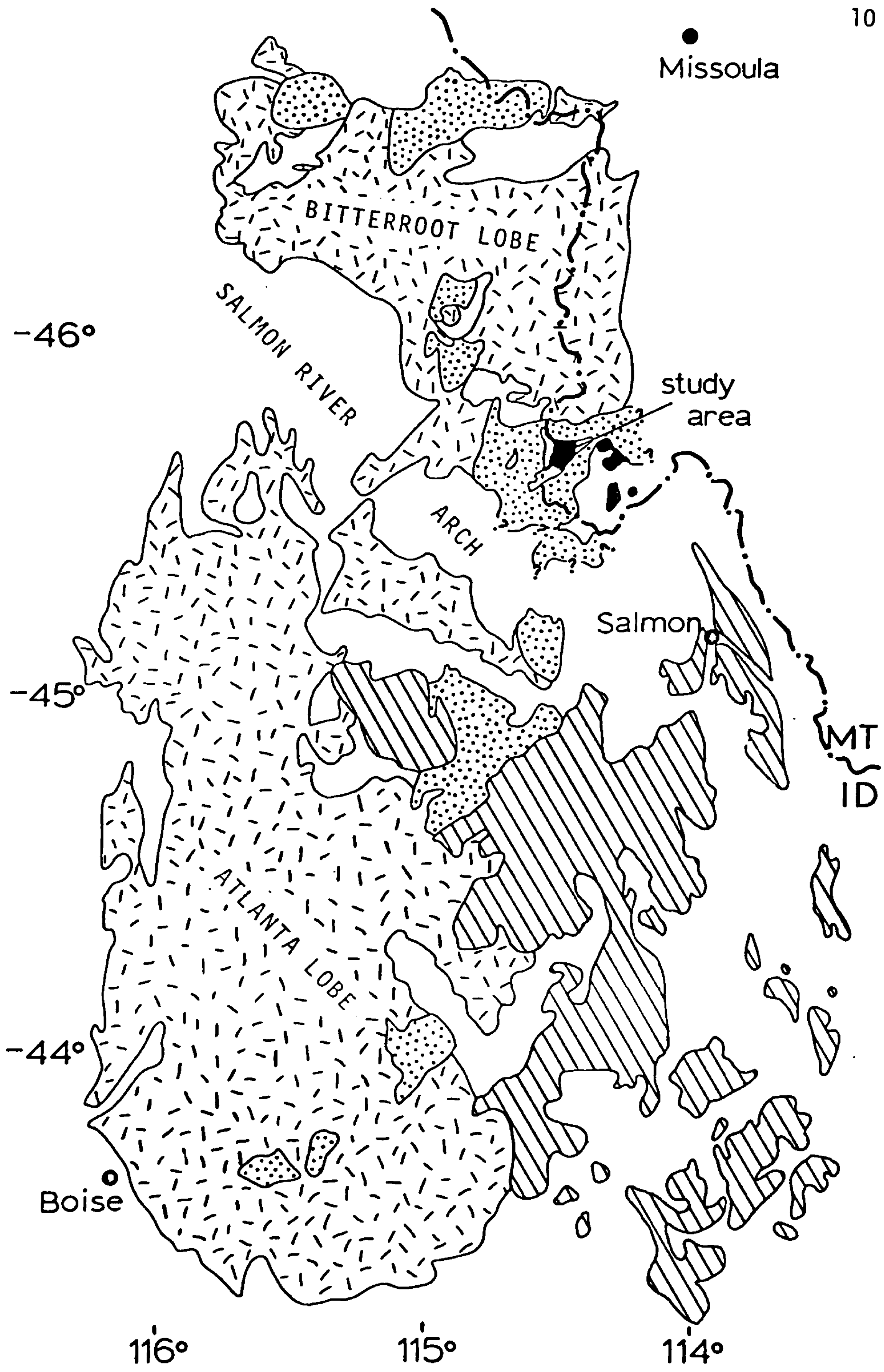
Missoula
BITTERROOT LOBE
SALMON RIVER
ARCH
study area
-46°
-45°
-44°
Salmon
MT
ID
ATLANTA LOBE
Boise
116°
115°
114°

The Challis Volcanics were originally defined by C.P. Ross (Ross, 1934; Ross, 1937; Ross, 1961). He applied the name to a thick sequence of flows, flow breccia, tuffs, and intercalated sedimentary rocks, which as a unit represent the lower part of the Tertiary deposits of central Idaho. The volcanic rocks constitute a calc-alkaline suite which ranges in composition from rhyolitic to basaltic. Silicic to intermediate rocks were said to predominate. Specifically excluded from the unit were basalts of the Snake River Plain and Columbia River Plateau. Subsequent mapping has shown that rhyolitic pyroclastic rocks, principally welded and unwelded ash-flow tuffs, comprise significant percentages of the Challis succession in many areas (Cater and others, 1973). Lateral facies variations within the volcanics are marked, hampering long-range correlation of sections (Ross and Forrester, 1958). The Challis Volcanics probably erupted from several major centers, only one of which, the Thunder Mountain cauldron, has thus far been described in detail (B.F. Leonard, in Cater and others, 1973). Figure 3 shows the distribution of the Challis Volcanics in relation to the area of the present study.

On the basis of paleontologic data, the Challis Volcanics were originally regarded as possibly or probably of Oligocene age and not younger than early Miocene (Ross, 1937, p. 65-68). However, more recent radiometric age determinations, summarized by Armstrong (1974) fall generally within the interval of 43.8 to 49.0 m.y. B.P. (Middle Eocene). Armstrong (1974) has also summarized the available radiometric dates on a series of Eocene granitic bodies, some of batholithic size, which occur throughout central Idaho in areas underlain by Challis volcanics. Ages on the intrusive rocks fall in the general range of 40.0 to 52.0 m.y. B.P., indicating a close temporal correlation between plutonism and Challis volcanism. Field relationships further substantiate this correlation: in the Idaho Primitive area of central Idaho, the 42.7 m. y. Casto pluton intrudes an overlying section of Challis Volcanics; the volcanics form a gently undulating, subhorizontal roof over the intruding granite (Cater and others, 1973). Ross and Forrester (1958, p. 27) noted that the Tertiary granitic rocks tend to occupy the cores of uplifts in the Challis Volcanics.

<u>The Idaho Batholith</u>. The Idaho batholith is one of the series of major Mesozoic granitic plutons which forms the backbone of the American Cordillera. The anomalous position of this pluton east of the general batholithic trend, and its division into two geographically-distinct parts, renders it unique among Cordilleran batholiths. The two parts of the body are separated by 1,500 m.y.-old high-grade metamorphic rocks of the Salmon River Arch (Armstrong, 1975). The names Bitterroot Lobe and Atlanta Lobe have been suggested for the northern and southern parts of the batholith, respectively (Armstrong, 1975). The study area is located near the southeastern margin of the Bitterroot Lobe (Figure 3).

The Idaho batholith is a composite body, consisting of numerous granitic to granodioritic plutons (Hyndman and Williams, 1977; Williams, 1977; Nold, 1974). Evidence for a mesozonal to catazonal depth of emplacement (see Hyndman, 1972, 1978) for most of these plutons includes: a prevalent weak foliation, regionally concordant and gradational contacts with the surrounding high-grade regionally metamorphosed sedimentary rocks, the subsolvus mineralogy of most plutonic rocks, the abundant migmatic textures, and the absence of genetically-related volcanic rocks. The bulk of the Idaho batholith was emplaced during Cretaceous time--the Atlanta Lobe about 75 to 100 m.y. B.P. and the Bitterroot Lobe about 70 to 80 m.y. B.P. (Armstrong and others, 1977).

Approximately 20% of the Bitterroot Lobe consists of plutons which have compositions and textures strikingly different from those described above (Hyndman and Williams, 1977). These plutons comprise rocks of granitic and alkali-granitic compositions; they are typically pink, coarse-grained, equigranular, and characteristically contain miarolitic cavities, indicating emplacement at shallow levels. These epizonal plutons intrude rocks of the Cretaceous mesozonal-catazonal suite. Scattered radiometric dates on rocks of the epizonal suite from throughout the Bitterroot Lobe fall in the range 40 to 50 m.y. B.P. (middle Tertiary). Intrusion of this younger suite probably accounts for the widespread re-setting of K/Ar dates on the deep-level rocks (Armstrong, 1975). Figure 4 shows Williams' (1977) ternary plots contrasting

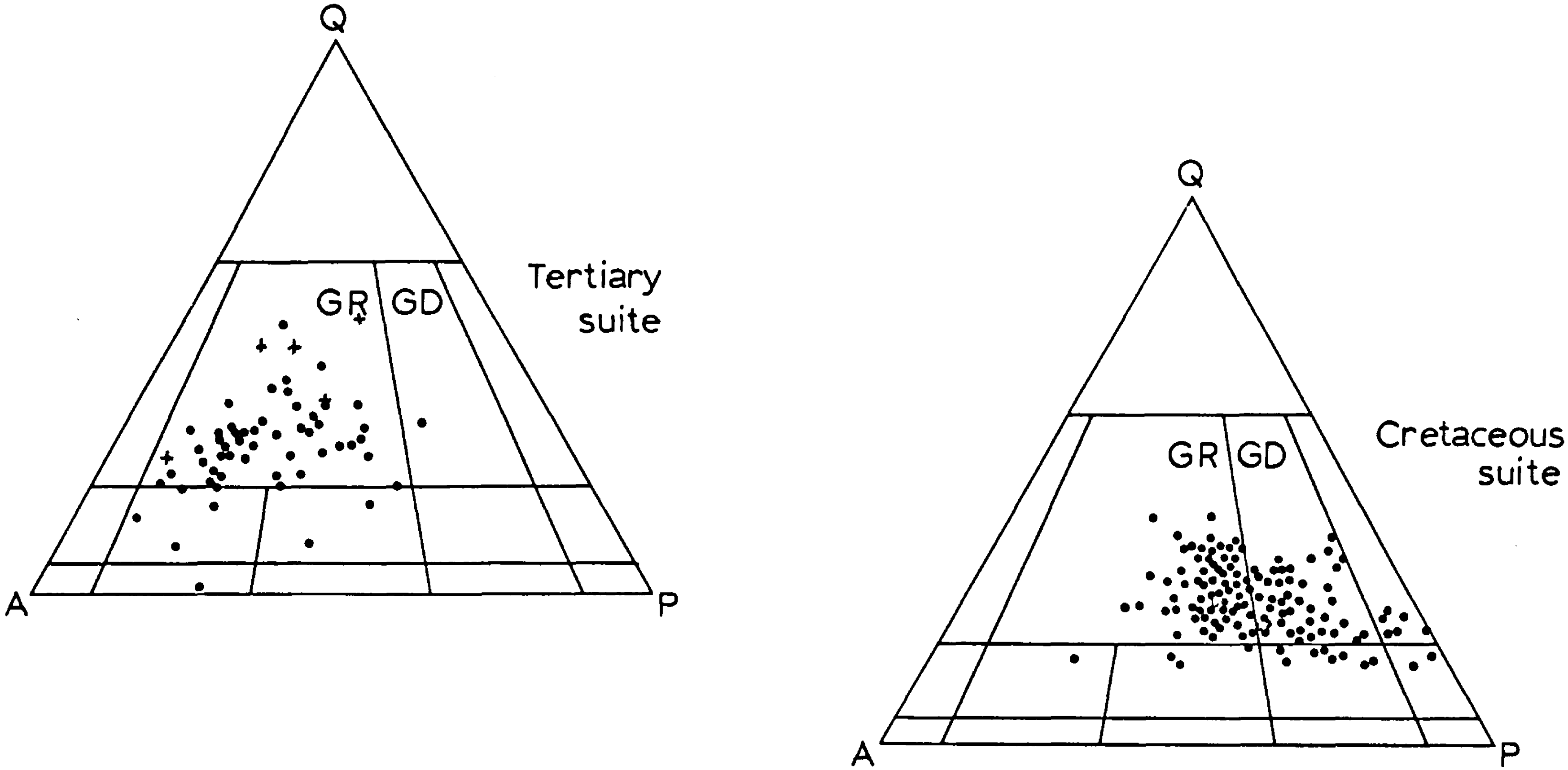

Figure 4. Ternary plots contrasting visual modes from the Cretaceous and Tertiary suites of the Bitterroot Lobe of the Idaho batholith. Tertiary samples from this study shown by crosses (modified from Williams, 1977).

visual modes from the Cretaceous and Tertiary suites of the Bitterroot Lobe.

In terms of age, texture, and mineralogy, the Tertiary plutons of the Bitterroot Lobe correlate with the Eocene plutons of central Idaho described above. The latter are associated with the southern, or Atlanta, lobe of the Idaho batholith, where they intrude rocks of the Cretaceous suite as well as the Challis Volcanics. The Challis Volcanics probably represent an extrusive phase of the Tertiary plutons of the Atlanta Lobe (Cater and others, 1973). The present study constitutes the first detailed examination of volcanic rocks believed to be the extrusive equivalents of one of the Bitterroot Lobe Tertiary plutons. The full areal extent of this epizonal pluton is not yet known. It underlies much of the region between the Selway River and the West Fork of the Bitterroot River and extends for an unknown distance to the south and west (Figure 2, 3). The pluton is a composite granitic body comprising several shallow-level plutonic and hypabyssal phases. The name "Painted Rocks pluton" has been proposed (Lund and others, ms; Mutschler and others, ms) for the body as a whole.

Eocene tectonic setting of the Pacific Northwest. Calc-alkaline volcanism, with subordinate related plutonism, was widespread in the greater Pacific Northwest during Eocene time. In addition to the Challis field, other volcanic centers active during this period include the Absaroka volcanic field (Montana and Wyoming) the Lowland Creek field (southwestern Montana), and the Clarno field (north-central Oregon) (Figure 5). The volcanic rocks in all four areas are dominantly

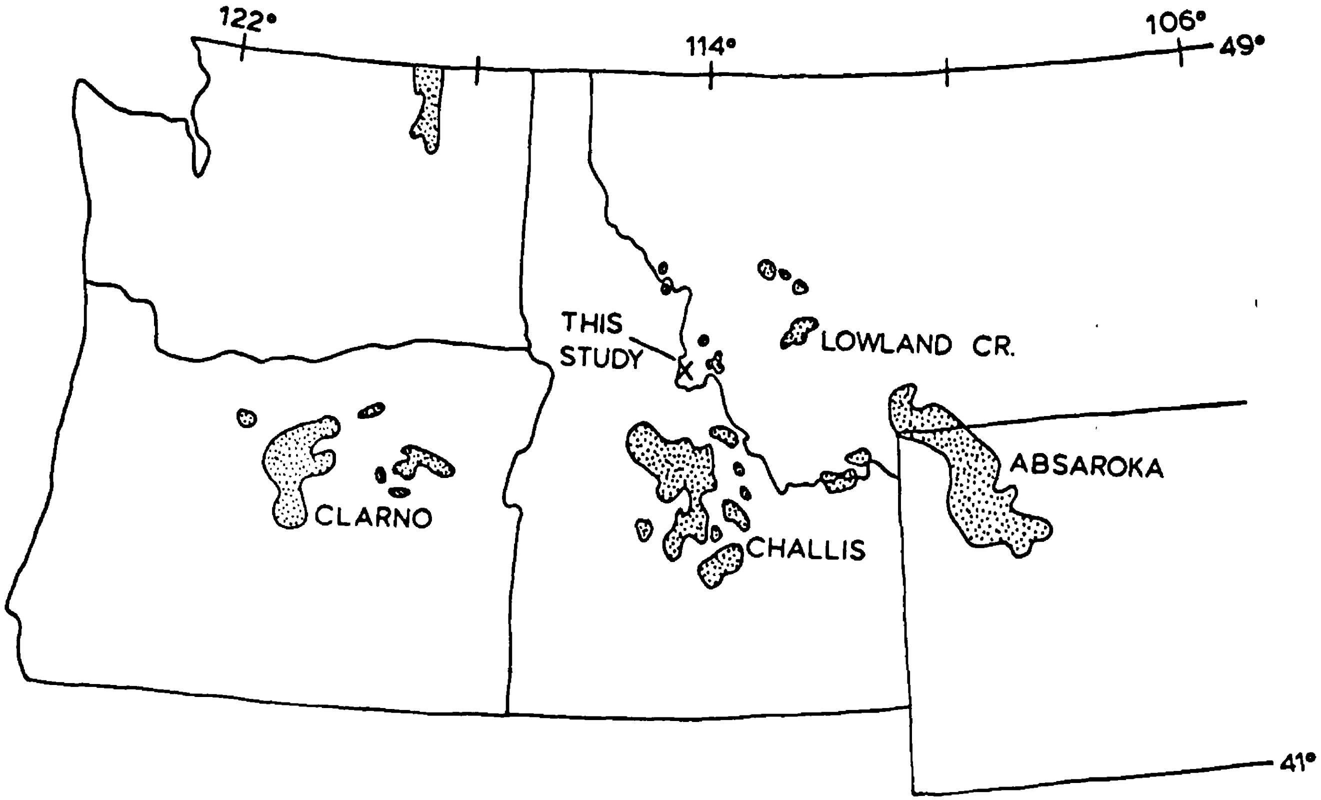

Figure 5. Felsic to intermediate Eocene volcanic fields of the Pacific Northwest. Fields discussed in the text are labeled (modified from Ross and others, 1955; Bond, 1978; and Stewart and Carlson, 1978).

intermediate in composition (andesite to rhyodacite), but include associated more silicic ash-flow tuffs (Lipman and others, 1972; Snyder and others, 1976; Chadwick, 1977; Prostka and others, 1977; Siems and Jones, 1977). K_2O/Si_2O ratios in these rocks tend to increase to the east (Lipman and others, 1972; Chadwick, 1977).

Volcanic rocks in present-day island arcs show similar overall intermediate calc-alkaline compositions. K_2O content in these rocks increases inland from the trench across the arc. These characteristics, coupled with Atwater's (1970) plate-tectonic reconstructions, have led many researchers to postulate a subduction-dominated tectonic regime for the Pacific Northwest during Eocene time (Lipman and others, 1972; Snyder and other, 1976). According to this model, volcanism occurred in response to eastward-directed subduction of the Farallon plate beneath the North American plate. Arc volcanism began in Canada about 55 m.y. B.P. and migrated southward over the next several million years (Lipman and others, 1972; Snyder and others, 1976; Prostka and others, 1977; Armstrong, 1978). Volcanic activity persisted for only about 5 to 10 m.y. in any given area.

Intersection of the North American plate with the East Pacific rise about 30 m.y. B.P. (Atwater, 1970) began the progressive destruction of the subduction system. Miocene and younger volcanic rocks in the western United States occur as fundamentally basaltic or biomodal basalt-rhyolite assemblages. They are presumably related to an extensional tectonic regime (Lipman and others, 1972) which formed after the cessation of subduction.

CHAPTER II

DESCRIPTIONS OF MAP UNITS

The study area is underlain by Precambrian quartzite, granodiorite of the Idaho batholith, Eocene volcanic and epiclastic rocks, Eocene epizonal coarse-grained and porphyritic intrusive rocks, and Quaternary sediments and talus. These rock units will be described in order of age, from oldest to youngest.

Precambrian Quartzite--Yq

Within the study area, quartzite crops out on ridgetops along and near the Montana-Idaho divide, at the mouth of the southwest boundary creek, and on Bare Cone Mountain.

Mineralogy. The unit includes rocks ranging from nearly pure orthoquarzites to meta-arkoses containing several volume percent plagioclase and potassium feldspar. Their color in hand specimen is generally pale greenish blue, and less commonly pink, maroon, pale grey, white, or dark green. Accessory minerals identified in thin section are zircon and magnetite, the latter altering to hematite. Muscovite is the only definite metamorphic mineral. The feldspars are typically altered to a low-birefringent clay. Undulatory extinction is a nearly ubiquitous feature of all three felsic minerals.

Textures. In thin section, grain boundaries range from polygonal in rocks with grains of fairly uniform size, to sutured in rocks where smaller grains are interstitial to larger. In both hand specimen and thin section, most rocks display a pronounced foliation, due primarily to the parellalism of muscovite flakes (Figure 6). In strongly foliated samples, quartz grains are also slightly elongated and exhibit a slight preferred crystallographic orientation. Heavy mineral bands are prominent in some locations. Crossbeds are uncommonly preserved as primary sedimentary structures.

Interpretation. The quartzites in the study area constitute only a small portion of a much larger sequence of quartz-rich metasedimentary rocks which crops out throughout southwestern Montana and adjacent parts of Idaho (see Berg, 1977; Lund and others, ms; Mutschler and others, ms). Berg (1977) subdivided the quartzites east of the study area into three groups on the basis of mineralogy and texture. All three groups are similar in appearance and composition to the Precambrian "Y" sedimentary rocks of nearby east-central Idaho (Berg, 1977). In this report, the quartzites are considered to be Precambrian "Y" in age (800 m.y. to 1,600 m.y. B.P.; Cohee, 1974), without assuming a direct correlation to any particular unit outside the study area.

Granodiorite of the Idaho Batholith--Ki

Two small patches of grey, foliated biotite granodiorite crop out on two ridges leading north off Castle Rock Ridge. The outcrops are

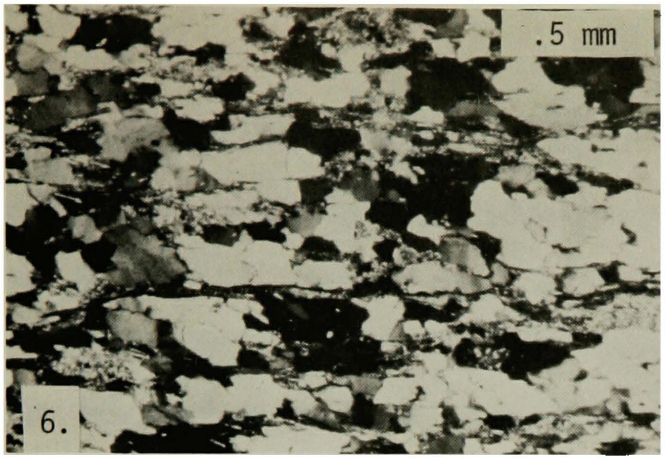

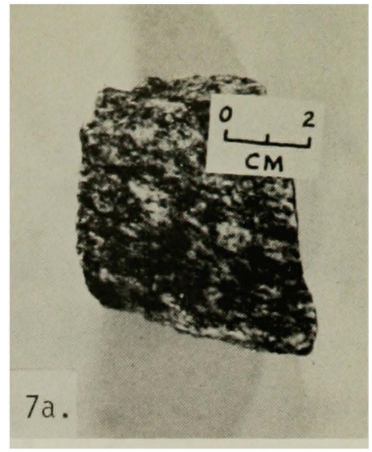

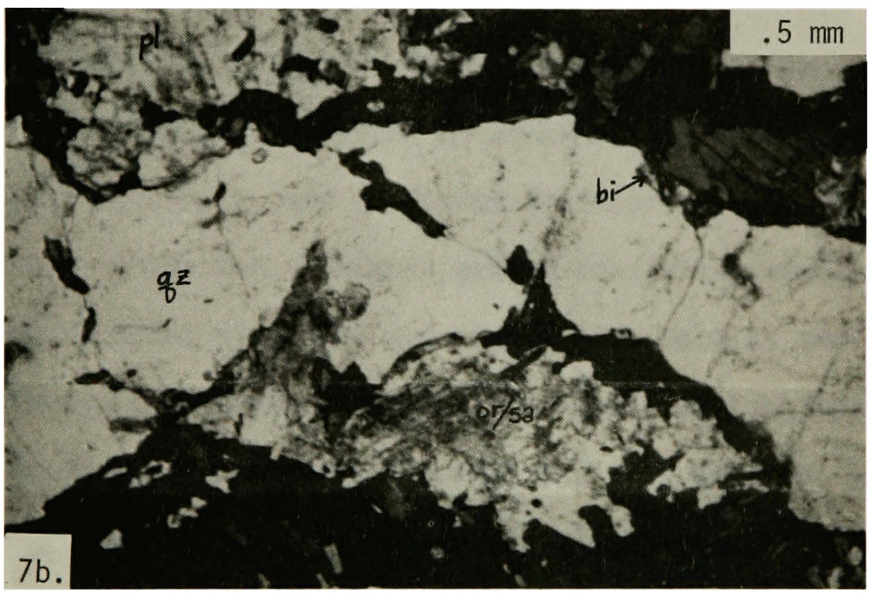

Figure 6. Photomicrograph of Yq quartzite, showing pronounced foliation of muscovite and felsic minerals. X polars.

Figure 7a. Hand specimen photograph of Ki granodiorite, showing biotite foliation.

Figure 7b. Photomicrograph of Ki granodiorite, showing biotite foliation.

entirely surrounded by coarse-grained eqigranular pink granites of the Tg unit. The granodiorite is mineralogically and texturally similar to rocks of the Cretaceous Idaho batholith, which crops out approximately 5 km to the north. These features suggest that the granodiorite outcrops are roof pendants of Idaho batholith rock, caught up by the younger magma during its ascent. Table 1 summarizes the mineralogy of this unit.

Textures. Grain boundaries of all three felsic minerals are typically sutured; although boundaries between two quartz grains or between two potassium feldspar grains may be polygonal. In places, patches of larger quartz, plagioclase, and potassium feldspar crystals appear to "float" in a sea of smaller, anhedral grains consisting mostly of quartz. Myrmekitic intergrowths of quartz and plagioclase form as small patches randomly scattered throughout the rock. The most striking textural feature of the rock, in both hand specimen and thin section, is a well-developed biotite foliation (Figure 7). In places, quartz shows a weak crystallographic orientation parallel to this foliation.

Interpretation. On the basis of their textural and compositional characteristics these rocks are assigned to the Cretaceous Idaho batholith. The two small outcrops are entirely surrounded by pink, coarse-grained, equigranular granite of the epizonal Tertiary suite. They are therefore interpreted as roof pendants of batholith rock caught up by the younger granite magma. The optical properties of the potassium feldspar in the Ki rocks show it to be sanidine rather than one of the

MINERAL/COLOR IN H.S.	% OF ROCK	GRAIN SIZE	GRAIN SHAPE	PROPERTIES	ALTERATION	TEXTURES/COMMENTS
Plagioclase white	74 to 85	0.2--3 mm	subhedral to euhedral laths	An_{21}--An_{30}* (oligoclase)	sericite and clay, gen. in fractures within individual crystals.	Undulatory extinction; concentric, normal zonation; albite twinning with subsidiary pericline twinning.
Quartz grey	23 to 38	0.1--1 mm	anhedral	anomalous 2V up to 10 or 15^{o}		Tendency for grain sizes to cluster around 0.1 and 1 mm, producing a bimodal distribution. Pervasive undulose extinction
Potassium feldspar pale buff to white	15 to 26	0.2--0.5 mm, some poikilitic megacrysts to 10 mm	anhedral sanidine	$2V_x = 30^{o}$ sanidine	low birefringent clay	Rare Carlsbad twinning; Poikilitic megacrysts contain biotite, plagioclase and quartz inclusions. Undulose extinction.
Biotite brown	9 to 15	0.1--0.4 mm	euhedral rectangular flakes	pleochroic, x'= medium cinnamon br., z'= slightly reddish brown	granular magnetite and hematite	flakes are bent and curved, strongly foliated. Zircon inclusions may create pleochroic haloes.
Primary accessory minerals: zircon, apatite						

* Centered bisectrix method (c.f. Tröger, 1958)

Table 1. Mineralogy of the Ki unit.

lower temperature polymorphs. Inversion of plutonic alkali feldspar to its high-temperature polymorph might have occurred as the granodiorite inclusions were engulfed by the Tertiary magmas (Jack Wehrenberg, pers. comm., 1980; Deer and others, 1966, p. 289). Alternatively, the mineral might be orthoclase with an exceptionally low sodium content (Deer and others, 1966, p. 308). Undulatory extinction documents post-crystallization strain which might further affect the optical properties of the mineral.

Massive Flow Unit--Tmf

Rocks of this unit are white-to-lilac biotite-quartz-plagioclase-sanidine porphyritic rhyolites (Figure 8a). The principal outcrops within the study area are on two ridges leading south off Castle Rock Ridge; a small outcrop also occurs on lower Jack the Ripper Creek, and another on the ridge east of that creek. Additional outcrops of this lithology are located immediately outside the southwest boundary of the study area. The unit is interpreted as a lava flow. Table 2 summarizes the mineralogy of this unit.

Groundmass and textures. Rocks of this unit have a felsite groundmass, consisting of a dense intergrowth of quartz and alkali feldspar microlites plus very fine-grained disseminated opaques (Figure 8b). In some thin sections the microlites have a sperulitic arrangement. The felsite intergrowth presumably represents devitrification of an original glassy groundmass.

MINERAL/COLOR IN H.S.	% OF ROCK	GRAIN SIZE	GRAIN SHAPE	PROPERTIES	ALTERATION	TEXTURES/COMMENTS
Sanidine glassy	7 to 15	0.5--2 mm, rarely to 4 mm	subhedral, rounded rectangular to equant			Characteristic Carlsbad twinning. Larger crystals have zonally-arranged inclusions of plagioclase and biotite. Fractured, with undulatory extinction, slightly to extremely embayed.
Plagioclase glassy	0 to 10	0.25--1.25 mm, ave. 0.75 mm	euhedral laths	An_{13}--An_{34}* (oligoclase to andesine)		Concentric zonation and albite twinning are ubiquitous; less common Carlsbad twinning. Crystals are fractured and have undulose extinction. Form 1--2mm diameter glomerocrysts.
Quartz grey	6 to 8	0.25--1.0 mm	rounded and embayed, with hexagonal cross sections	anomalous 2V of 5-10^{o}		Slight undulatory extinction. Commonly fractured. Forms glomerocrysts, which rarely contain sanidine, but do not contain plagioclase.
Biotite black	4 to 5	0.1--0.5 mm, rarely to 1.25 mm	long, slender rectangular laths or hexagonal basal sections	pleochroic, with x'= light blond-brown, z'= dark brown	minute "beads" of magnetite on rims of flakes	Abundance of biotite, and shape of laths are characteristic features of this unit. Rare pleochroic haloes surround zircon inclusions in a few flakes.
Primary accessory minerals: zircon, apatite, magnetite, allanite						

* Centered bisectrix method (c.f. Tröger, 1958)

Table 2. Mineralogy of the Tmf unit.

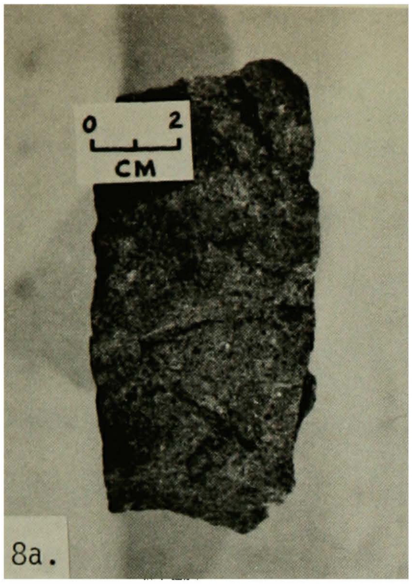

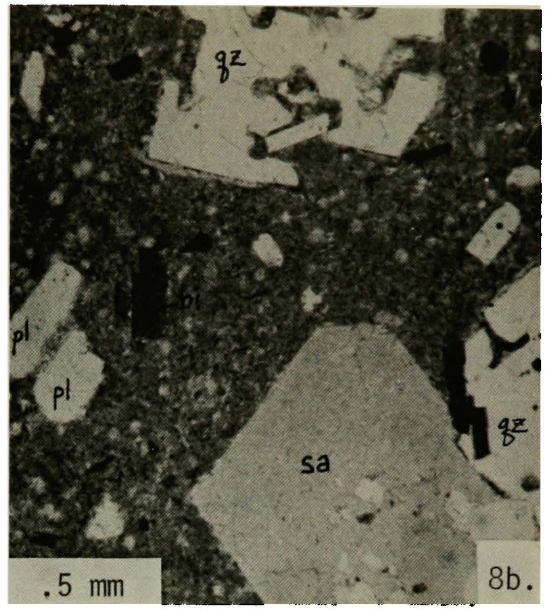

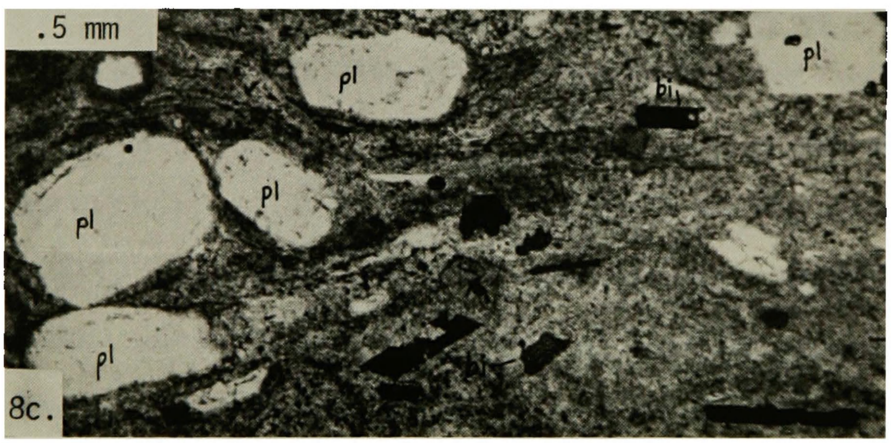

Figure 8a. Hand specimen photograph of Tmf massive flow unit. Dark spots are quartz phenocrysts, light spots are sanidine phenocrysts.

Figure 8b. Photomicrograph of Tmf showing randomly-oriented phenocrysts in a devitrified felsite groundmass.

Figure 8c. Photomicrograph of Tmf showing parallel orientation of phenocrysts and layered aspect to groundmass.

Out of 18 samples of this unit examined in thin section, 7 are massive, 5 show orientation of phenocrysts (best developed in biotite, but also present in the smaller plagioclase laths), and 6 show both phenocryst orientation and a layered aspect to the groundmass (Figure 8c). The latter is usually accentuated by a differential coarseness of the devitrification minerals. Thin, mm-scale fluidal banding is continuous on hand specimen scale. The unit normally crops out as piles of blocky rubble, and the extent of layering on an outcrop scale cannot usually be determined. Where outcrops are good, the banding is continuous for at least several centimeters. In thin section, the layering is in places highly contorted; this is interpreted as a primary flowage feature. In most cases, the rock appears massive on both hand specimen and outcrop scale. In both massive and layered rocks, there is a conspicuous absence of broken crystals, recognizable pumice fragments, glass shards, and lithic inclusions. Granophyric intergrowths of sanidine and quartz are common, occurring as phenocryst-sized clots or as broad rims on sanidine phenocrysts.

Interpretation. The Tmf unit is interpreted as a rhyolite lava flow. The general absence of prominent layering may attest to the relatively low viscosity of the unit (Williams and McBirney, 1979, p. 117-118). A lava flow rather than ash flow origin is strongly indicated by the almost total absence of broken crystals and accidental inclusions, and by the complete absence of glass shards, pumice, or eutaxitic structures (see Ross and Smith, 1961). Although fracturing of quartz crystals is commonly seen, this appears to have occurred in place. Fracturing may derive from the inversion of high-temperature β-quartz to low-temperature α-quartz (Blatt and others, 1972) and provides no information on the mode of extrusion. The excellent preservation of plagioclase glomerocrysts and of granophyric overgrowths on sanidine may also argue against an explosive origin for the unit; these structures contain inherent inhomogeneities which would render them particularly unstable during a violent eruption (Vance, 1969). Biotite flakes in welded tuffs are commonly bent and crumpled during compaction (Williams and McBirney, 1979, p. 163), whereas those in the Tmf unit are undeformed.

Outcrops of this unit are separated from one another by distances of up to 1.5 km and are found at varying elevations (Plate 1). The relative importance of original distribution, erosion, and faulting in creating the present outcrop pattern is unknown. Detailed statistical measurement of phenocryst orientation in oriented thin sections (e.g., Smith and Rhodes, 1972) might provide information on the source area for the flows; such measurements are beyond the scope of the present examination.

Laminated Flow Unit--Tlf

Outcrops of this unit are restricted to the western margin of the study area. In outcrop the rocks are typically dark maroon to purple and show an irregular lamellar color banding, which in places is highly contorted. The rock displays a platy fracture which is oriented parallel to the banding (Figure 9a). In addition to the layering, a distinctive characteristic of this unit is the paucity of phenocrysts: only scattered, weathered feldspar crystals are identifiable in hand specimen. The rocks are highly fractured and coated with manganese-oxide stain. The unit is interpreted as a lava flow. Table 3 summarizes the mineralogy of this unit.

Groundmass and textures. In thin section, it can be seen that the prominent fluidal banding of this unit results primarily from different amounts and coarseness of the devitrification and alteration products (clays, silica minerals, alkali feldspar, and disseminated opaques). The groundmass in sample 64A contains 0.1 mm-thick drawn-out voids(?) lined with varpor-phase crystals of quartz (inverted from the original tridymite--Ross and Smith, 1961) (Figure 9b). These parallel the contorted layering in the rock, and presumably occurred during volatile loss and shearing of the nearly-solidified lava. The same mechanism may have caused the platy fracture characteristic of the unit (Williams and McBirney, 1979, p. 118). In thin section, sample 67A shows a well-developed trachytic texture produced by minute oriented plagioclase microlites (Figure 9c). These diverge around the phenocrysts. Phenocryst orientation is poorly developed in sample 64A, perhaps due to turbulence in the lava.

MINERAL/COLOR IN H.S.	GRAIN SIZE	GRAIN SHAPE	COMPOSITION	ALTERATION	TEXTURES/COMMENTS
Plagioclase buff	0.75--2 mm, ave. 1 mm	euhedral laths		extensively altered to clays and sericite	Fractured; many phenocrysts are sufficiently altered to be entirely removed during thin section manufacture, leaving only a rectangular void or skeletal network of sericite microveinlets.
Biotite dark brown	0.25--0.75 mm	long, slender or short, stubby euhedral laths	pleochroic, x'= pale blond-brown, z'= dark brown	granular magnetite on rims	Generally shows strong flow-alignment.
Primary accessory minerals: zircon, apatite, magnetite; one apparent amphibole end-section seen in thin section					

Table 3. Mineralogy of the Tlf unit.

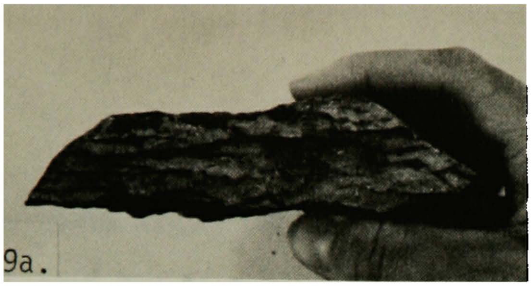

Figure 9a. Hand specimen photograph of Tlf, laminated rhyolite flow, showing platy fracture oriented parallel to color banding.

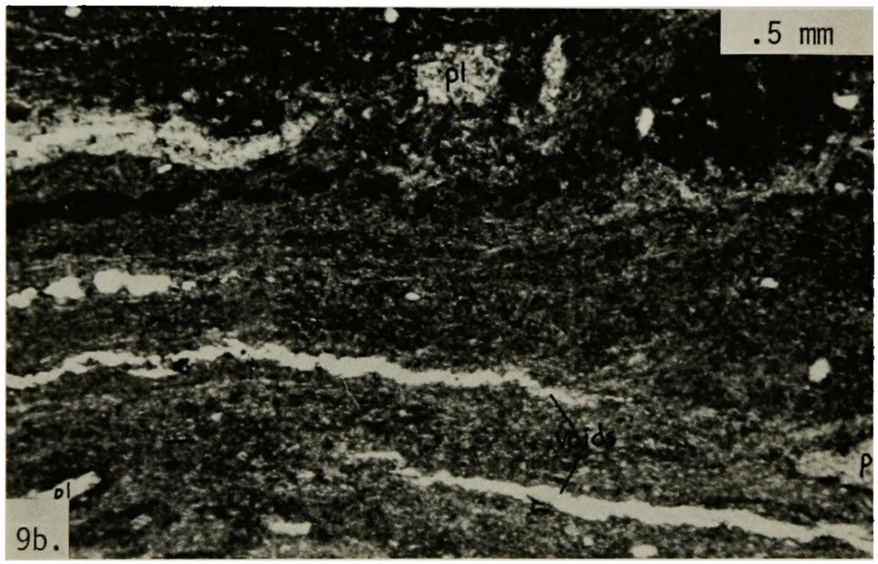

Figure 9b. Photomicrograph of Tlf, showing flow banding and drawn-out voids(?) lined with vapor-phase minerals.

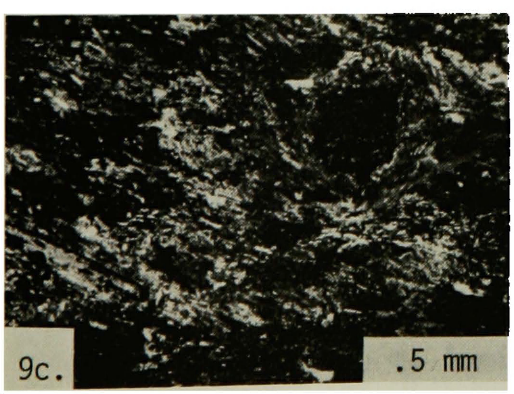

Figure 9c. Photomicrograph fo Tlf showing trachytic texture produced by parallel orientation of plagioclase microlites. X polars.

Interpretation. As with the massive flow unit, there is no evidence in these rocks of features indicative of a pyroclastic origin. The fluidal banding is continuous in both outcrop and thin section. The trachytic texture of sample 67A is positive evidence of a lava flow origin (Williams and others, 1954). The turbulent nature of the groundmass in sample 64A in comparison to the more regular lamellar appearance in thin sections from other samples, may indicate that it lies closer to the source of the flow (Williams and McBirney, 1979, p. 117). The limited outcrop extent of this unit presumably reflects the higher viscosity and/or smaller volume of this flow in comparison to the massive flow unit.

Volcanic Rocks, Undivided--Tvc

Description. This unit comprises a texturally and compositionally diverse suite of rhyolitic extrusive rocks which underlies most of the southern two-thirds of the study area (Plate 1). The unit typically does not form resistant or laterally-continuous outcrops, and was generally mapped from rubble.

Tvc rocks are apparently interbedded and partly coeval with those mapped as Tlf, Tmf, and Tt. They are also partly younger, since the upper part of the unit overlies the epiclastic conglomerates of the Ttc unit.

These are massive to laminated, off-white, grey, green, and purple rhyolitic volcanic rocks. Phenocryst content ranges from less than 1% to 30% of the rock. Phenocryst species occur in widely varying relative

FEATURE \ SAMPLE	53A	54A vitrophyre (flow?)	55B vitrophyre (flow?)	56A welded tuff	61A flow	65A welded tuff	68A banded obsidian flow	68B flow
Crystals--whole or broken (abbreviations, see below)	mainly whole al hb pl zr sa qz	whole al pl bi ap qz zr sa	brecciated al bi	(1) bi zr qz ma pl sa	sparcely crystalline sa altered pl?	whole pl bi zr	whole pl ap ma zr sa bi→he	whole pl al sa zr bi→he ma→he
Secondary crystallization	extensive	very clean	abundant	abundant	extensive; much vapor phase; xals altered	extensive; much vapor phase; xals altered	extensive in groundmass	moderate; bi xals much altered; felds less so
Glass shards	--	--	--	within pumice fragments; none seen in groundmass	--	--	--	--
Pumice fragments	--	--	--	compressed, randomly oriented lapilli	--	--	--	--
Bent biotite flakes	no biotite	--	generally not	those inside pumice fragments may be protected from crushing	no biotite	--	--	--
Axiolitic texture	--	--	--	possible	--	possible	--	--

SAMPLE / FEATURE	53A	54A vitrophyre (flow?)	55B vitrophyre (flow?)	56A welded tuff	61A flow	65A welded tuff	68A banded obsidian flow	68B flow
Eutaxitic structure / lamination	massive	parallel fractures--poss. tension shears?	--	--	contorted layering	layered aspect to devitrification coarseness	layered--diff. xal abundance and coarseness of devitr.	massive, except for voids (2)
Perlitic cracks	--	present	remnant	--	--	--	--	--
Microlites or trichytes	--	--	--	--	--	--	--	possible trichytes
Glomerocrysts, granophyric intergrowths	--	glomerocrysts and granophyric intergrowths	a few glomerocrysts	a few glomerocrysts (1)	--	a few glomerocrysts	abundant glomerocrysts	abundant glomerocrysts

Mineral abbreviations:

al	allanite	ch	chlorite	pl	plagioclase	sp	sphene
ap	apatite	hb	hornblende	qz	quartz	zr	zircon
bi	biotite	he	hematite	sa	sanidine		
ca	carbonate	ma	magnetite	se	sericite		

Table 4. Mineralogy and textural features of the Tvc unit.

SAMPLE / FEATURE	71A flow	73AI vitrophyre (flow?)	73AII flow	74A	79A flow	83A	95A	109A
Crystals--whole or broken	mostly whole qz zr sa al pl ma bi hb	whole qz hb sa pl zr	mostly whole qz zr sa hb pl al	broken qz ma sa pl bi	whole qz sp sa hb pl ch ap	whole qz hb pl zr sa bi	whole sa zr qz pl hb	whole pl bi hb ap
Secondary crystallization	extensive; xals are fresh	extensive; xals are fresh	extensive	extensive	extensive; poss. vapor phase; xals are altered	extensive; felsic xals fresh, mafic are altered	extensive; felsic xals fresh, mafic are altered	extensive; poss. vapor phase; xals are altered
Glass shards	--	--	--	--	--	--	--	--
Pumice fragments	--	--	--	--	--	--	--	--
Bent biotite flakes	--	no biotite	no biotite	--	--	--	no biotite	--
Axiolitic texture	--	--	--	--	--	--	--	poss. seen in h.s.

SAMPLE / FEATURE	71A flow	73AI vitrophyre (flow?)	73AII flow	74A	79A flow	83A	95A	109A
Eutaxitic structure / lamination	massive	massive	massive	massive	massive	massive	massive	layered, shown by diff. coarseness of devitr.
Perlitic cracks	--	remnant	remnant	--	remnant	--	--	--
Microlites or trichytes	feldspar microlites?	--	trichytes?	--	--	--	trichytes?	--
Glomerocrysts, granophyric intergrowths	a few glomerocrysts	a few glomerocrysts	a few glomerocrysts	--	--	a few glomerocrysts	a few glomerocrysts	--

Table 4. (cont'd).

FEATURE \ SAMPLE	123A	141B vitrophyre (flow)	145A tuff breccia	147B flow?	154 welded tuff	155A welded tuff	157I flow?	157II flow?
Crystals--whole or broken	whole pl bi	in-place brecciation qz al sa hb pl ap	whole qz zr felds ap bi → sp + ch	whole bi hb ap pl → ca	broken qz sa pl	whole? sa qz bi	whole pl ap bi hb ma → he	whole pl ap bi hb ma → he
Secondary crystallization	extensive; varying coarseness	extensive in groundmass; felsic xals fresh; mafic are altered	extensive; felds. very altered	extensive	extensive	extensive; xals are fresh	moderate; felsic xals very altered	moderate; felsic xals very altered
Glass shards	--	--	only in pumice fragments	--	ghosts?	see "axiolitic texture"	--	--
Pumice fragments	possible	--	compressed, randomly oriented lapilli	--	present	--	--	--
Bent biotite flakes	--	no biotite	no biotite	--	no biotite	--	--	--
Axiolitic texture	--	--	possible	--	in ghost shards	possible	--	--

SAMPLE / FEATURE	123A	141B vitrophyre (flow?)	145A tuff breccia	147B flow?	154 welded tuff	155A welded tuff	157I flow?	157II flow?
Eutaxitic structure / lamination	layering, may diverge around xals, or be cut by them	massive	massive	discontinuous elongate shapes--tension shears? (2)	some layering to shards(?), but not consistent	eutaxitic	discontinuous elongate shapes--tension shears? (2)	turbulent layering; diff. coarseness of devitr.
Perlitic cracks	--	remnant	--	--	present (post-welding?)	--	--	--
Microlites or trichytes	--	--	--	--	--	--	--	trichytes?
Glomerocrysts, granophyric intergrowths	a couple small glomerocrysts	--	possible; too altered to be sure	--	--	--	--	--

Table 4. (cont'd).

FEATURE \ SAMPLE	158A	164A tuff breccia	174A flow	235BI flow	236AII flow	236B flow	239A	257A
Crystals--whole or broken	whole pl zr bi hb ap	whole pl bi ap	whole qz zr felds al bi→he ap	whole qz pl sa hb	whole bi ap felds→ca+se	whole pl al bi hb zr	brecciated in-place pl ap hb bi	brecciated in-place? pl hb qz al sa zr bi
Secondary crystallization	moderate to extreme in groundmass; felsic xals very altered	moderate	extensive; felds are very altered	moderate	moderate; felds are very altered	moderate to extreme in groundmass; mafic xals very altered	moderate in groundmass; pl and hb are altered	extensive; abundant vapor phase
Glass shards	--	present; very little compression	--	--	--	--	--	--
Pumice fragments	--	cannot distinguish individual lapilli	--	--	--	--	--	--
Bent biotite flakes	--	possible	--	no biotite	--	--	--	--
Axiolitic texture	--	--	--	--	--	--	--	present?

SAMPLE / FEATURE	158A	164A tuff breccia	174A flow	235BI flow	236AII flow	236B flow	239A	257A
Eutaxitic structure / lamination	turbulent layering	massive	massive	trachytic layering;	trachytic layering; drawn-out amygdules?(3)	trachytic layering; drawn-out amygdules?(3)	--	--
Perlitic cracks	--	--	remnant	--	--	--	--	--
Microlites or trichytes	--	--	--	microlites	microlites	trichytes	microlites	--
Glomerocrysts, granophyric intergrowths	a couple glomerocrysts	a couple glomerocrysts	possible; to altered to be sure	--	--	--	a few glomerocrysts	a few glomerocrysts

Table 4. (cont'd).

SAMPLE / FEATURE	262A	263BI flow?	263BII	267A	301	303A vitrophyre (flow?)	303B tuff or tuff breccia
Crystals--whole or broken	whole pl hb sa ap qz bi→he	whole pl bi sa zr qz ap	whole qz zr sa pl hb	whole pl zr sa ap qz hb	whole qz sa pl zr	whole qz al sa pl hb	broken and whole pl zr qz ap sa al hb
Secondary crystallization	patchy throughout groundmass	extensive; xals are unaltered	extensive	extensive, with no relationship to layering	extensive; felsic xals are fresh	very clean	moderate; shards still visible
Glass shards	--	--	--	--	--	--	present
Pumice fragments	--	--	--	wispy laminae--compressed lapilli?	--	--	present
Bent biotite flakes	--	no biotite	no biotite	no biotite	no biotite	no biotite	no biotite
Axiolitic texture	--	--	--	--	--	--	present

SAMPLE / FEATURE	262A.	263BI flow?	262BII	267A	301	303A vitrophyre (flow?)	303B tuff or tuff breccia
Eutaxitic structure / lamination	layering, diff. devitr. coarseness color layered in h.s.	faint elongation of possible amygdules	massive	thin, dark layers with no relationship to devitr.	massive	faint trichyte layering	massive
Perlitic cracks	--	--	--	--	--	present	--
Microlites or trichytes	--	--	--	trichytes?	--	faint trichytic layering	--
Glomerocrysts, granophyric intergrowths	--	possible	--	--	possible	a few	--

(1) Crystals enclosed in pumice lapilli might be protected from fragmentation during explosive eruption.

(2) Elongate voids, filled with vapor-phase minerals and oriented parallel to or at a slight angle to layering may be tension shears produced during laminar flow (Williams and others, 1954, p. 122)

(3) Elongate voids, rimmed with quartz or tridymite--possible amygdules?

Table 4. (cont'd).

proportions; in overall order of abundance these are: Quartz ≅ sanidine > plagioclase > biotite > hornblende ≅ allanite ≅ primary magnetite > zircon > apatite > sphene. Alteration minerals include chlorite, hematite, carbonate, sericite, and magnetite.

Possible former hot springs activity of limited extent is recorded by the presence of abundant botryoidal, chalcedony-filled globules at two localities. These outcrops of highly silicified Tvc rocks form resistant knobs on the top of present-day ridges. The deposits probably formed late in the volcanic history of the area.

Table 4 summarizes the textural and mineralogical features of 39 samples from the Tvc unit. Because of their wide range in textures and phenocryst mineralogy, the rocks grouped within this unit probably represent a sequence of several lava flows and welded ash-flow tuffs. These rocks could not be separated in the field due to limited outcrop exposures. Maximum preserved thickness of the unit as a whole is approximately 550 m.

Interpretation. Features used in Table 4 to assign an ash-flow origin to a particular sample were:

(1) glass shards, produced by the explosive disintegration of chilled frothy magma. (1)*

*Number in parentheses following feature refers to references:
(1) Ross and Smith, 1961
(2) Donald Peterson, pers. comm., 1979
(3) Williams and McBirney, 1979
(4) Williams and others, 1954
(5) Vance, 1969

(2) pumice fragments, which are present in almost all ash-flow tuffs. (1)

(3) eutaxitic structure, due mainly to flattening of pumice fragments during compaction of the tuffs. The result is a discontinuous, streaky foliation in both hand specimen and thin section. (1)

(4) broken phenocrysts, produced by explosive eruption. (2) Ross and Smith (1961) do not consider this feature to be especially diagnostic of a pyroclastic origin.

(5) bent biotite flakes resulting from differential compaction. (3) This feature might only be apparent in densely welded tuffs having a high percentage of other phenocrysts between which the biotite flakes might be trapped.

(6) axiolitic texture, a devitrification texture consisting of fibers of alkali feldspar and a silica mineral (generally tridymite) which grow normal to particle walls (generally a glass shard or pumice fragment) and radiate inward. (1)

Features used in Table 4 to assign a lava flow origin to a particular sample were:

(1) presence of microlites (minute, birefringent crystals) or trichytes (curved, hairlike, non-birefringent crystallites). (4)

(2) glomerocrysts, which might be expected to not survive an explosive eruption. (5)

(3) perlitic cracks formed from glassy magmas which absorbed a few percent water while cooling. (4)

(4) turbulent or laterally-continuous fluidal lamination. (1,3,4)

Parallelism of tabular phenocrysts may be produced by laminar flow in either lavas or ash flows, or by compression in welded ash-flow tuffs; its occurrence was not therefore considered diagnostic of either mode of origin. Likewise, spherulitic structures developed during devitrification of welded tuffs are in no way different from those formed in lava flows (Ross and Smith, 1961). Lithophysae (large vesicular cavities produced by the escape of volatiles during devitrification) seem to be much less common in welded tuffs than in lava flows (Ross and Smith, 1961) but have essentially the same characteristics in both. Foreign crystals or rock fragments derived from vent walls or picked up from the surface may be incorporated into both ash flows and lava flows; they are not necessarily diagnostic of either. "Secondary crystallization" as used in Table 4 refers to both devitrification, the fine-grained intergrowth of alkali feldspar and silica minerals produced by the breakdown of felsic glasses, and to vapor-phase crystallization, the growth of crystals from a vapor phase, in pore spaces. Devitrification and vapor phase crystallization may occur in both rhyolitic lava flows and welded ash-flow tuffs.

On the basis of these criteria, 19 of the thin sections described in Table 4 are interpreted as representing lava flows, and 7 are interpreted as representing welded ash-flow tuffs or tuff breccias (Figure 10).

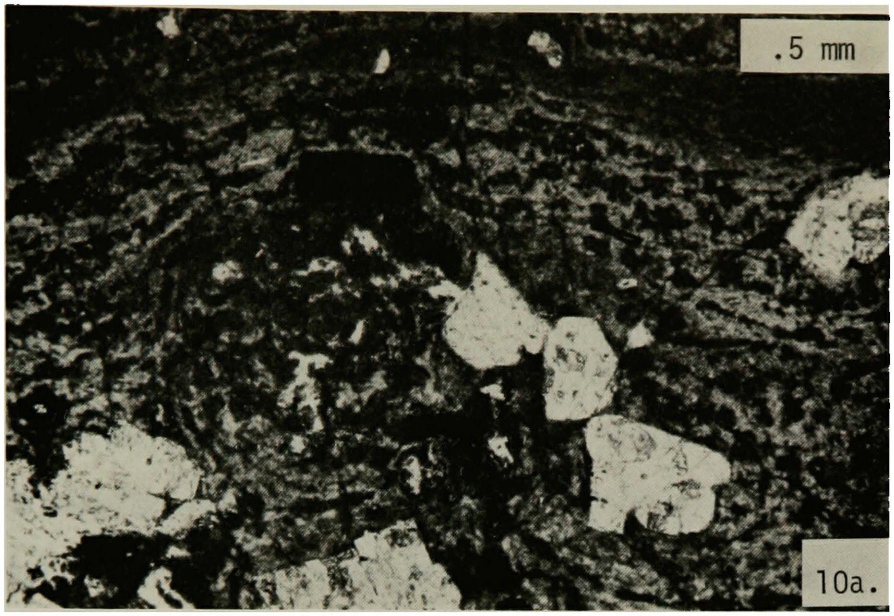

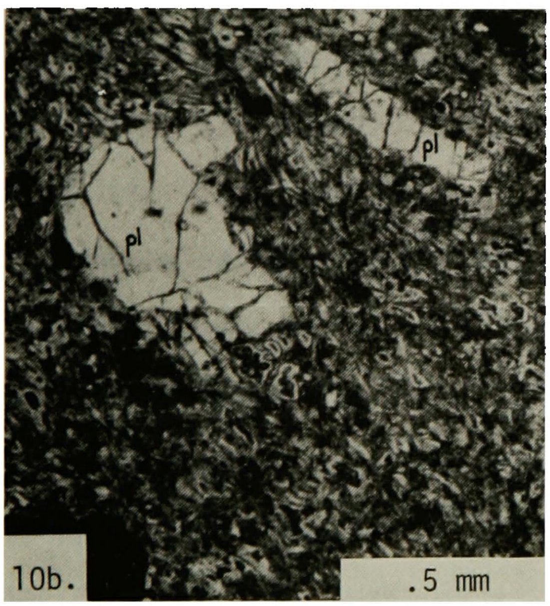

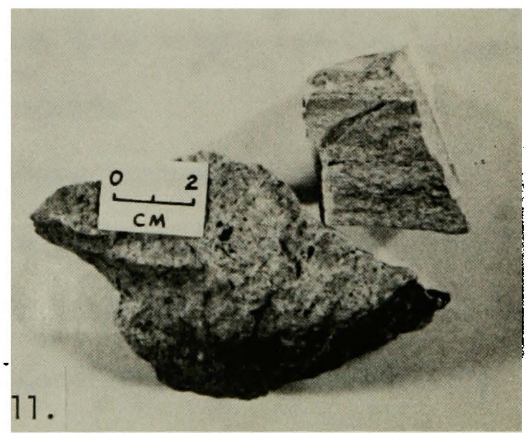

Figure 10a. Lava flow-rock from Tvc unit. Photomicrograph showing turbulent flow-layering. Phenocrysts are altered plagioclase and oxidized biotite.

Figure 10b. Ash-flow tuff from Tvc unit. Photomicrograph showing slightly distorted circular glass shards.

Figure 11. Hand specimen photograph of Tt airfall tuff. Large sample contains dark fragments of charcoal; small sample shows fine scale lamination.

Of the remaining 12 slides, 11 lacked the diagnostic features given above (due either to secondary crystallization or to non-occurrence) and 2 showed contradictory evidence of origin. Most ash-flow tuffs are readily recognizable by means of thin-section studies, as their distinctive pyroclastic characteristics are rarely completely obscured by devitrification or other late-stage alteration (Ross and Smith, 1961). On the other hand, glassy rhyolite flow-rocks can be essentially featureless, consisting of phenocrysts set in a glassy or felsitic groundmass which may or may not show fluidal banding. On the basis of admittedly negative evidence, that is the absence of pyroclastic features, it is therefore tempting to propose a lava flow origin for the 11 samples which lack diagnostic features in thin section.

Regardless of whether these samples are included, there appears to be a predominance of flow rocks over welded ash-flow tuffs or tuff breccias within the 39 rocks described in Table 4. Sampling of the Tvc unit in the field was not carried out according to any statistically random design. Nevertheless, as Plate 1 shows, samples were collected from throughout the unit, at a wide range of elevations. The suite of samples examined in thin section may therefore be taken as broadly representative of the unit as a whole.

The Tmf and Tlf units described above are also interpreted as lava flows. The particular volcanic environment encompassed by the study area must be one which allowed the formation of over 13.2 km^3 of rhyolitic lava flows apparently containing only minor amounts of interbedded pyroclastic material.

Airfall Tuff--Tt

Only one outcrop of definite airfall material was mapped within the study area. It consists of approximately seven vertical meters of very thinly-laminated white crystal-vitric tuff. The isolated exposure could not be traced laterally for more than approximately eight meters due to thick soil and vegetative cover. The lithology is significant because of its use for K/Ar age determination (Chapter I), and will therefore be described in detail.

Mineralogy. Phenocryst minerals are quartz, sanidine, biotite, plagioclase, and very minor amounts of allanite and zircon. The felsic minerals occur as well-sorted, angular, broken fragments measuring 0.1 to 0.25 mm in diameter. Extinction in all felsic minerals is highly undulatory. Quartz greatly predominates over feldspar. Plagioclase shows albite twinning, and possible concentric zoning. Biotite occurs as rounded to euhedral flakes which are black in hand specimen, and are pleochroic with x' = greenish tan and z' = medium dark brown. Zircon forms euhedral to slightly rounded crystals. Small (0.25 to 0.3 mm) rounded pumice fragments are also present.

Groundmass and textures. The rock shows a prominent millimeter-scale lamination produced by parallel orientation of the biotite flakes and by variations in the size and amount of felsic phenocrysts. The groundmass consists of glass shards and volcanic dust. The shards are indistinct, but appear to be unwelded, and are altering to clays or devitrification minerals. The phenocryst minerals appear to be very fresh, and in general, this unit is much less altered than many of the other volcanic lithologies, a fact which prompted its selection as a dating locality.

A striking feature is the small fragments of charcoal which occur randomly scattered throughout the rock (Figure 11). These are small twig fragments approximately 0.5 to 1 cm long, some of which contain unburned cores. Apparently the hot falling ash pelted down through some small bushes, stripping away the thinner twigs, flash-charring them, and incorporating them in the deposit.

Interpretation. The thin laminae, good sorting, and overall fine grain size of this unit indicate that it formed as an airfall deposit. The material was still hot as it fell, as shown by the charcoal fragments, and therefore may have been relatively near its source. On the other hand, the ash was not hot enough to cause welding of its constituent glass shards.

There are no signs, such as the presence of ripples, crossbedding, or channels, to suggest stream reworking of the ash. Airfall deposits typically occur as veneers which uniformly mantle topography (Williams and McBirney, 1979, p. 136, 175-176). In contrast, the Tt unit crops out as an isolated 7 m-thick body. This suggests that the tuff may have formed by deposition of airfall material into a small lake or pond. Airfall material washed in from surrounding slopes or precipitated directly from the air would have settled slowly through the water, producing the fine laminae and parallel orientation of biotite characteristic of the unit.

The overall paucity of airfall tuffs within the study area may signify a relatively low volatile content for the volcanic system as a whole. Other indications of low volatile content include the very minor amount of pumice in this and the other units, and the predominance, noted above, of lava flow-rocks over pyroclastic deposits.

Tuffaceous(?) Conglomerate and Sandstone--Ttc

Epiclastic tuffaceous(?) conglomerates, lithic-rich arkoses, and thinly-laminated lithic-lapilli-crystal tuffs(?) crop out primarily in the central portion of the study area, along Castle Rock Ridge and the ridge northeast of Jack the Ripper Creek. Although the outcrops may be lumped into the three divisions given above, they display great textural and compositional variability. The outcrops each have different colors, depending on the color and relative amounts of matrix and clasts. The clasts are quartzite and numerous volcanic lithologies; granitic clasts have not been recognized in either hand specimen or thin section.

Lithic-rich arkose. Only one outcrop of this rock-type was found within the study area, near the intersection of the Castle Rock trail and the Montana-Idaho divide. In hand specimen the pale grey rock is so crystal-rich that it resembles a fine-grained granite. In thin section (Figure 12a) the rock consists of well-sorted, angular, broken crystals of quartz, plagioclase, and sanidine, with lesser bent biotite flakes. Allanite, zircon, and sphene(?) are present as accessory minerals. Lithic fragments are present in varying amounts, and consist of porphyritic or aphanitic volcanic lithologies, quartzite, and

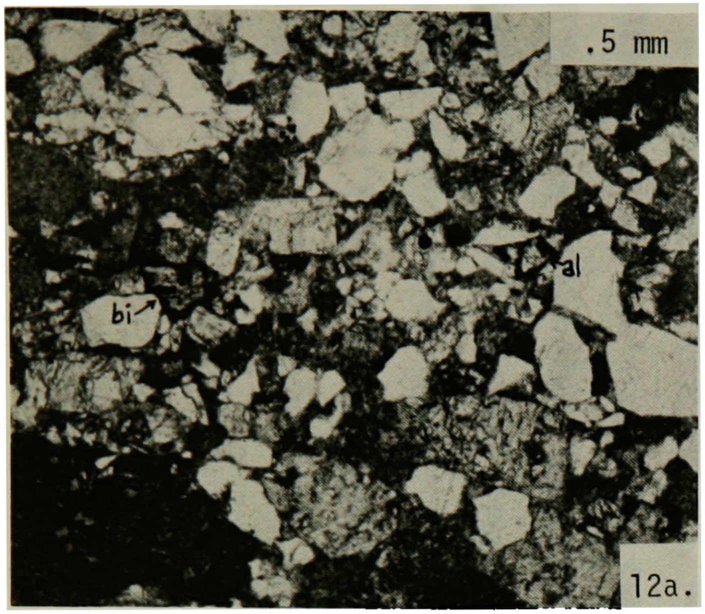

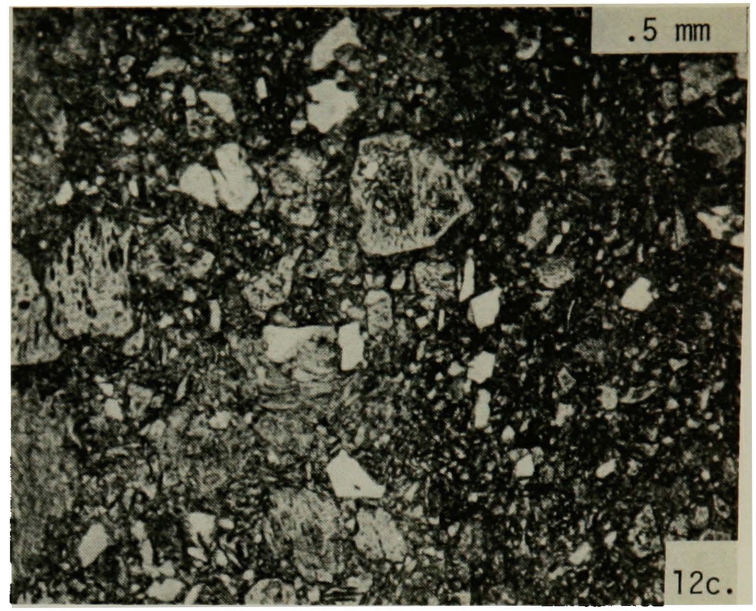

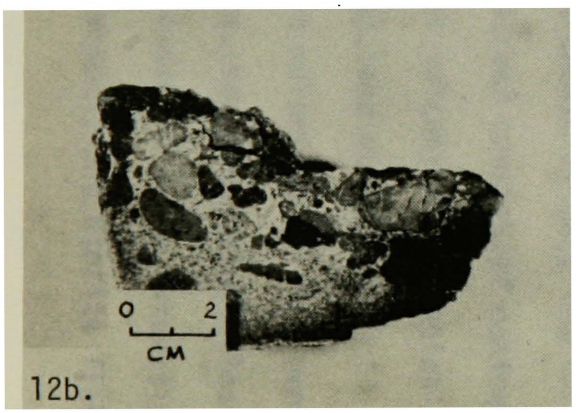

Figure 12a. Photomicrograph of Ttc lithic-rich arkose, showing lithic fragments, crystals of quartz, sanidine, biotite, plagioclase, and allanite.

Figure 12b. Hand specimen photograph of Ttc tuffaceous(?) conglomerate. Clasts are quartzite and volcanic lithologies.

Figure 12c. Photomicrograph of Ttc lithic-lapilli-crystal tuff(?), showing compositional layering of pumice-rich (left) and crystal-rick (right) laminae.

possibly pumice fragments. The arkose is clast-supported. Matrix material comprises only a few percent of the rock; its composition is uncertain, but it could consist of volcanic ash and dust. Glass shards were not recognized in thin section.

Both laminated and massive samples were found, but graded bedding was not observed in either outcrop or hand specimen. Throughout the unit as a whole, grain size ranges from 15 mm (fine sand) to 2 mm (very coarse sand). In spite of a wide range in grain densities in clasts of the same size (compare allanite, S.G. = 3.4 to 4.2, with pumice, S.G. = 2.0-2.5--Marshall, 1935; Gilbert, 1938) there is no evidence of sorting by clast type or density. Sparse rounded to subangular clasts of quartzite up to 15 cm in diameter were found in some pieces of rubble. The lithic-rich arkose may have been formed by sheetwash off an eroded surface of quartzite and volcanic rocks.

Tuffaceous(?) conglomerate. Poorly-sorted, massive, matrix- and clast-supported pebble to cobble conglomerates crop out in several places along Castle Rock Ridge and the ridge northeast of Jack the Ripper Creek. Clasts range from 0.5 mm to 6 cm, and consist of pumice, perlitic vitrophyres, various porphyritic felsic volcanic lithologies (both lava flow-rocks and welded ash-flow tuffs), and quartzite (Figure 12b). Clasts are mostly subrounded, and colors range from green to purple, maroon, and grey. Crystals of quartz, sanidine, plagioclase, biotite, magnetite, zircon, allanite, and hornblende fill the interstices between the larger clasts. Most crystals are broken, and biotite flakes are bent. The matrix material is a very fine-grained, low-birefringent material, possibly representing volcanic ash and dust, altering to clay. Glass shards were not recognized in thin section.

Lithic-lapilli-crystal tuff(?). These well-sorted, thinly-laminated rocks occur as interbeds within outcrops of the tuffaceous(?) conglomerate. Broken, angular crystals of quartz, sanidine, plagioclase, biotite, allanite, and zircon range from 0.05 to 2 mm in diameter. Subangular to subrounded lithic fragments and pumice lapilli range from 0.25 to 3.5 mm. Some samples show a compositional layering from crystal-rich into pumice-rich laminae (Figure 12c). Unfortunately, no oriented thin sections were made to show whether this gradation is upward from small crystals into larger pumice fragments (possible airfall into water) or upward from pumice into crystals (possible airfall on land or deposition from a flow). The groundmass is the same featureless, low birefringent material as in the tuffaceous(?) conglomerates. The laminated nature of these rocks is similar to that of the airfall tuffs of the Tt unit, but there are significant differences between the two: biotite is foliated in the airfall tuff and randomly oriented in this rock. In addition, these rocks contain far more lithic fragments than does the airfall tuff; some layers also contain broken fragments of carbonaceous plant trash.

Interpretation of tuffaceous(?) conglomerates and lithic-lapilli-crystal tuff(?). The textural and compositional variability of these units appears to document a high degree of local source control. The absence of sedimentary structures such as crossbedding, imbrication, and channeling argues against their deposition in a purely fluvial environment. Some size gradation exists between smaller crystals and larger pumice fragments in the lithic-lapilli-crystal tuff(?), but this may actually result from density-sorting. A likely origin for the tuffaceous(?) conglomerates is deposition as a volcanic mudflow, or lahar. A branch of petrified wood found in tuffaceous(?) conglomerate showed no sign of being charred, and may signify that the lahar was cold, rather than hot. Rounding of the constituent clasts in the conglomerate could have occurred during transport in the flow (Williams and McBirney, 1979, p. 177-178) or may have occurred during an earlier period of stream reworking. As with flows of any kind, lahars would seek topographic lows and could easily incorporate stream material over which they passed. Such incorporation would also explain the variability of this unit between one outcrop and the next. The laminated, fine-grained lithic-lapilli-crystal tuff(?) interbeds would then represent reworking of the tops of successive laharic deposits under upper flow regime conditions, presumably by sheetwash. The transition from conglomerate to fine-grained material is abrupt, rather than gradational as might be expected from rapid, turbidity current-like deposition of debris into a body of standing water (Reineck and Singh, 1975).

Epizonal Granite--Tg

Buff to salmon, medium- to coarse-grained biotite granite crops out in two spatially-distinct parts of the study area. Outcrops on the lower parts of the ridges trending north off Castle Rock Ridge are steep walls of bare granite, in marked contrast to the gentle, vegetated slopes formed on the overlying volcanic rocks (Figure 13). Somewhat less striking outcrops of granite are exposed in the south-eastern corner of the study area. The overall pinkish color of these granites readily distinguishes them from the grey to black-and-white granodiorite of the Idaho batholith. In outcrop or hand specimen, other distinctive features include small, 1-2 mm miarolitic cavities, the abundance of potassium feldspar, the deeply-weathered and friable nature of most outcrops, and the equigranular, non-foliated fabric of the lithology.

In texture and composition, rocks of the Tg unit are comparable to the epizonal Tertiary granites mapped elsewhere in the Bitterroot and Atlanta lobes of the Idaho batholith. Outcrops of the Tg unit within the study area are part of a larger, compound epizonal pluton of batholithic dimensions (Figure 2,3). The name "Painted Rocks pluton" has been proposed for this body (Lund and others, ms; Mutschler and others, ms). Preliminary K/Ar dates on this body indicate a probable age within the range 45-50 m.y. P.B. (Robert Fleck, pers. comm., 1980), making it age-equivalent to the other epizonal plutons, as well as to the Castle Rock volcanics. Table 5 summarizes the mineralogy of this unit.

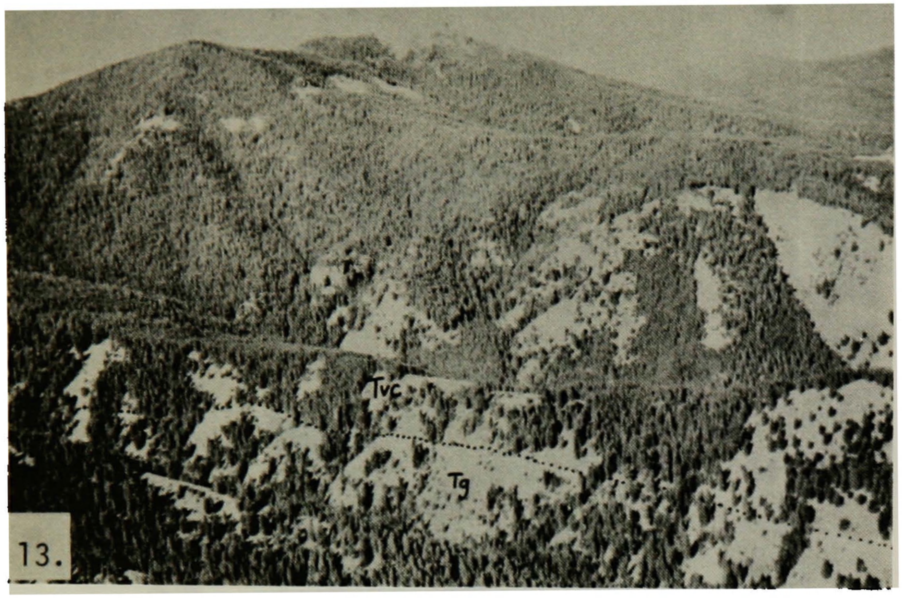

Figure 13. Photograph showing subhorizontal contact between Tvc volcanic rocks and Tg granite. Ridge north from Castle Rock Ridge in vicinity of sample locations 143--150.

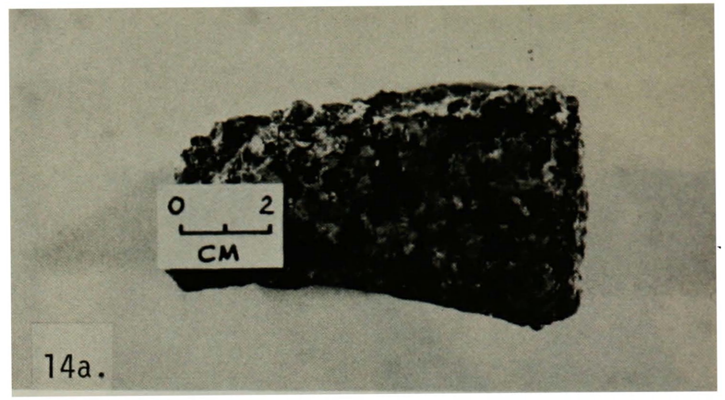

Figure 14a. Hand specimen photograph of Tg granite showing massive, equigranular intergrowth of orthoclase (light grey), quartz (medium grey), and chloritized biotite (dark grey).

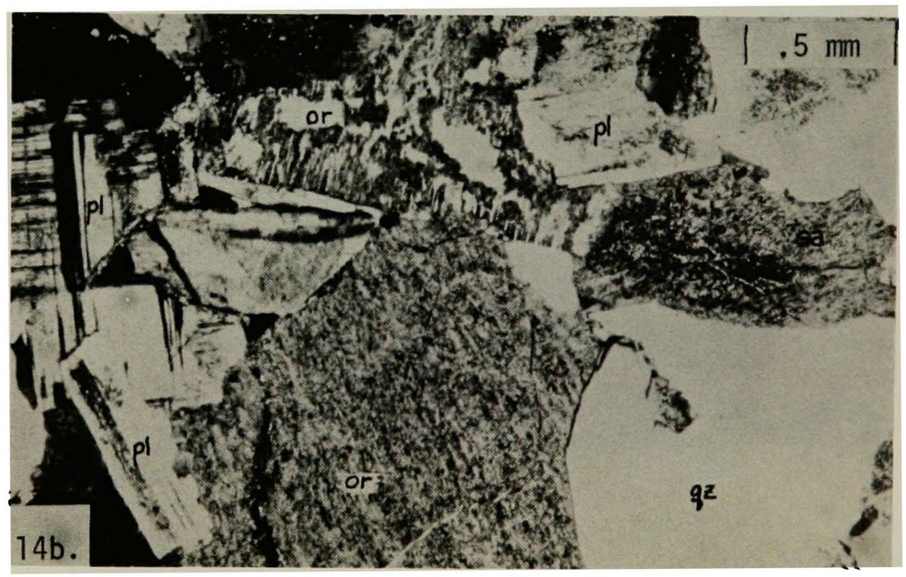

Figure 14b. Photomicrograph of equigranular Tg granite showing interlocking crystals of orthoclase (exsolving albite), twinned plagioclase, and quartz. X polars.

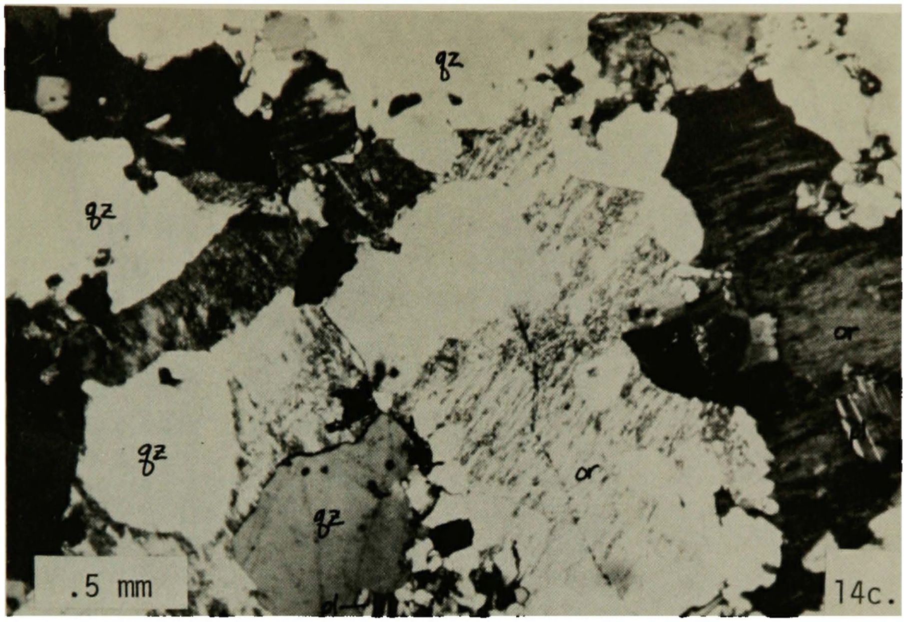

Figure 14c. Photomicrograph of Tg sample 120A showing bimodal size distribution of felsic crystals. Orthoclase exsolving albite. X polars.

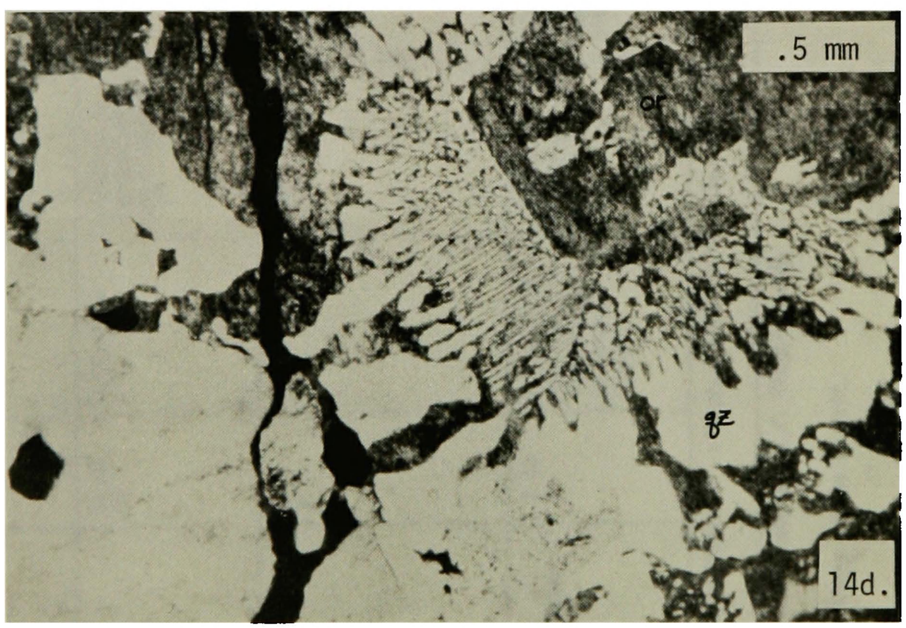

Figure 14d. Photomicrograph of Tg sample 265A showing micrograno-phyric intergrowths of orthoclase and quartz. X polars.

MINERAL/COLOR IN H.S.	% OF ROCK	GRAIN SIZE	GRAIN SHAPE	PROPERTIES	ALTERATION	TEXTURES/COMMENTS
Potassium feldspar pink, salmon, or buff	22 to 63	0.5--6 mm	anhedral to subhedral, with straight to irregular grain boundaries	absence of grid twinning suggests orthoclase	extensively altered to clays	Typically shows undulatory extinction. Perthitic exsolution is very well-developed, with albite exsolving as stringers and irregular blebs.
Quartz grey	23 to 50	0.25--3 mm	anhedral to rounded polygonal crystals	small anomalous 2V		Generally forms monomineralic glomerocrysts up to several mm diameter. Quartz-quartz grain boundaries are both crenate and polygonal. Abundant fluid inclusions. Undulatory extinction.
Plagioclase white	11 to 31	0.5--2 mm	euhedral laths	An_{20}--An_{32}* (oligoclase to andesine)	most crystals altering to clay; many have a thin (0.04mm) unaltered rim, even on xals which do not show concentric zonation	Well-developed albite and lesser pericline twinning. Forms glomerocrysts, which may also contain orthoclase and biotite and, very rarely quartz. Commonly concentrically zoned.
Biotite greenish-brown	.5 to 7	0.2--0.5 mm, generally in ragged clots of several flakes	slender to stubby euhedral laths	pleochroic, x'= greenish tan, z'= dark greenish brown	altered to chlorite + magnetite + sphene-- pervasive, but incomplete	Distinctive "ribbon texture"--many flakes appear to be shredded apart perpendicular to their cleavage planes.
Primary accessory minerals: zircon, apatite, fluorite, allanite						

* Centered bisectrix method (c.f. Tröger, 1958)

Table 5. Mineralogy of the Tg unit.

Textures. As a whole, rocks of the Tg unit are medium- to coarse-grained, with a massive interlocking texture (Figure 14). Both quartz and plagioclase form dominantly monomineralic clots reminiscent of volcanic glomerocrysts. Orthoclase appears to have begun crystallizing after quartz and plagioclase and fills interstices between the other minerals; in particular, orthoclase forms thin, macroscopically-visible "septa" between small quartz glomerocrysts. Plagioclase inclusions in orthoclase are uncommon. In contrast, thin, irregular rims of plagioclase on orthoclase crystals are very common. Whether this is a nucleation effect, indicating comtemporaneous or sequential crystallization of orthoclase and plagioclase, or a variety of exsolution, cannot be determined from the texture.

Two samples have textures distinctly different from the other five samples of this unit examined in thin section: Sample 120A is characterized by a pronounced bimodal size distribution of quartz, orthoclase, and plagioclase crystals (Figure 14). Large, 0.5 to 3 mm, subhedral to anhedral crystals are surrounded by an intricate intergrowth of very small (generally .1-.3 mm), almost bubble-shaped anhedral crystals. These fill interstices between the larger crystals, in a sense constituting the "matrix" of the rock. The margins of many larger crystals, particularly quartz, contain abundant inclusions of the small anhedral crystals. The texture suggests a two-stage crystallization history:

(1) slow crystallization of the corase crystals to produce a crystal mush, followed by (2) rapid crystallization of the matrix under conditions of reduced temperature, reduced vapor pressure, or both. Whereas the more normal equigranular granites are all immediately overlain by silicic volcanic rocks, sample 120A is from an area of granite which is separated from the quartzite country rock by intrusive porphyritic rhyolite and porphyritic fine-grained granite of the Tpr unit.

Sample 265A displays a very pronounced "micrographophyric" texture (Figure 14). This outcrop is not spatially-continuous with the main body of equigranular granites but may be connected to it at depth. Sphene in these rocks is both primary, as shown by a 5 mm-long, euhedral crystal with well-developed cleavage, and secondary (granular sphene associated with chloritization of biotite). The Tpr dike which cuts across this outcrop also shows a conspicuous graphic texture in thin section.

Interpretation. Textural, and to some extent mineralogical, features of the Tg granite show it to be an epizonal plutonic body, probably emplaced at depths of no more than approximately 6 km (Hyndman, 1972), and probably much less. These diagnostic features are: (1) miarolitic cavities; (2) a massive, dominantly equigranular texture; (3) the absence of observable contact metamorphic effects on the surrounding country rocks; and (4) the sharp boundary between the granite and the country rocks.

The Tg unit contains both potassium and plagioclase feldspar. Epizonal granites are normally characterized as hypersolvus, "one-feldspar" plutonic rocks (Figure 15a) in contrast to the "subsolvus", "two-feldspar" composition of deeper-seated granitic rocks (Figure 15b). Consideration of the phase diagram shows that this condition applies to rocks formed in the system $KalSi_3O_8$--$NaAlSi_3O_8$. Addition of even a small amount of calcium to the plagioclase structure results in the expansion of the solvus (Figure 15a) (Hyndman, pers. comm., 1980). Plagioclase in the Tg unit granites has the composition An_{20-32}; this is sufficient to alter the phase diagram and enable crystallization of two discrete feldspar phases.

Several petrographic features of these rocks appear to document late-stage "quenching" and movement of the nearly-solidified melt: (1) Biotite habitually occurs as bent or otherwise deformed flakes. These demonstrate internal movement of the granite after crystallization of both the biotite and the felsic crystals between which the biotite flakes are trapped. (2) Compositional zonation in most plagioclase crystals is shown by a diffuse concentric extinction and by the unaltered rim surrounding an altered core on many crystals. Such compositional zonation indicates cooling of the magma too rapidly to allow equilibration between crystals and residual melt. (3) The bimodal size distribution of crystals in sample 120 and the abundance of inclusions in the outer margins of large crystals in the same sample are disequilibrium textures reflecting rapid crystallization of interstitial melt.

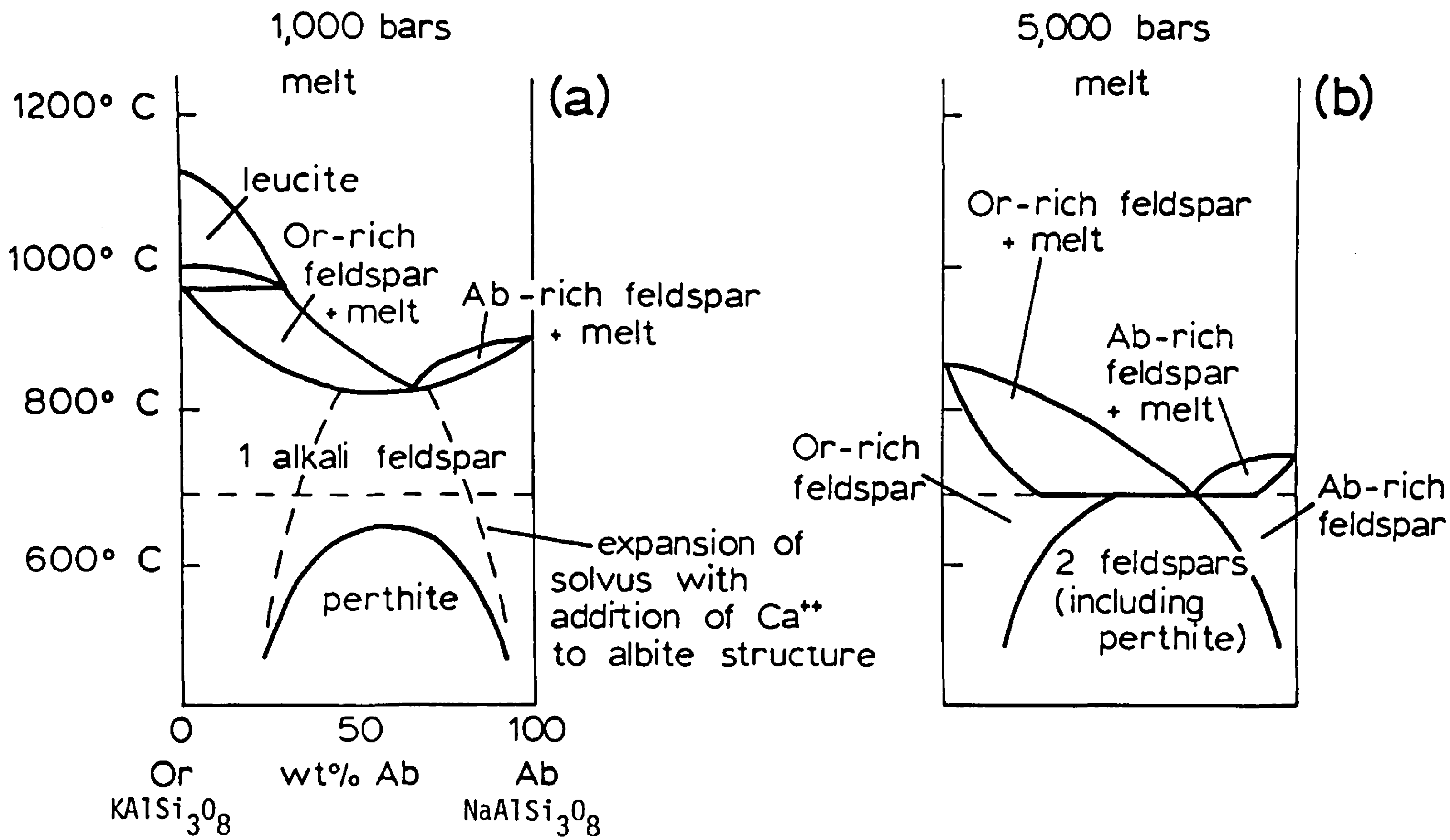

Figure 15. Binary phase diagrams for the system $KAlSi_3O_8$--$NaAlSi_3O_8$: (a) low-P_{H_2O} configuration; (b) high-P_{H_2O} configuration (modified from Hyndman, 1972, p. 18).

(4) The pronounced granophyric texture in sample 265A can be considered a product of rapid crystallization under a strong chemical or energy gradient (Spry, 1969; Barker, 1970), as for example, a sudden decrease in water or load pressure. (5) The distinctive "ribbon texture" (Table 5) of many biotite flakes might have resulted from a process such as hydration or expansion of contained water due to a sudden pressure release.

Intrusive Porphyritic Rhyolite and Porphyritic Fine-grained Granite, Undivided -- Tpr

Lithologies included in this unit were grouped together primarily on the basis of similarities in their texture and inferred origin. Where they are found in outcrop, these massive, porphyritic rocks show definite cross-cutting dike relationships to plutonic or quartzite country rocks. Out of 22 thin sections examined for this unit, 17 were of porphyritic rhyolite; the remainder were classifed as porphyritic fine-grained granites. Rhyolites grade into granites with increasing crystallinity of the groundmass (Figure 16). The terms "rhyolite" and "granite" are used here in a very general way to mean felsic igneous rocks containing phenocrystic and groundmass quartz, plagioclase, and sanidine; the dominant mafic mineral is biotite. The rocks contain highly variable amounts of the three felsic minerals and may have correspondingly variable compositions within the family of granitic rocks. Three samples, analysed by XRF, have the composition of high-silica

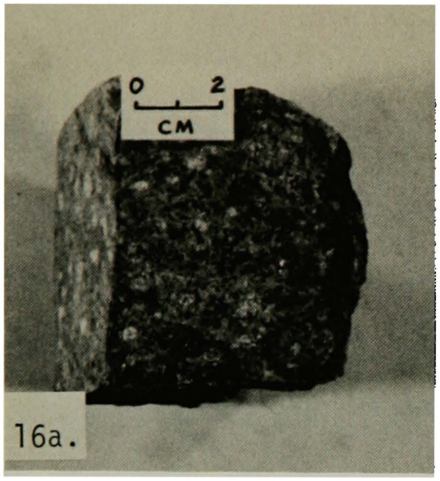

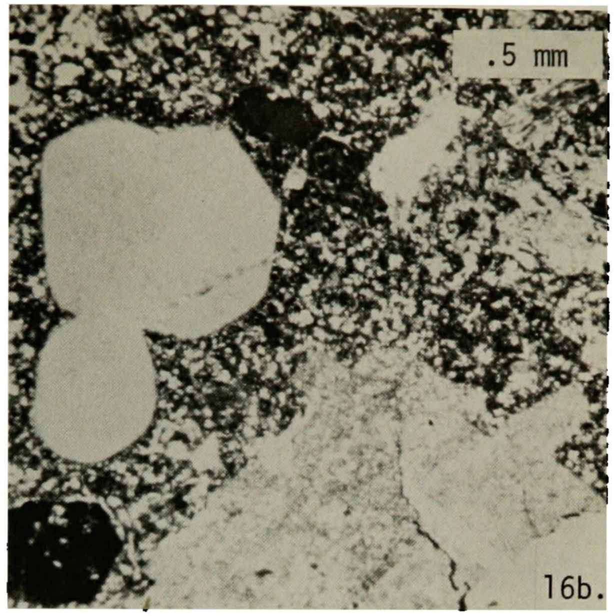

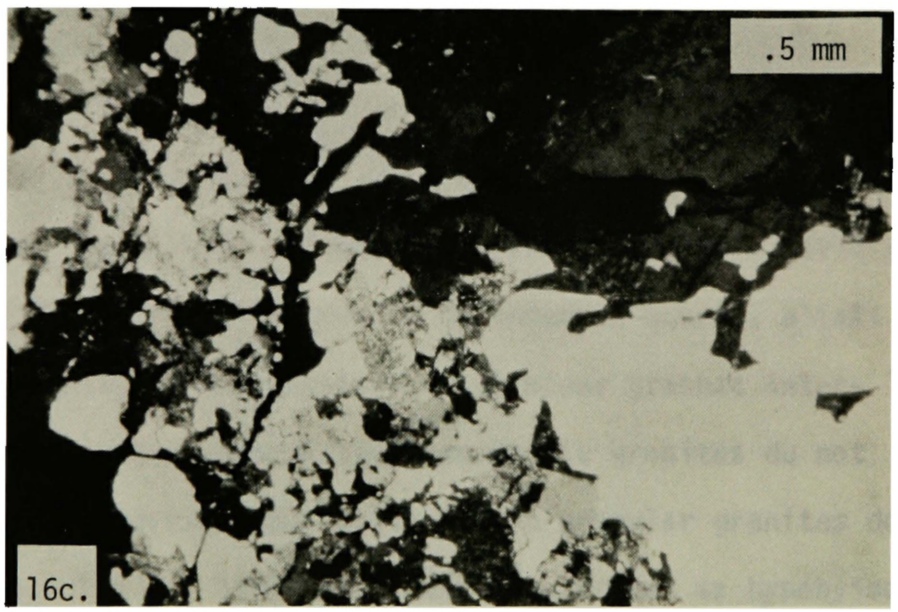

Figure 16a. Hand specimen photograph of Tpr porphyritic rhyolite. White spots are felsic phenocrysts, dark spots are chloritized biotite.

Figure 16b. Photomicrograph of Tpr porphyritic rhyolite. X polars.

Figure 16c. Photomicrograph of Tpr porphyritic fine-grained granite, showing granophyric intergrowth of sanidine (dark) and quartz (light). X polars.

rhyolites (Chapter III). With the exception of outcrops in the southeastern corner of the study area, rocks of this unit are found only on the ridges running north and east off Castle Rock Ridge (Plate 1). Table 6 summarizes the mineralogy of this unit.

Groundmass and textures. The groundmass in the rhyolites consists of very fine-grained intergrowths of alkali feldspar and a silica mineral. The intergrowths may take the form of (1) discrete patches, (2) massive felsite, very similar to the Tprc unit (see below) and (3) feathery spherulites, 0.25 - 0.5 mm diameter, which in many cases nucleate on phenocrysts. There is no evidence of phenocryst flow-orientation either in hand specimen or in thin section (Figure 16). In the granites, the groundmass forms (1) a dense spherulitic/granophyric intergrowth of quartz and alkali feldspar with rare miarolitic cavities, and (2) a granular "bubble-like" aggregate of anhedral quartz, alkali feldspar, and lesser plagioclase crystals, with minor graphic intergrowths. Phenocrysts in the spherulitic/granophyric granites do not show irregular grain boundaries, but those in the granular granites do.

Interpretation. The Tpr lithologies are interpreted as hypabyssal off-shoots of the Tg granite. Definite cross-cutting relationships are uncommon within the study area due to poor exposure but can be seen in outcrops in its far southeastern corner and north of Nez Perce Creek. In outcrop, the Tpr lithologies are most commonly found as rubble in areas underlain by either Tertiary granite or Precambrian quartzite.

MINERAL/COLOR IN H.S.	GRAIN SIZE	GRAIN SHAPE	ALTERATION	TEXTURES/COMMENTS
Quartz grey	0.5--3 mm	rhyolites: rounded to deeply embayed, with hexagonal outlines. granites: outer rims are irregularly indented in contact with groundmass		Crystals occur singly and in mono-mineralic glomerocrysts. Undulatory extinction is common.
Plagioclase off-white	0.5--2.5 mm, rarely to 8 mm	euhedral laths	commonly altered to clay, sericite, or carbonate--slightly to extensively altered	Albite twinning is common; Carlsbad is rare. Typically forms glomerocrysts, which may also contain sanidine or biotite. Grain boundaries in granites are irregular.
Sanidine buff to off-white	0.5--5 mm, ave. 1--2 mm	euhedral, slightly rounded	variably altered to clays; rarely to carbonates	Habitually shows Carlsbad twinning. Crystals typically fractured and show undulatory extinction. Grain boundaries in granites are irregular.
Biotite green	0.25--0.5 mm	euhedral stubby to elongate flakes	ubiquitously altered to chlorite and granular sphene	Occurs as chloritized masses with remnant pleochroic haloes around zircon inclusions. Chlorite shows anomalous blue interference colors.
Primary accessory minerals: zircon, magnetite, allanite, fluorite				

Table 6. Mineralogy of the Tpr unit.

Tpr rubble is only rarely found in areas underlain by volcanic rock; exceptions are a few localities on some of the ridges north of Castle Rock and east of Bare Cone.

The lithologies of the Tpr unit appear, then, to represent an approximately 1 km-thick sequence of closely-spaced hypabyssal dikes which form the "cap" of the Tertiary pluton in this area (Figure 17a). Similar porphyritic rocks may form the roof facies of the Casto pluton in the Challis volcanic field (Cater and others, 1973). Fiske and others, 1963, described a fine-grained porphyritic chill zone 100 or more meters thick adjacent to the roof of the Miocene Tatoosh pluton in Mt. Rainier National Park (Figure 17b). The granophyric groundmass displayed by some of their rocks is remarkably similar to that found in Tpr rocks in the study area. They attributed this texture to a sudden final crystallization that took place after most of the melt had solidified. This rapid crystallization may have followed a sudden loss of heat and volatiles brought on when the hypabyssal rocks vented to the surface (Fiske and others, 1963). The same effect (ie, rapid crystallization of interstitial melt) may also be achieved in a water-bearing magma by a sudden decrease in pressure with rapid uplift of the magma (Figure 18; Hyndman, ms). Biotite in Tpr rocks is much more highly chloritized than that in either the coarse-grained granites or the volcanic rocks. This might reflect a greater concentration of water and other volatiles in the roof zone of the pluton. As magma vented to the surface, the

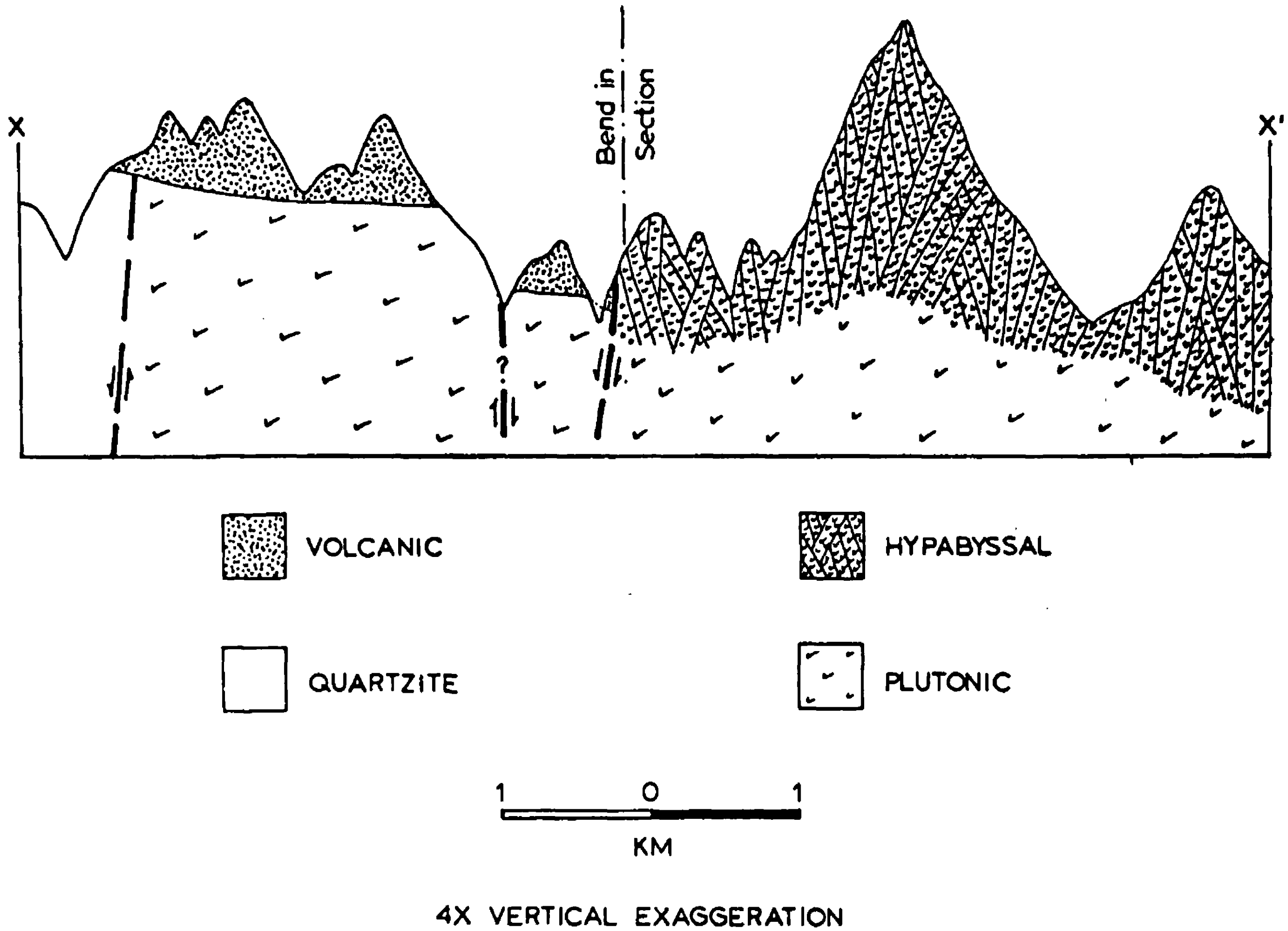

Figure 17a. Schematic cross section showing porphyritic "cap" of Painted Rocks pluton in study area. Section drawn along line X—X', Plate 2.

Symbols: Tdi, sills and dikes; Tg, granodiorite and related rocks; Tv, pyroclastic rocks; To, Ohanapecosh Formation; Ts, Stevens Ridge Formation; Tf, Fifes Peak Formation.

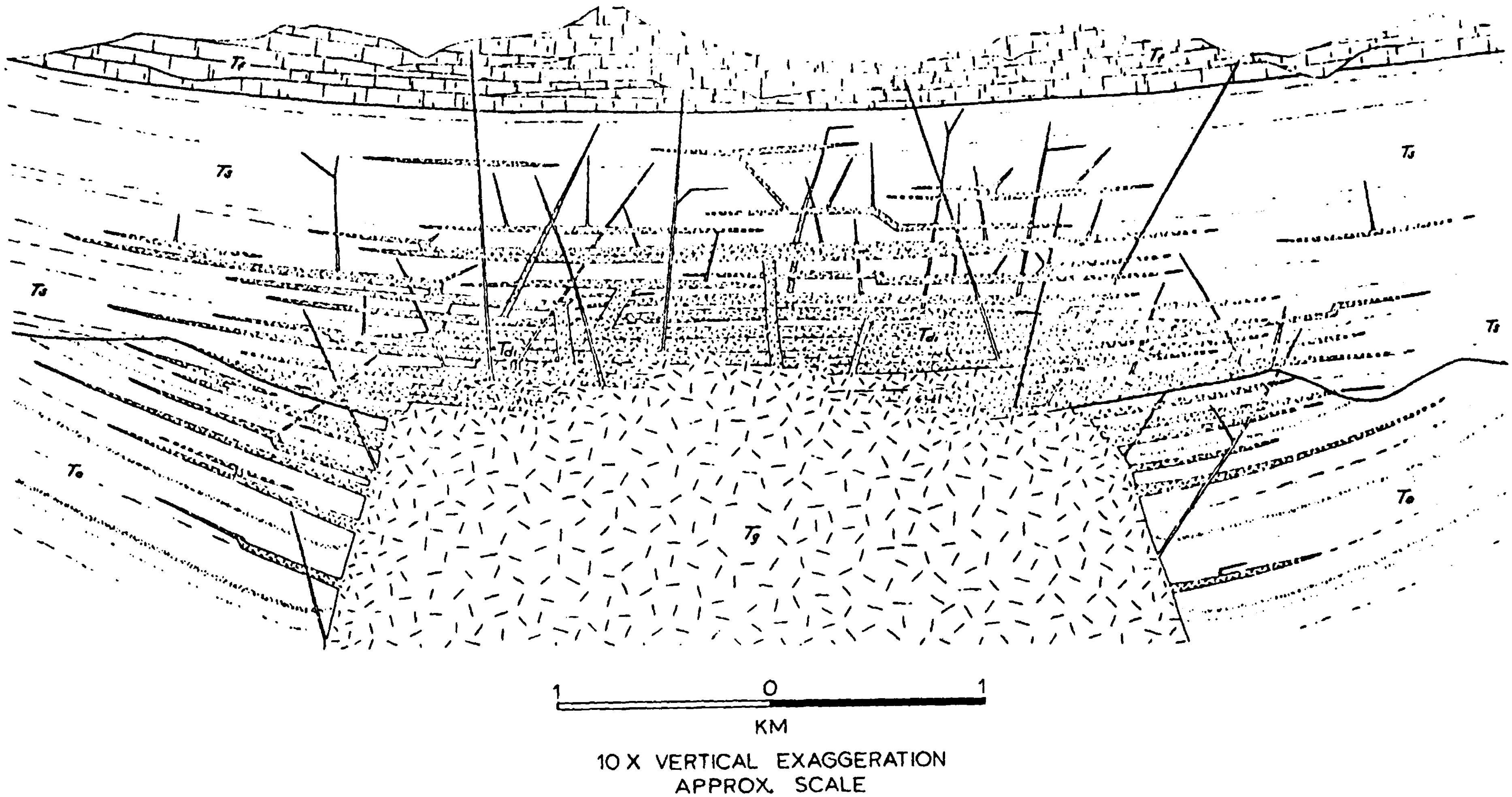

Figure 17b. Schematic cross section showing porphyritic "roof-zone" of the Tatoosh pluton, Mt. Rainier National Park (Fiske and others, 1963).

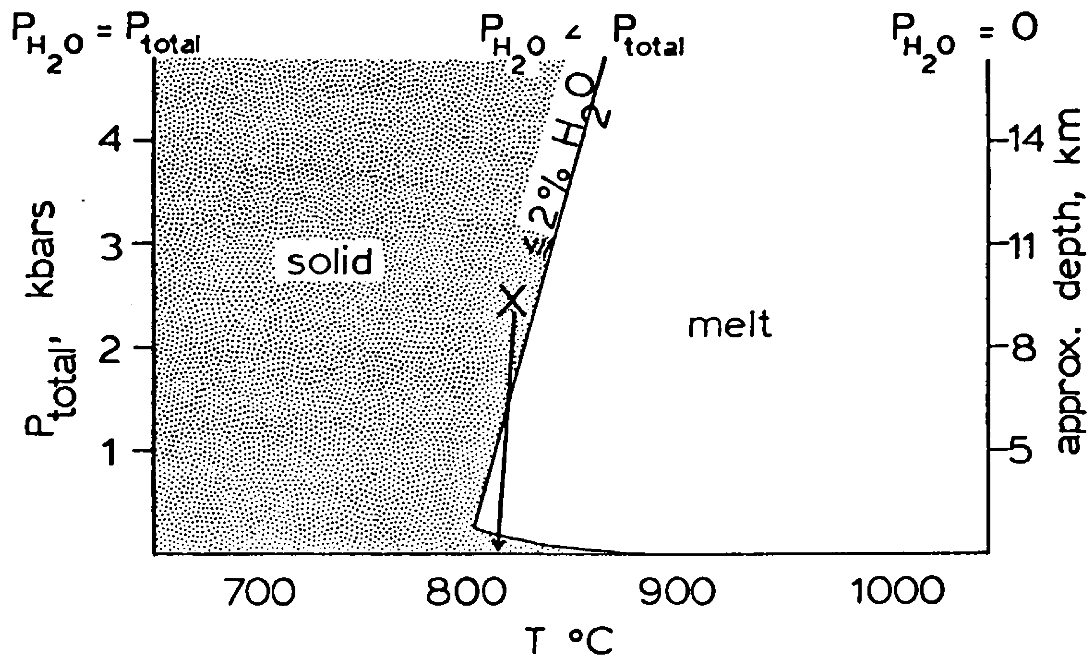

Figure 18. Pressure-temperature curve for water-bearing granitic magma, showing path of crystallization with decreasing P_{total}. Curve drawn for granitic magma containing ≦ 2% H_2O (Whitney, 1975) (modified from Hyndman, 1972, p. 70).

volatiles may have been rapidly lost, explaining the relatively unchloritized condition of the biotite in most of the volcanic units.

As mentioned above, Tpr rubble is rarely found in areas underlain by volcanic rocks. If the volcanic rocks constitute the country rock "roof" above the pluton, then there should be a wide zone of hypabyssal rocks separating granite from volcanic rocks, just as there is separating granite from quartzite on the ridges north of Bare Cone. Perhaps in those places where the hypabyssal "cap" is missing, the underlying pluton itself rose to shallow levels, engulfing its porphyritic chilled border zone as a foundered stope block (Figure 17a).

The granite and dike rocks may be essentially coeval. Both gradational and intrusive contacts between equigranular and porphyritic rocks are very well displayed along the Nez Perce Fork-Magruder Corridor road immediately north of the study area. The top of a pluton which is subject to venting to the surface is presumably an area of rapid and irregular fluctuations of lithostatic load, water pressure, and the volatile content of the differentiating magma. The interplay of these various fluctuations could create the complex relationship of porhyritic and eqigranular rocks seen within the study area.

Intrusive Porphyritic Rhyolite of Castle Rock--Tprc

This unit crops out as a small plug, Castle Rock, and at least three nearby related dikes. Outcrops are characterized by resistant, almost vertical cliffs with strong vertical and less distinct subhorizontal jointing (Figure 19a). Weathered surfaces show iron- and

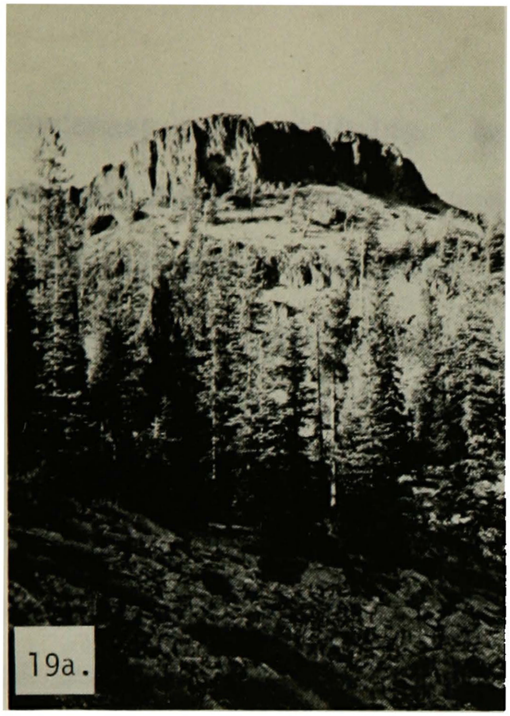

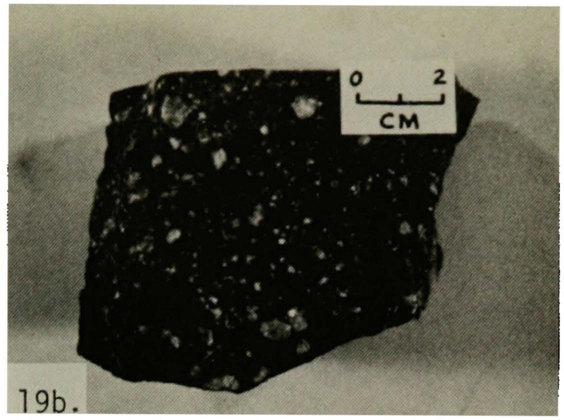

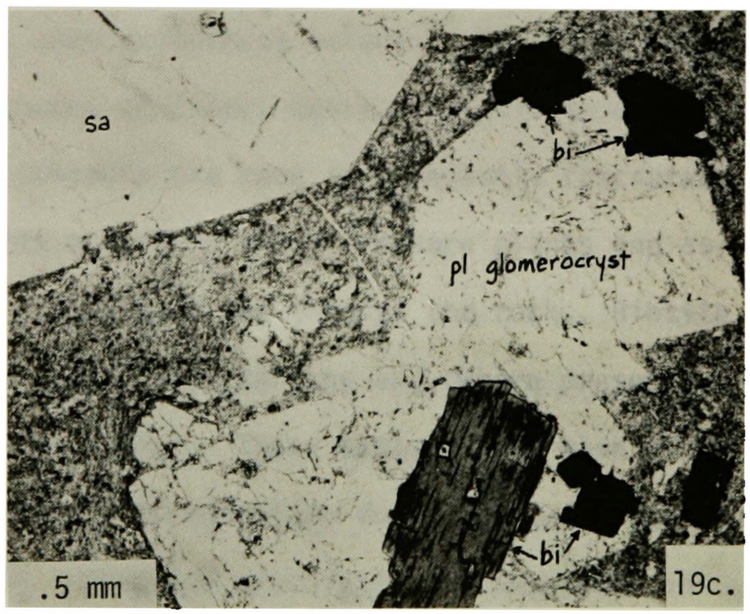

Figure 19a. Photograph of Castle Rock plug, taken from vicinity of sample locality 23-50-300.

Figure 19b. Hand specimen photograph of Tprc rhyolite. Large white phenocrysts are mostly sanidine.

Figure 19c. Photomicrograph of Tprc rhyolite showing phenocrysts in a devitrified felsite groundmass.

manganese-oxide staining. In outcrop, the rock is a massive, biotite-plagioclase-quartz-sanidine porphyritic rhyolite with a dense, grey-purple aphanitic groundmass (Figure 19b). A weak flow(?) banding is rarely seen in the groundmass but phenocryst orientation was not seen in hand specimen or in thin section. Relative and absolute percentages of phenocryst minerals may vary considerably, even over a distance of only a few meters. Phenocryst size is likewise variable, but in general the coarse grain size of the phenocrysts is a prominent feature of this lithology.

Near contacts with the country rocks, the dikes are brecciated and hydrothermally altered. The groundmass becomes irregularly banded or swirled and colored in shades of lilac, ochre, and buff as a result of alteration. Near these contacts the rock is abundantly fractured, with silicified microbreccias occurring along fracture planes and as wispy trains of comminuted crystals waving through the rock. Biotite is generally absent in these brecciated margins and, where present, is extensively altered to iron oxides. These textures may have been produced by volatile-streaming or fluidization during dike emplacement (Myers, 1975; Pitcher, 1978). In-place brecciation, represented in thin section by a "jig-saw puzzle fit" of broken crystals, apparently documents late-stage movement of the almost-solidified dike. A similar origin would explain the abundant slickensides observed in rubble from the outer edges of the Castle Rock plug. Open spaces in the breccias are coated with drusy rinds of tiny (0.025 mm) terminated quartz crystals. These may have formed as a low-temperature inversion of an original vapor-phase mineral such as tridymite (Ross and Smith, 1961). Table 7 summarizes the mineralogy of this unit.

Groundmass and textures. As with the Tmf unit, the groundmass of Tprc rocks consists of a massive intergrowth of quartz and alkali feldspar devitrification products (Figure 19c). The original groundmass was presumably glassy, perhaps with a few trains of tiny microlites; two samples show what may be remnant trachytic texture, and what appear to be remnant perlitic cracks in a now-devitrified groundmass.

Interpretation. The intrusive nature of the lithology is readily seen in outcrop. Castle Rock itself is a Tprc plug approximately 250 m in diameter (Plate 1). It is surrounded on all sides by a "skirt" of blocky talus but discontinuous outcrops of epiclastic tuffaceous(?) conglomerate completely encircle the rock. Xenoliths of this epiclastic material can be found in the Castle Rock plug and the Tprc dike to the west. The conglomerate in these xenoliths is extremely silicified, and appears to have been "fused", either by conduction of heat from the surrounding intrusion or by lowering of its melting temperature as intergranular water was converted to steam (Williams and McBirney, 1979, p. 137-138).

Williams (1932) distinguished between volcanic domes which are "exogenous" and formed by surface effusion of lava from a central vent, and those which are "endogenous" and formed by continued addition of

MINERAL/COLOR IN H.S.	% OF ROCK	GRAIN SIZE	GRAIN SHAPE	PROPERTIES	ALTERATION	TEXTURES/COMMENTS
Quartz grey	7 to 11	0.5--3 mm, ave. 1.5 mm	rounded embayed crystals with remnant hexagonal outlines	slight anoma-2V		Undulose extinction; uncommonly forms glomerocrysts.
Sanidine glassy to buff	4 to 18	0.5--3 mm, rarely to 8 mm	euhedral to subhedral, may be rounded or embayed			Well-developed Carlsbad twinning can be seen in hand specimen. May form monomineralic glomerocrysts. Undulatory extinction; zonally-arranged inclusions of plagioclase and biotite in some larger crystals. Fairly commonly shows zoned extinction.
Plagioclase glassy	3 to 9	0.5--2 mm	euhedral laths	An_{23}--An_{40}* (oligoclase to andesine)	sericite	Commonly forms glomerocrysts which may contain biotite or sanidine. Highly fractured, particularly in cores. Concentrically zoned, with well-developed albite twinning; Carlsbad twinning also occurs.
Biotite black	2	0.2--1 mm	euhedral laths and basal sections	pleochroic, x'= blond-brown, z'= dark brown	very fresh	Zircon inclusions are rare, and do not all create pleochroic haloes
Primary accessory minerals: zircon, apatite, magnetite						

* Centered bisectrix method (c.f. Tröger, 1958)

Table 7. Mineralogy of the Tprc unit.

magma and expansion from within, generally beneath an overlying layer. Endogenous domes may be later exposed by erosion. Various features of the Castle Rock plug may be cited in support of either of these modes of formation. As seen today, Castle Rock occupies a topographic high. This is in part due to the more resistant nature of the Tprc lithology, but could also be a reflection of the original exogenous nature of the plug. If the Castle Rock plug is exogenous, its flat top could be an original feature, or it might be due partly to contraction and partly to reduction of volatile pressure during the closing stages of intrusion (Williams, 1932). On the other hand, jointing, which is a prominent feature of Castle Rock, is best developed in endogenous domes (Williams, 1932). However, jointing in endogenous domes is generally vertical, and either radiating or concentric. The dominant joint sets in Castle Rock are vertical, but their trend varies through only a small angle (Figure 20). The fact that the jointing does not continue into the surrounding rocks indicates that this feature probably resulted from cooling or pressure-release during the late stages of intrusion and solidification of the plug, rather than at some later time.

In texture and mineralogy, the rhyolite of Castle Rock is not significantly different from lithologies in the Tpr unit. The main petrographic difference between the two units is the greater degree of alteration in Tpr rocks. If Castle Rock and its related dikes vented to the surface, volatile constituents would have escaped. Perhaps in the wholly(?) intrusive Tpr dikes these volatiles were "sealed in" and allowed to react with earlier-formed phenocryst minerals.

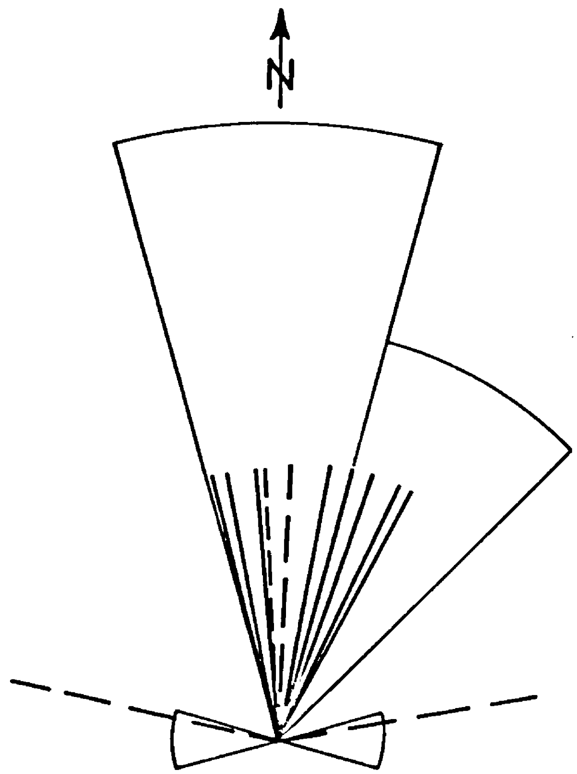

— — — sub-horizontal joints (≤ 35°, ave. 22° dip)

———— high-angle joints (= 55°, ave. 79° dip)

Figure 20. Rose diagram plotting trends of joints from Castle Rock plug.

Unconsolidated Deposits, Undivided--Qu

Quaternary deposits consist of morainal material, possible lake sediments in a few localities (Winegar, 1974), and alluvium.

Talus--Qt

This unit designation is applied to trains of blocky rubble of mappable extent, which can be traced to bedrock outcrops. Both of these criteria are met only by the thick skirt of blocky talus eroded off the steep walls of the Castle Rock plug. Bedrock units crop out through this cover in only a few places.

Summary

The bedrock units in the study area can be grouped into three general categories: (1) the Precambrian quartzite country rock; (2) intrusive granitic rocks, comprising the Tpr hypabyssal dike rocks and the Tg granite with its included blocks of Idaho batholith rock; and (3) the Castle Rock volcanics. The hypabyssal intrusive rhyolite of Castle Rock is included in the last category because of its definite cross-cutting relationship to the volcanics, and because of the possibility that it may have vented to the surface.

The extrusive units of the Castle Rock volcanics consist primarily of rhyolite lava flows, with subordinate pyroclastic deposits. The significance of this fact is discussed in Chapter V, but presumably it reflects the relatively low volatile content of the parent magma. A similar low volatile content in the Tg granite magma is indicated by the small size of miarolitic cavities, by the absence of contact metamorphic effects, and by the fact that the body was able to rise to within less than 1,000 m of the surface, judging from the thickness of the volcanic cover within the study area.

The Castle Rock volcanics and the subjacent plutonic rocks have a similar mineralogy, are coeval, and occur together in close spatial proximity. The parent magma for each group of lithologies was a relatively low-volatile granitic melt. Chapter III presents the chemical data for these rocks and discusses the implications of their observed similarities.

CHAPTER III

WHOLE-ROCK CHEMISTRY

Table 8 gives whole-rock chemical analyses for 22 intrusive and extrusive rocks: 15 samples from within the study area, 5 for comparison from areas on its margin, and 2 replicate samples. All are X-ray fluorescence analyses performed by the Department of Geology, Washington State University . Also given are the compositions for Nockold's (1954) average calc-alkaline granite and calc-alkaline rhyolite, and values for the 5 USGS standards run with the rocks of this study. Agreement of replicated samples and standards (both run as unknowns) is very good. Normative minerals for the study area rocks were calculated using a computer program from Dartmouth College.

With one exception, all samples contain greater than 66% silica, and may be classified as acidic or felsic igneous rocks (Figure 21). Sample 283, with 63.14% silica, would be classified as intermediate; the rock was described in the field as an andesite. Sample 270B, with the next-lowest silica value, 68.9%, was also mapped as an andesite; its higher silica value may be the result of quartz-filled amygdules. Sample 269A shows an abnormally high silica value of 80.89%; in hand specimen this rock shows evidence of secondary silicification. Because of their suspect nature, the analyses for samples 269A and 270B will not be utilized in the following discussion. Samples 159 and 206 are

Table 8a. Whole-rock XRF chemical analyses of study area rocks.

	22A Tprc	176B Tprc	54A Tvc	83A Tvc	303A Tvc	66A Tlf	70A Tt	260A Tmf	279A Tmf	85A Tpr	106A Tpr	146C Tpr
SiO_2	77.60	78.16	73.22	77.92	76.23	71.44	74.95	69.20	73.66	77.01	76.98	78.70
TiO_2	0.13	0.13	0.27	0.06	0.12	0.22	0.26	0.29	0.24	0.11	0.16	0.08
Al_2O_3	12.22	12.31	14.66	12.71	13.35	15.74	14.10	16.49	14.50	12.91	13.08	12.99
FeO (1)	1.18	0.73	1.52	0.46	1.05	2.38	1.44	1.73	1.61	1.24	1.24	0.28
MnO	0.02	0.01	0.03	0.01	0.03	0.02	0.02	0.02	0.03	0.01	0.00	0.00
MgO	0.20	0.19	0.41	0.09	0.39	0.23	0.44	0.43	0.46	0.13	0.17	0.12
CaO	0.27	0.56	1.47	0.23	0.90	1.48	1.64	1.14	1.19	0.28	0.39	0.39
Na_2O	2.41	2.95	3.23	3.21	3.03	3.57	1.28	3.14	3.07	3.43	3.01	2.36
K_2O	5.92	4.91	5.10	5.26	4.88	4.82	5.79	7.44	5.15	4.76	4.93	5.04
P_2O_5	0.05	0.04	0.09	0.04	0.02	0.08	0.07	0.11	0.09	0.03	0.05	0.03
Total	100.00	99.99	100.00	99.99	100.00	99.98	99.99	99.99	100.00	99.91	100.01	99.99

	159A Tg	206A Tg	253C Ttc	269A Tprs	270B Tvs	283A Tvu	286A Tvu	293A Tvu	70A(2) Tt	260A(2) Tmf
SiO_2	73.01	75.81	74.78	80.89	68.99	63.14	78.67	76.69	74.61	69.29
TiO_2	0.27	0.13	0.24	0.14	0.83	0.78	0.08	0.09	0.26	0.29
Al_2O_3	14.58	13.51	14.84	11.86	14.37	18.43	11.98	12.98	14.22	16.43
FeO	2.10	1.16	1.12	0.16	5.24	4.63	0.75	0.55	1.46	1.74
MnO	0.04	0.02	0.02	0.01	0.04	0.07	0.01	0.64	0.02	0.02
MgO	0.16	0.21	0.28	0.20	2.10	0.44	0.20	0.28	0.49	0.54
CaO	0.26	0.66	1.96	0.00	0.54	2.49	0.01	0.17	1.51	1.13
Na_2O	3.61	3.50	1.91	0.40	0.82	4.14	3.43	2.61	1.43	3.06
K_2O	5.91	4.95	4.79	6.39	6.63	5.61	4.82	5.96	5.94	7.41
P_2O_5	0.06	0.04	0.05	0.04	0.38	0.28	0.04	0.04	0.06	0.10
Total	100.00	99.99	99.99	100.09	99.94	100.01	100.09	100.00	100.00	100.01

(1) Total iron reported as FeO

(2) Replicate sample

	SiO_2	Al_2O_3	TiO_2	Fe_2O_3	FeO	MnO	CaO	MgO	K_2O	Na_2O	P_2O_5
BCR1(378)	55.04	13.92	2.19	6.02	6.89	0.18	6.87	3.27	1.82	3.43	0.37
BCR1	55.28	13.90	2.19	5.95	6.81	0.18	6.93	3.16	1.79	3.44	0.36
BCR1(Given)	55.05	13.79	2.26	6.04	6.92	0.19	7.02	3.32	1.69	3.35	0.37
AGV1(378)	60.35	17.43	1.08	3.13	3.59	0.10	5.07	1.48	3.08	4.20	0.49
AGV1	60.25	17.31	1.07	3.22	3.69	0.10	5.04	1.58	3.07	4.18	0.49
AGV1(Given)	60.36	17.40	1.11	3.05	3.50	0.09	5.09	1.53	2.96	4.43	0.49
GSP1(378)	67.79	15.39	0.69	1.98	2.27	0.04	2.14	1.09	5.44	2.88	0.29
GSP1	67.79	15.35	0.68	1.92	2.20	0.04	2.13	1.17	5.43	3.01	0.29
GSP1(Given)	68.05	15.40	0.67	1.93	2.21	0.04	2.04	0.97	5.59	2.83	0.28
G2(378)	69.84	15.71	0.50	1.19	1.36	0.03	1.69	0.93	4.60	4.00	0.15
G2	69.69	15.58	0.50	1.17	1.34	0.03	2.02	0.86	4.56	4.10	0.14
G2(Given)	69.45	15.48	0.51	1.42	1.63	0.03	1.95	0.77	4.54	4.09	0.14
PCC1(378)	44.28	0.73	0.00	3.85	4.42	0.12	0.53	46.06	0.00	0.00	0.00
PCC1	44.48	0.76	0.00	3.87	4.43	0.12	0.54	45.79	0.00	0.00	0.00
PCC1(Given)	44.26	0.78	0.02	4.03	4.61	0.13	0.54	45.61	0.01	0.01	0.00

Table 8b. Values for U.S.G.S. standards run as unknowns with study area samples. All analyses normalized on a volatile-free basis, with Fe recorded as 44% Fe_2O_3 and 56% FeO.

	(I)	(II)
SiO_2	72.08	73.66
TiO_2	0.37	0.22
Al_2O_3	13.86	13.45
FeO	2.53	2.00
MnO	0.06	0.03
MgO	0.52	0.32
CaO	1.33	1.13
Na_2O	3.08	2.99
K_2O	5.46	5.35
H_2O^+	0.53	0.78
P_2O_5	0.18	0.07
Total	100.00	100.00

(I) ave. calc-alk granite

(II) ave. calc-alk rhyolite + rhyolite-obsidian

Table 8c. Chemical compositions of average calc-alkaline granite and rhyolite + rhyolite-obsidian. Values from Nockolds, 1954.

	22A	176B	54A	83A	303A	66A	70A	260A	279A	85A	106A	146C
Quartz	39.97	40.75	31.20	38.53	37.27	28.47	41.18	19.46	32.86	37.88	39.46	44.75
Corundum	1.49	1.23	1.39	1.42	1.50	2.17	2.93	1.49	1.95	1.69	2.22	3.02
Orthoclase	34.98	29.01	30.14	31.08	28.84	28.48	34.21	43.96	30.43	28.13	29.13	29.78
Albite	20.39	24.96	27.33	27.16	25.64	30.21	10.83	26.57	25.98	29.02	25.47	19.97
Anorthite	0.98	2.49	6.64	0.85	4.32	6.77	7.63	4.86	5.26	1.17	1.58	1.72
Enstatite	0.50	0.47	1.02	0.22	0.97	0.57	1.10	1.07	1.15	0.32	0.42	0.30
Ferrosilite	0.52	0.24	0.51	0.21	0.48	1.09	0.47	0.58	0.62	0.57	0.47	0.04
Magnetite	0.80	0.49	1.03	0.30	0.71	1.61	0.97	1.17	1.09	0.84	0.84	0.19
Ilmenite	0.25	0.25	0.51	0.11	0.23	0.42	0.49	0.55	0.46	0.21	0.30	0.15
Hematite	--	--	--	--	--	--	--	--	--	--	--	--
Rutile	--	--	--	--	--	--	--	--	--	--	--	--
Apatite	0.12	0.09	0.21	0.09	0.05	0.19	0.17	0.26	0.21	0.07	0.12	0.07

	159A	206A	253C	269A	270B	283A	286A	293A	70A(rep.)	260A(rep.)
Quartz	28.39	34.67	40.74	53.81	34.78	11.75	39.83	37.78	39.56	19.95
Corundum	1.93	1.30	3.08	4.29	5.84	1.76	1.12	2.03	2.85	1.58
Orthoclase	34.92	29.25	28.30	37.76	39.18	33.15	28.48	35.22	35.10	43.79
Albite	30.54	29.61	16.16	3.38	6.94	35.03	29.02	22.08	12.10	25.89
Anorthite	0.86	2.99	9.36	--	--	10.34	--	0.56	7.06	4.89
Enstatite	0.40	0.52	0.70	0.50	5.40	1.10	0.50	0.70	1.22	1.34
Ferosilite	0.88	0.51	0.31	--	1.83	1.59	0.33	0.57	0.48	0.60
Magnetite	1.42	0.78	0.75	--	3.54	3.13	0.51	0.80	0.99	1.17
Ilmenite	0.51	0.25	0.46	0.21	1.58	1.48	0.15	0.17	0.49	0.55
Hematite	--	--	--	0.07	--	--	--	--	--	--
Rutile	--	--	--	0.03	--	--	--	--	--	--
Apatite	0.14	0.09	0.12	0.09	0.90	0.66	0.09	0.09	0.14	0.24

Table 8d. Normative mineral content, in weight %, of study area samples; analyses listed in Table 8a.

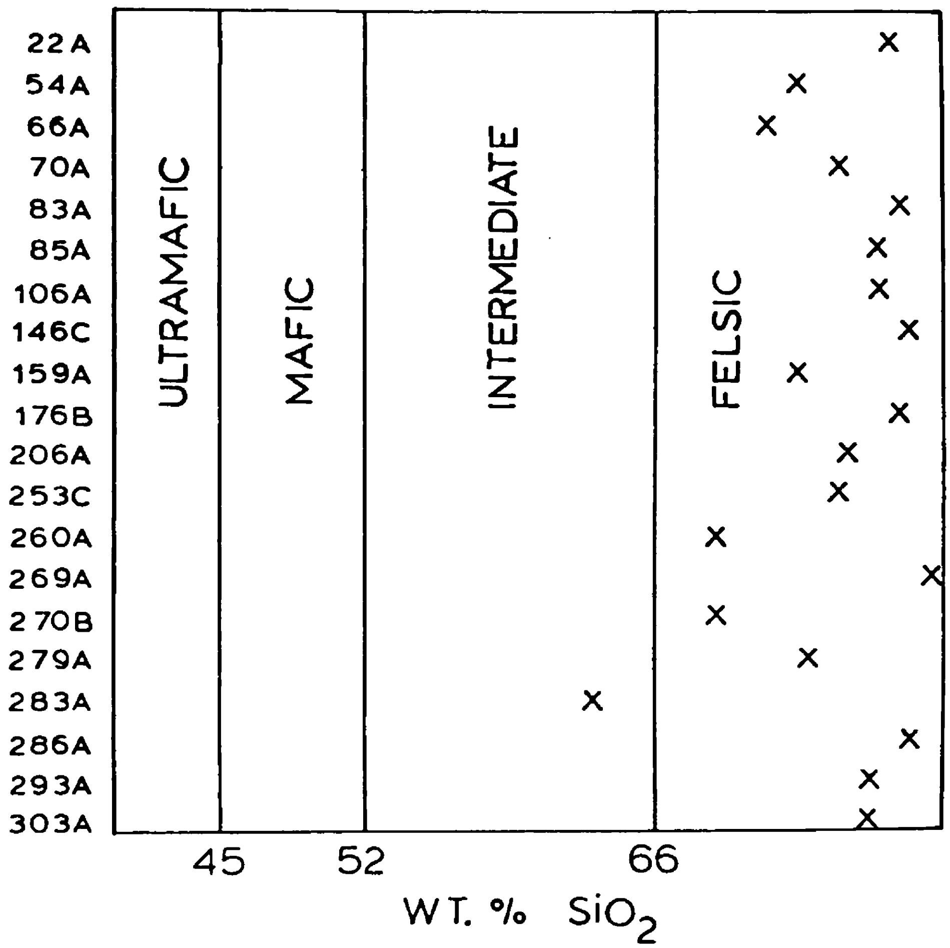

Figure 21. Silica percentages of analysed samples. Values from Table 8.

coarse-grained plutonic rocks of the Tg unit which by virtue of their silica contents would be classified as granites. This is substantiated by the results of point counts.

The remaining fifteen felsic rocks consist of extrusive flows and tuffs, and porphyritic intrusive dike rocks. Of these, two contain silica in the range 65-72%, five contain 72-76% silica, and eight contain silica in excess of 76%. These divisions correspond to the "quartz latite", "low-silica rhyolite", and "high-silica rhyolite" categories used by Byers and others (1976) for rocks of the Timber Mountain-Oasis Valley caldera complex of southern Nevada. There is considerable disagreement in the literature regarding the meaning of the term "quartz latite". In older classifications, "quartz latite" refers to a felsic volcanic rock containing plagioclase as 1/3 to 2/3 of the total feldspar and having greater than 10% quartz (Peterson, 1961). However, Streckeisen (1979) has recently redefined "quartz latite" to mean a volcanic rock containing these same proportions of alkali and plagioclase feldspars, but having 5-20% modal quartz. In order to avoid confusion in nomenclature, those rocks containing silica in the range 65-76% are referred to in this report as "low-silica rhyolites" and those containing greater than 76% silica are called "high-silica rhyolites". Figure 22 shows all fifteen low- and high-silica rhyolites plotted on Church's (1975) triaxial classification diagram for volcanic rocks.

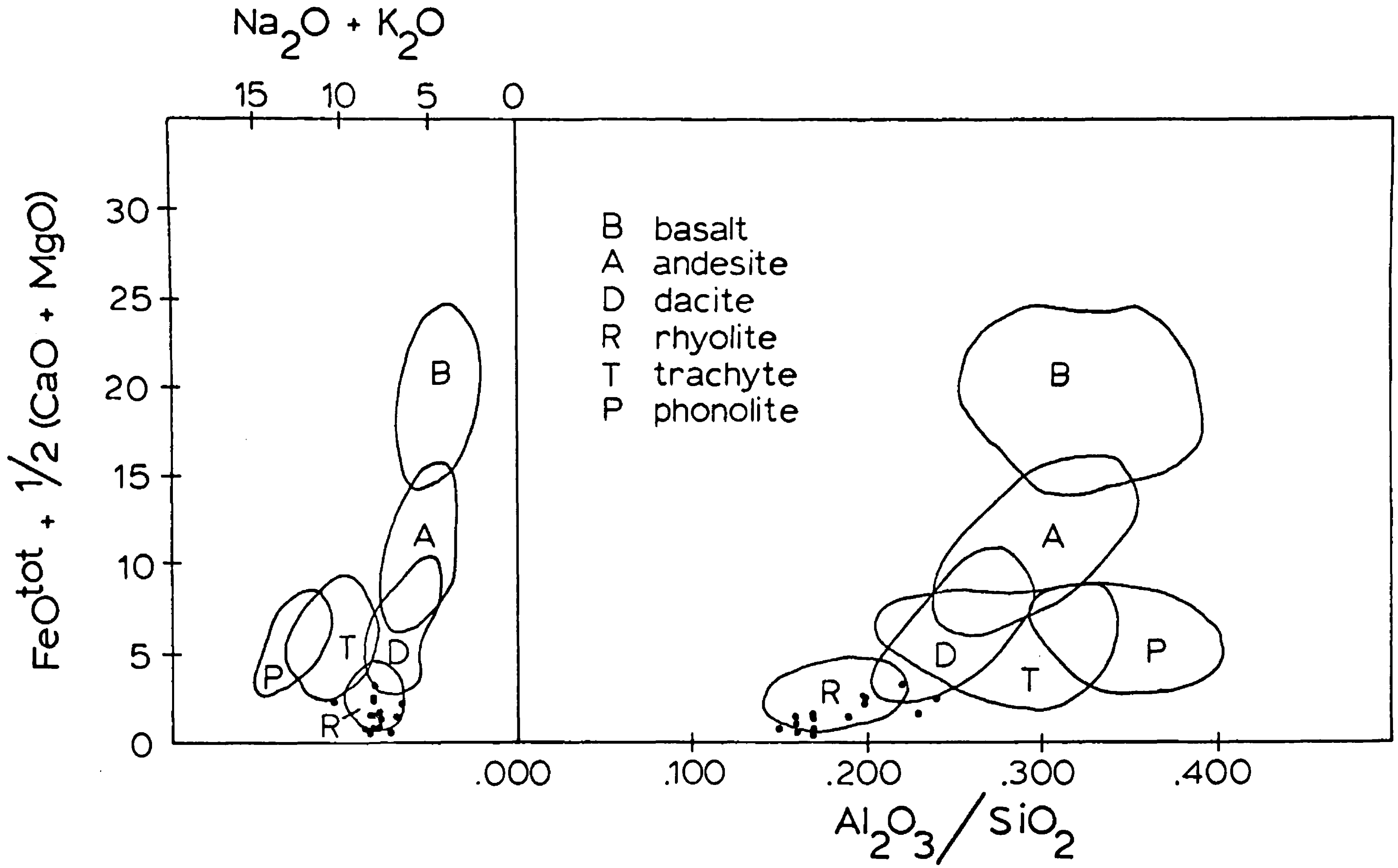

Figure 22. Composition of high- and low-silica rhyolites of the Castle Rock volcanics. Values from Table 8 (classification of Church, 1975).

Examination of Table 8 reveals an interesting compositional distinction between the hypabyssal, plutonic, and volcanic rock-groups. All six hypabyssal rocks contain greater than 76% silica--they are all high-silica rhyolites, as might be expected from lithologies representing the highly-differentiated "cap" of a granitic pluton. Both coarse-grained granite samples contain less than 76% silica.

In contrast to the fairly restricted range of silica contents exhibited by the hypabyssal rocks, the extrusive rhyolites show a range of silica values from 78.5% to 69.2%. Such variability might result from several factors, including: (1) original silica variations within the magma chamber. Tapping different levels of a compositionally-zoned magma chamber could produce different silica contents in the resultant volcanic rocks (Smith, 1960; Lipman and others, 1966; Hildreth, 1979; Smith, 1979). The same effect would follow from tapping the same level in the magma chamber, but at different times. (2) varying amounts and species of phenocryst minerals in the volcanic rocks. Crystal settling and incorporation of xenocrysts could produce eruptive rocks have a range of compositions. (3) post-eruptive processes such as flow-concentration and density sorting. These mechanisms would affect the phenocryst content of the rocks, and as a consequence, their chemical composition as well. (4) variability in porosity and permeability of the volcanic rocks. As a result, their susceptibility to alteration and leaching of various constituents would likewise be highly irregular. As a corollary, the hypabyssal rocks show a tight grouping with respect to their contents of silica and many of the other oxides; this could follow from their uniformly dense nature and consequently enhanced resistance to alteration. This topic is discussed further below.

Figure 23 is a variation diagram of silica plotted against nine other oxides for the eighteen reliable analyses given in Table 8. Replicate samples and U.S.G.S. standards were not plotted. Elements which form linear trends on such diagrams are considered to have a common derivation along the liquid line of descent (Wilcox, 1979; Hyndman, ms)--ie, they are cogmamatic. Inspection of Figure 23 shows that for TiO_2, Al_2O_3, FeO^{tot}, MnO, and P_2O_5 the intrusive and extrusive rocks plot on just such a tight linear trend.

In contrast, the plots for MgO, CaO, Na_2O, and K_2O show moderate fit for the hypabyssal rocks, but considered scatter for the volcanic samples. The plot of K_2O versus silica forms an essentially flat line, with virtually no correlation between K_2O content and silica percentage.

I believe that the lack of tight fit on these four variation diagrams is best explained as the result of syn- or post-emplacement hydrothermal alteration, which affected the porous volcanic rocks to a greater degree than their denser intrusive equivalents.

Discussion of Alteration Mineralogy and Reactions

Hydrothermal alteration is essentially a metasomatic process involving the addition and removal of constituents from a rock and its

Figure 23. Variation diagram. Values from Table 8.

▲ Volcanic

● Hypabyssal

■ Plutonic

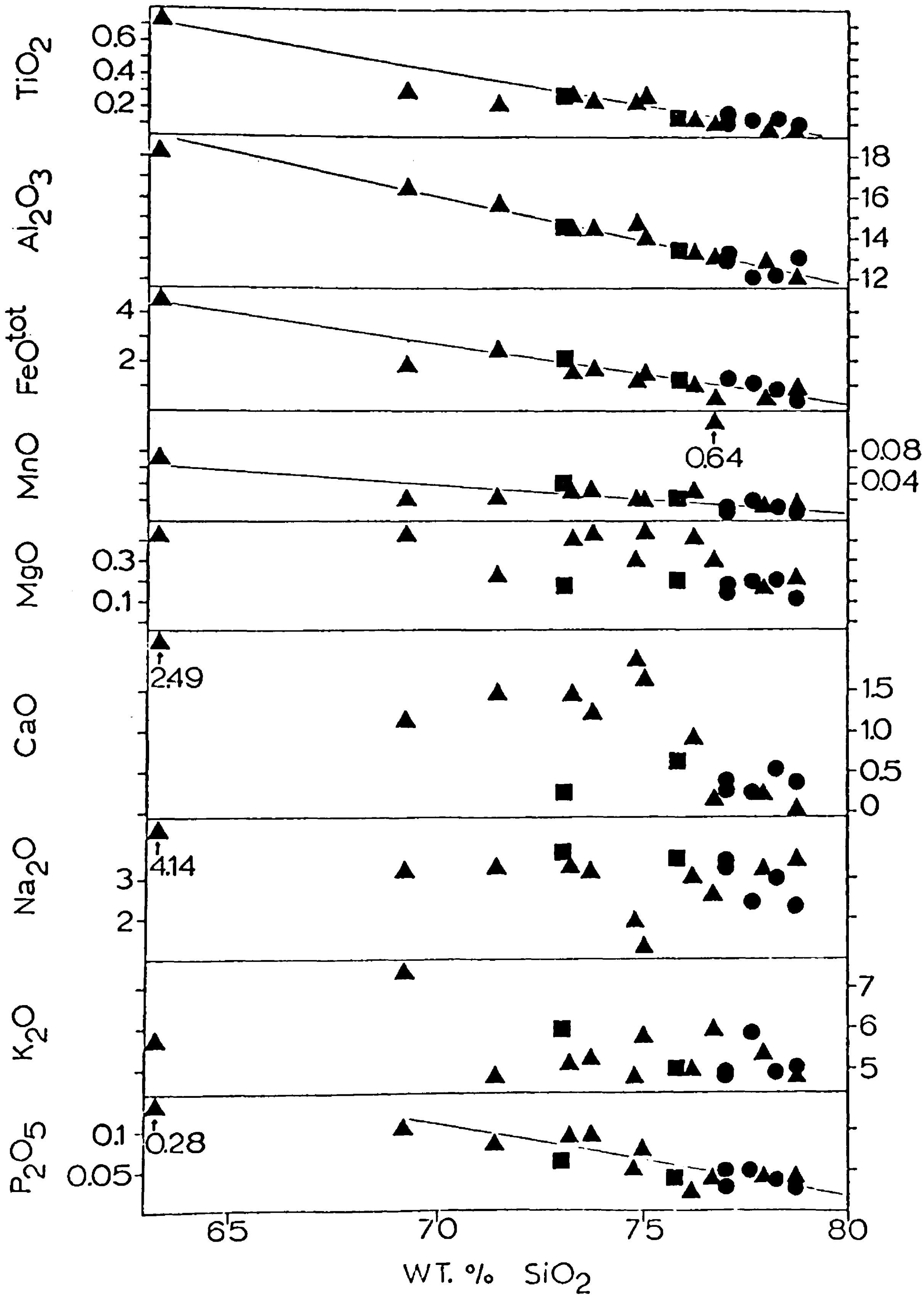
TiO2
0.6
0.4
0.2
Al2O3
18
16
14
12
FeOtot
4
2
MnO
0.64
0.08
0.04
MgO
0.3
0.1
CaO
2.49
1.5
1.0
0.5
0
Na2O
4.14
3
2
K2O
7
6
5
P2O5
0.1
0.28
0.05
65
70
75
80
WT. % SiO2

minerals. In particular, hydrogen metasomatism involves the addition of H+ ions to a rock and the concomitant release of a mole-equivalent amount of base-metal cations (Meyer and Hemley, 1967). In general, hydrothermal fluids readily and extensively deplete near-source regions in magnesium, calcium, and sodium; aluminum is relatively immobile, and silica and potassium contents may increase. The more-mobile elements are precipitated in areas farther away from the fluid source (Hemley and Jones, 1964; Meyer and Hemley, 1967). The behavior of iron is quite variable, but for the most part Fe is oxidized and remains with the altered material instead of being carried away in solution (Krauskopf, 1979, p. 83). It is best to remember that these changes in base-metal content may be either relative or absolute; thus an apparent increase in any given constituent may simply be a reflection of its relative stability in contrast to the mobility of the other cations.

Petrographic examination of rocks from the study area, including those listed in Table 8, reveals the following evidence of fairly pervasive alteration, the intensity of which may be highly variable:

(1) sericitization of plagioclase

(2) chloritization of biotite

(3) formation of secondary carbonate--primarily as a replacement of plagioclase, but rarely of alkali feldspar as well

(4) alteration of both alkali and plagioclase feldspar to clay--most extensively developed with plagioclase

(5) devitrification/alteration of groundmass glass to an intergrowth of alkali feldspar and a silica mineral

(6) oxidation of biotite to form magnetite and hematite

(7) iron- and manganese-oxide coatings on fracture surfaces

These alteration products are typical of those found in the argillic-sericitic assemblages formed by intermediate-intensity hydrogen metasomatism (Hemley and Jones, 1964). Representative reactions are:

(a) $$\underset{\text{(andesine)}}{0.75Na_2CaAl_4Si_8O_{24}} + 2H^+ + K^+ = \underset{\text{(sericite)}}{KAl_3Si_8O_{10}(OH)_2} + 1.5Na^+ + 0.75Ca^{+2} + \underset{\text{(quartz)}}{3SiO_2}$$

(b) $$\underset{\text{(biotite)}}{2K(Mg,Fe)_3AlSi_3O_{10}(OH)_2} + 4H^+ = \underset{\text{(chlorite)}}{Al(Mg,Fe)_5AlSi_3O_{10}(OH)_8} + (Mg,Fe)^{+2} + 2K^+ + \underset{\text{(quartz)}}{3SiO_2}$$

(c) $$\underset{\text{(andesine)}}{Na_2CaAl_4Si_8O_{10}} + 4H^+ = \underset{\text{(montmorillonite)}}{2M_xAl_{2+x}Si_{4-x}O_{10}(OH)_2} + 2Na^+ + Ca^{+2}$$

where M = base cation

Among the feldspars, plagioclase typically breaks down more readily than does potassium feldspar (Hemley and Jones, 1964; Krauskopf, 1979, p. 84). The loose bonding of sodium and calcium within the montmorillonite structure further facilitates their removal during alteration (Meyer and Hemley, 1967). Sericitization commonly results from a net increase in potassium within the altered rock; in addition, the resulting dioctahedral micas may contain considerable amounts of sodium and magnesium. Remobilization of magnesium also occurs during carbonatization and chloritization. Reactions (a) and (b) produce by-product quartz. Within the study area, silicification is especially evident in the two fossilized hot springs. Remobilization of silica is also reflected in the widespread devitrification of groundmass glass. Groundmass devitrification may represent a decrease in the density of a rock from its original glassy state. This agrees with the observation that alteration products commonly occupy a smaller volume than their precursors (Hemley and Jones, 1964; Meyer and Hemley, 1967).

In most igneous rocks, the content of potassium shows a sympathetic relation to that of silica. This does not appear to be the case in the analysed samples of volcanic, hypabyssal, and plutonic rocks from the study area. As Figure 23 shows, the potassium content of these rocks varies only from 4.76% to 7.44%, and is independent of silica content. There are two ways to account for the potassium values shown in Figure 23: (1) the potassium values result from the original composition of the lithologies analysed; or (2) the potassium content was altered during post-crystallization metasomatism.

At first glance, the first possibility seems unlikely. A positive correlation between potassium and silica contents is a feature of most igneous rock suites, and has even been utilized as a means of classifying different suites (c.f.: Peacock, 1931). Nevertheless, exceptions to this general rule do exist: in a detailed examination of the chemistry and mineralogy of the Bishop Tuff, Hildreth (1979) found that potassium varied inversely with silica for his samples in the range of 75-77 weight percent silica. It is conceivable, therefore, that the flat curve for potassium in Figure 23 is an original feature of the rocks.

The second possibility is that the potassium content reflects metasomatic alteration of rocks which presumably had original positive correlations between their potassium and silica contents. Uniform addition or subtraction of potassium would have shifted the position of the original K_2O/SiO_2 curve, but would not have caused the flattening seen in Figure 23. Furthermore, the absolute amount of K_2O in the analysed samples averages 5.22%, which is very close to the value for Nockold's average calc-alkaline rhyolite (Figure 23; Nockolds, 1954). There is no textural evidence for the late-stage addition of large amounts of potassium in rocks from the study area. Sericitization of plagioclase is widespread, but is generally only moderately well-developed. The breakdown of groundmass glass has produced a fine-grained intergrowth of alkali feldspar and a silica mineral. This breakdown is typical of glassy rocks under normal surface conditions and does not require the addition of large amounts of potassium to the rock. Phenocrystic potassium feldspars show no evidence of secondary crystallization; many show resorbed outlines indicative of an igneous origin. Textural evidence for large-scale leaching of potassium is likewise lacking.

These considerations suggest that the observed K_2O values may be due to a redistribution of potassium within the magma prior to crystallization.

Relative to the positive slope of a typical K_2O/SiO_2 variation curve, the study area rocks appear to reflect an addition of potassium to the lower silica rocks, and depletion of potassium in the higher silica rocks. The lower silica samples are all from extrusive volcanic rocks, whereas higher silica rocks are both extrusive and intrusive. Perhaps the granitic magma chamber itself was compositionally zoned, with an upward concentration of SiO_2, Na_2O, and volatiles, leaving deeper levels enriched in K_2O and the more "mafic" oxides (c.f.: Hildreth, 1979). The relatively low-SiO_2, high-K_2O volcanic rocks may represent direct tapping of these deeper levels. Later, or possibly synchronous, tapping of the more highly differentiated upper levels would have produced the relatively high-SiO_2 , low-K_2O volcanic and extrusive rocks. The bulk of the volcanic rocks in the study area are lava flow-rocks rather than ash-flow tuffs, presumably reflecting the low volatile content of the deeper-level magma.

Additional analyses of samples representing all levels within the magma chamber might reveal more of a pattern to potassium variation than is evident from Figure 23. The above hypothetical explanation is offered merely as a first approximation, and to indicate an interesting avenue for further research.

There remains the question of the possible source for the alteration fluids. The relative importance of magmatic and meteoric waters can only be determined by isotopic studies which are beyond the scope of this investigation. In any event, the extent and nature of the alteration assemblage would be essentially the same, regardless of the fluid source.

Summary and Conclusions

The important points in the preceding discussion may be summarized as follows:

(1) Variation diagrams for TiO_2, Al_2O_3, FeO^{tot}, MnO, and P_2O_5 show good linear trends for both intrusive and extrusive rocks. Such trends are commonly taken as evidence for comagmicity of the analysed samples.

(2) The scatter recorded on the diagrams for MgO, CaO, and Na_2O is consistent with that produced by hydrogen metasomatism. There is abundant textural and compositional evidence in the rocks for this type of alteration. The flat curve on the variation diagram for K_2O may also be a result of alteration, or may reflect original variations in the granite magma.

In addition to their close chemical affinity, the intrusive and extrusive rocks in the study area are coeval, have a similar mineralogy, and occur in close spatial proximity. On the basis of these four criteria, I conclude that the two suites are comagmatic. Measured Sr values of the intrusive and extrusive rocks are also consistent with their derivation from a common parent (Robert Fleck, pers. comm., 1980). Based on their outcrop distribution, the porphyritic intrusive rocks appear to represent the "cap" of a zoned, shallow-level granitic pluton. This is substantiated by their high-silica rhyolite composition. The extrusive rocks show a wide range of silica contents which may signify their derivation from several levels within the differentiating magma chamber. The extrusive rocks show greater scatter on variation diagrams for Mg, CaO, Na_2O and K_2O than do the intrusive rocks. This is probably due to their greater susceptibility to metasomatic alteration.

CHAPTER IV

STRUCTURE

Four structural features provide important information for interpreting the geologic setting and evolution of the study area. These are (1) the contact between the Castle Rock volcanics and the Precambrian quartzite country rocks; (2) the contact between the volcanics and the epizonal granite pluton and its related Tpr dikes; (3) the contact of the pluton and dikes with the quartzites; and (4) faults which offset all three major lithologic groups.

Volcanic--Quartzite Contact

Actual bedrock contacts between quartzite and epiclastic or volcanic rocks were not seen in the field. However, mapping on the basis of rubble indicates that contacts between these lithologies are slightly to steeply inclined. The best exposures are on hill 359M and near the mouth of the creek marking the southwestern boundary of the study area (Plate 1). The upper surface of the quartzite is nearly horizontal at hill 359M and dips gently to the southeast at the creek. Along the western margin of the area, the quartzite--volcanic contact appears to be fairly steep, but then flattens out on the north side of the Castle Rock Ridge. Contacts between quartzite and a small patch of volcanic and hypabyssal rocks on the ridge east of Bare Cone are very steep, and could represent the walls of a narrow stream valley or a narrow fault block. The vertical north-south contact between volcanic rocks and quartzite in the eastern half of the area is interpreted as a fault (see below). Quartzite pebbles and cobbles are a characteristic feature of the epiclastic conglomerates and sandstones and also occur in some of the volcanic rocks. The well-rounded nature of many of these clasts suggests a period of stream transport and abrasion prior to their incorporation in the volcanic rocks.

These outcrop and textural features imply that the pre-volcanic landscape may have been one of varying topographic relief, with hills and ridges of quartzite separated by stream valleys. Lahars, lava flows, and ash flows debouching onto this landscape would have filled in the valleys and formed sheet-like deposits on the less-dissected surfaces.

Granite--Volcanic Contact

Where best exposed, contacts between the volcanic rocks and the granite are either subhorizontal (ridges north and northeast of Castle Rock) or nearly vertical (south of Bare Cone). The subhorizontal contacts are marked by a prominent topographic ledge of granite overlain by rounded, vegetated slopes formed on volcanic rocks (Figure 13). No granite clasts were found within either epiclastic or extrusive volcanic rocks. There is no evidence, such as the presence of grus, to suggest development of an erosional surface on top of the granite prior to the onset of volcanic activity. Moreover, radiometric age determinations on volcanic rocks within the study area and on granite immediately to the northwest show these two lithologies to be essentially coeval (Robert Fleck, pers. comm., 1980). Based on these considerations, I interpret the coarse-grained granites as intrusive into the compositionally-similar and essentially coeval volcanic rocks. However, contact metamorphic effects are absent, apparently due to the low volatile content of the intruding granite.

Granite--Quartzite Content

Although commonly obscured by vegetation, the contact between these two units also appears to be subhorizontal in some places and nearly vertical in others. For the most part, the granite--quartzite contact does not seem to be as sharply-defined as that between the granite and the volcanics. Rather, plutonic and country rocks are separated by an approximately 1 km-wide zone of Tpr rhyolitic and granitic dikes (Figure 17a; Plate 1). This feature is most clearly seen on the east boundary ridge and on the ridge leading north from Bare Cone. Porphyritic Tpr lithologies show clear cross-cutting relationships in quartzites on the upper parts of these ridges; lower down most outcrops are of porphyritic lithologies, but pink coarse-grained granite grus is obiquitous, and granite crops out in a few places. In the southeastern corner of the area, the transition from granite to both quartzites and volcanic rocks is abrupt, without a porphyritic transition zone, although a prominent Tpr dike cuts across the granite. This may be a fault (see below). I interpret the coarse-grained granite as intrusive into the quartzite country rock. Contact metamorphic effects were not observed.

Faults

Structural features such as faults are difficult to detect within the study area, due to the heavy vegetative cover on most slopes. An exception is the small northwest-trending normal fault which offsets the upper surface of granite on the ridge northeast of Castle Rock (Plate 1). On the downthrown northern side of the fault, the granite appears to pass upward into porphyritic dike rocks, which have been eroded off the upthrown southern side.

The 4 km-long north-south-trending contact between quartzite and porphyritic intrusive rocks on the east and granite and volcanic rocks on the west is interpreted as a high-angle fault, with the west side down. The nature of the juxtaposed lithologies north of Castle Rock Ridge suggests that faulting may have been synchronous with intrusion of the granite: east of the fault the porphyritic "cap" is present, whereas to the west the rising pluton appears to have stoped its "cap" and is in direct contact with volcanic rocks (Figure 17a). Outcrops of volcanic rocks on the downthrown western block terminate abruptly at the fault. The fault itself appears to be cut off by the intrusive(?) granite contact in the southeastern corner of the study area.

Volcanic rocks do not crop out north of Nez Perce Creek or south of Blue Joint Creek. This fact, coupled with the linearity of the two streams, suggests that the study area may occupy a graben downdropped between faults situated along each creek. Shearing along an east-west trend is pronounced in the granite along Nez Perce Creek near Nez Perce Camp. Adjacent to the study area shearing has not been seen in outcrops parallel to Blue Joint Creek, but has been noted in quartzite on the north side of the creek southwest of the study area (Karen Lund, pers. comm., 1979). It is perhaps significant that the trend of the creek lines up with the intrusive(?) granite contact in the southeastern corner of the study area. This contact lines up with a fault mapped by Berg and Goldberg (1973) which likewise juxtaposes quartzite against granite; this contact in the study area may actually be a fault. Outcrops are rare on the south side of Blue Joint Creek due to the vegetative cover, thus hindering determination of structure.

Vertical displacement of the blocks north and south of the study area must have measured several hundred meters in order to completely erode a volcanic cover comparable to the 600 m of volcanic rocks preserved in the possible graben. If, on the other hand, the original thickness of volcanic rocks had diminished rapidly on all sides away from the study area, the displacement need not have been so great.

The timing of this hypothetical faulting is not known. If faulting and volcanism were synchronous, then the non-occurrence of extrusive rocks outside of the study area could be ascribed to ponding of volcanics within the subsiding graben. In such a case, however, the marginal faults along the creeks might be expected to contain rhyolitic dikes. There is no evidence that this was ever the case. If faulting post-dated cessation of volcanic and plutonic activity, then the nonoccurrence of volcanic rocks outside of the graben might be due primarily to their removal by erosion, coupled with a possible lesser original thickness in these areas.

Interpretation of Structures

In summary, the structural relationships of the three major lithologic groups--plutonic rocks, volcanic rocks, and quartzite--document the following generalized sequence of events:

(1) extrusion and deposition of rhyolitic lava flows and subordinate pyroclastic and epiclastic rocks onto a quartzite surface having variable topographic relief. Possible sources for the volcanic rocks are discussed in Chapter V, but may have been the fissures now occupied by the Castle Rock plug and dikes.

(2) intrusion of the epizonal pluton into both the quartzite country rocks and the recently-erupted volcanics. Contact relationships show that the pluton had a box-like shape, with an essentially flat top and straight, vertical sides. As load-pressure decreased, more volatile-rich magma at the top of the rising pluton shot out into the brittle host rocks to form the porphyritic "cap".

Box-like shapes such as these are a common feature of high-level granitic plutons in subvolcanic caldera environments around the world (Hills, 1959; Branch, 1967; Pitcher, 1978, 1979). In such environments, the granite intrudes primarily by stoping and engulfing large blocks of overlying brittle country rock. A dramatic example of this mechanism is seen in the Coastal batholith of Peru. Here "bell-jar-shaped", structurally isotropic, epizonal plutons rose to within 3 to 8 km of the surface, accomplishing their rise by stoping blocks of country rock and comagmatic volcanic rocks from the overlying caldera sequence (Pitcher, 1978). In these plutons, the transition from steep walls to flat roof typically occurs within a vertical distance of 50 m (Myers, 1975).

There is evidence that the granite pluton in this study reached its present position via this same mechanism. Apparent foundered blocks of quartzite in granite have been mapped immediately west and south of the study area (Karen Lund and Felix Mutschler, pers. comm., 1979); reconnaissance mapping by the author shows that they may also be present immediately to the north. In the central part of the study area, the porphyritic "cap" of the pluton is missing; possibly upwelling magma from beneath stoped the already-solidified porphyritic carapace, juxtaposing coarse-grained granite immediately against a roof of recently-erupted volcanic rocks (Figure 17a).

The Peruvian volcano-plutonic complexes formed within a subduction-dominated continental margin setting. Similar intrusive relationships are extensively developed in continental interior environments as well. In 1967, Hamilton and Myers proposed that the Boulder batholith of Montana had risen into a roof of comagmatic and coeval volcanic rocks. More-recent studies of the Boulder batholith and its related volcanic rocks have revealed the probable existence of several caldera structures (W. R. Greenwood, _in_ Hyndman and others, 1980). Similarly, a strong negative Bouguer gravity anomaly which underlies the San Juan volcanic field of southwestern Colorado is interpreted as an expression of a shallow underlying granitic batholith (Plouff and Pakiser, 1972). The sequential development of the several San Juan calderas is believed to reflect the progressive emplacement of the different high-level plutons of this composite batholith (Steven and Lipman, 1976), each pluton rising into a cover of slightly older comagmatic volcanic rocks. The same conclusion was reached by Elston and others (1976) for the extensive Mogollon-Datil volcanic field of southwestern New Mexico, which they interpreted as overlying a composite granitic pluton 125 km in diameter. The central plutons of granitic ring complexes such as those of northern Nigeria (Jacobson and others, 1958) may represent the root zones of similar calderas whose volcanic complement has been almost entirely eroded off.

Thus, the general configuration, of an epizonal granitic pluton forcibly intruding its coeval and comagmatic volcanic cover, is one which finds characteristic expression in both continental margin and continental interior caldera environments. I propose that the volcano-plutonic association described in this study formed within such a caldera environment during Eocene time. This conclusion is based on the following observations:

(1) The volcanic rocks in the study area consist of rhyolitic lava flows, ash-flow tuffs, and subordinate airfall and epiclastic material. Lithologies of this type characteristically erupt from or are associated with calderas situated above shallow granitic magma chambers (Smith, 1979; Stevens and Lipman, 1976; Chapin and Elston, 1979).

(2) Within the study area, the volcanic rocks are intruded by a coeval, comagmatic epizonal granite pluton. The pluton is box-shaped, with steep sides and an essentially flat roof. It appears to have risen by stoping large blocks of the overlying quartzite and volcanic rocks. Plutons demonstrating this geometry and style of intrusion have been interpreted as a characteristic feature of caldera environments; their intrusion occurs relatively late in the caldera cycle.

(3) The Castle Rock volcanics are probably correlative with the Challis Volcanics of central Idaho. Detailed mapping of the Challis field has delineated at least one caldera (B.F. Leonard, _in_ Cater and others, 1973); further investigations will undoubtedly reveal the presence of several more (Siems and Jones, 1977). During Eocene time the study area was thus located within a region tectonically favorable for caldera formation.

In the final chapter, the geologic setting and evolution of the study area are discussed in the context of this proposed caldera environment.

CHAPTER V

DISCUSSION

General Features of Calderas

The term "caldera" is used here in the sense of Williams' (1941) definition of "collapse caldera"--a more-or-less circular volcanic depression which results from the withdrawal of magma at depth. Such withdrawal may be achieved by voluminous extrusion of lava or pyroclastic material, or by a combination of both.

The concept of a caldera cycle provides a model to explain the spatial and temporal relationships observed between certain felsic to intermediate volcanic rocks and their intrusive equivalents. Smith and Bailey (1968) provided the first elucidation of this concept in a synthesis of the available data on eight major calderas, most of them located in the western United States. They proposed a seven-stage cycle of volcanic, structural, sedimentary, and plutonic events. Few calderas demonstrate all stages of activity, but as a whole the cycle shows wide applicability. Briefly, these stages are:

(I) regional tumescence consisting of broad upwarping in response to increasing magma pressure in a differentiating epizonal granitic melt.

(II) explosive pyroclastic eruption of material, especially ash flows, from the upper portion of the magma chamber.

(III) collapse of the volcanic edifice to form a structural caldera; this stage may overlap considerably in time with stage (II).

(IV) post-collapse sedimentation, perhaps accompanied by minor volcanism. Avalanches from the walls partially fill the caldera depression; lakes may also form.

(V) resurgent doming due to rise of the central subvolcanic pluton. Possible volcanic activity, and continued caldera filling.

(VI) major ring-fracture volcanism, especially lava flows and domes, and possible stoping by the central pluton. Continued caldera filling.

(VII) terminal furmarolic and hot springs activity with accompanying hydrothermal alteration and possible mineralization. Crystallization of the subvolcanic pluton, and erosion of the topographic caldera.

Subsequent work has made modifications to this sequence, while preserving its essential features. In the extensive San Juan volcanic field, Steven and Lipman (1976) found a close correlation between the volume of erupted material and the type as well as size of caldera structure formed. Large volume ($>500\ km^3$) eruptions produced well-developed calderas which resurgently domed shortly after subsidence. Smaller-volume eruptions produced either no collapse at all, or only a one-sided "trapdoor" style of subsidence. Virtually none of the smaller calderas in the San Juan field show evidence of post-collapse resurgence.

The Study Area Within a Caldera Setting

In the preceding chapter I proposed that during Middle Eocene time, approximately 46 m.y. B.P., the study area was located in the region of a caldera. Because of its age and its location in an area which was extensively glaciated during the Pleistocene, and which is now heavily forested, any topographic expression of this hypothetical caldera has long since been removed or obscured. Any argument for its existence must therefore be made on the basis of observable structures, lithologies, and age relationships. In this section I offer two models for the possible caldera "facies" represented by the study area.

Model I--Caldera-margin sequence. Most of the volcanic rocks within the study area were emplaced as lava flows; this includes rocks mapped as Tlf, Tmf, and most of the Tvc unit. Pyroclastic material comprises only the Tt airfall tuff and a minor amount of the Tvc lithologies. Another style of emplacement is represented by the intrusive rhyolite of Castle Rock, which forms a plug and three dikes. The nearby porphyritic rhyolite of Steep Hill (Plate 2) appears to be a similar intrusive body. A review of several major calderas in the western United States (Smith and others, 1961; Smith and Bailey, 1968; Byers and others, 1976; Steven and Lipman, 1976) shows that this association of rhyolitic lava flows and intrusive plugs and dikes most typically occurs as a post-collapse caldera-margin sequence. Model I interprets the study area as this type of caldera "facies". As such, the study area is only part of a postulated caldera structure which extends eastward to beyond Painted Rocks Lake on the West Fork of the Bitterroot River (Figure 24).

Published descriptions of the geology east of the study area (Fisk, 1969; Berg, 1973; Winegar, 1973; Berg, 1977; Badley, 1978) and reconnaissance investigations by the author around Took, Slate, Overwich, Hughes, and Salt creeks provide tentative substantiation for this hypothesis. The volcanic sequences immediately east and south of Painted Rocks Lake appear to contain significantly more ash-flow tuff material than is found within the study area. Lithologies found between the lake and the study area include extrusive volcanic rocks, epiclastic deposits, and an intrusive(?) porphyritic rhyolite. Of particular interest is an unusual breccia containing clasts of porphyritic rhyolite tuff(?) and quartzite. This lithology crops out both east and west of Painted Rocks Lake, and could represent caldera-collapse breccias formed as material avalanched off the caldera walls during collapse (c.f.: Lipman, 1976). In particular, extremely coarse "megabreccias" produced during initial collapse should be present near the base of a deeply-eroded caldera sequence (Lipman, 1976). On the basis of flow-banding in volcanic rocks, Winegar (1973) proposed a possible vent area on Thunder Mountain, southeast of Painted Rocks Lake. A zone of high-angle faults extends along the West Fork of the Bitterroot River (Berg, 1973, 1977). Berg (1977) felt that this faulting may have pre-dated volcanism, but his hypothesis has not been verified. Possibly, faulting and volcanism were synchronous, with both related to caldera development.

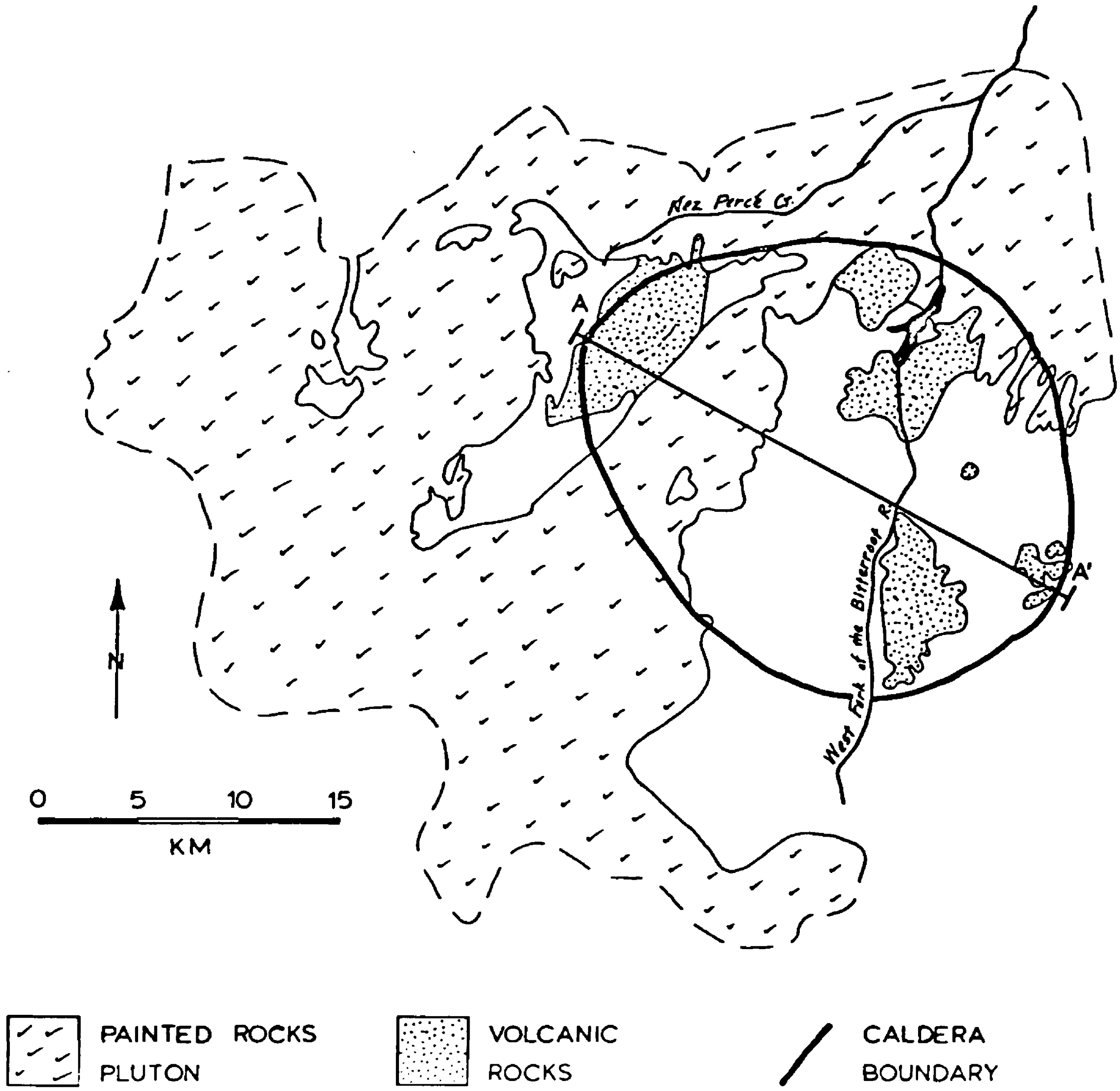

Figure 24. Sketch map of Model I caldera.

Volcanic rocks are not continuously exposed in the areas around Painted Rocks Lake. Rather, they crop out in four discrete areas: around Took Creek; between Mine and Crandell creeks; around Slate, Overwich, and Coal creeks; and between Hughes and Salt creeks. Intervening rocks are Precambrian quartzite and coarse-grained epizonal granite. The juxtaposition of these three major lithologic groups is probably due to the same combination of faulted, intrusive, and depositional relationships proposed for these groups within the study area. These relationships might be expected in the roots of a caldera, where foundered blocks of the quartzite and volcanic roof have been stoped or intruded by the rising subvolcanic pluton.

There is admittedly little gross structural evidence to support the Model I interpretation. This may not pose a significant problem. Because of extensive erosion and the present vegetative cover, an Eocene caldera, if present, might expectedly have no topographic expression today. Furthermore, the structural boundary of a collapsed caldera can be a fairly subdued feature: the boundary of the Lake City caldera in the San Juan field is nearly everywhere a single fault, marked by only a meter or so of gouge and minor hydrothermally altered rock (Steven and Lipman, 1976). The distance from Castle Rock to the east side of Painted Rocks Lake is slightly over 13.5 km. This distance is comparable to the diameter of many of the San Juan calderas, including the Lake City structure (Figure 25). According to Model I, however, the volcanic rocks east of Painted Rocks Lake represent an intra-caldera

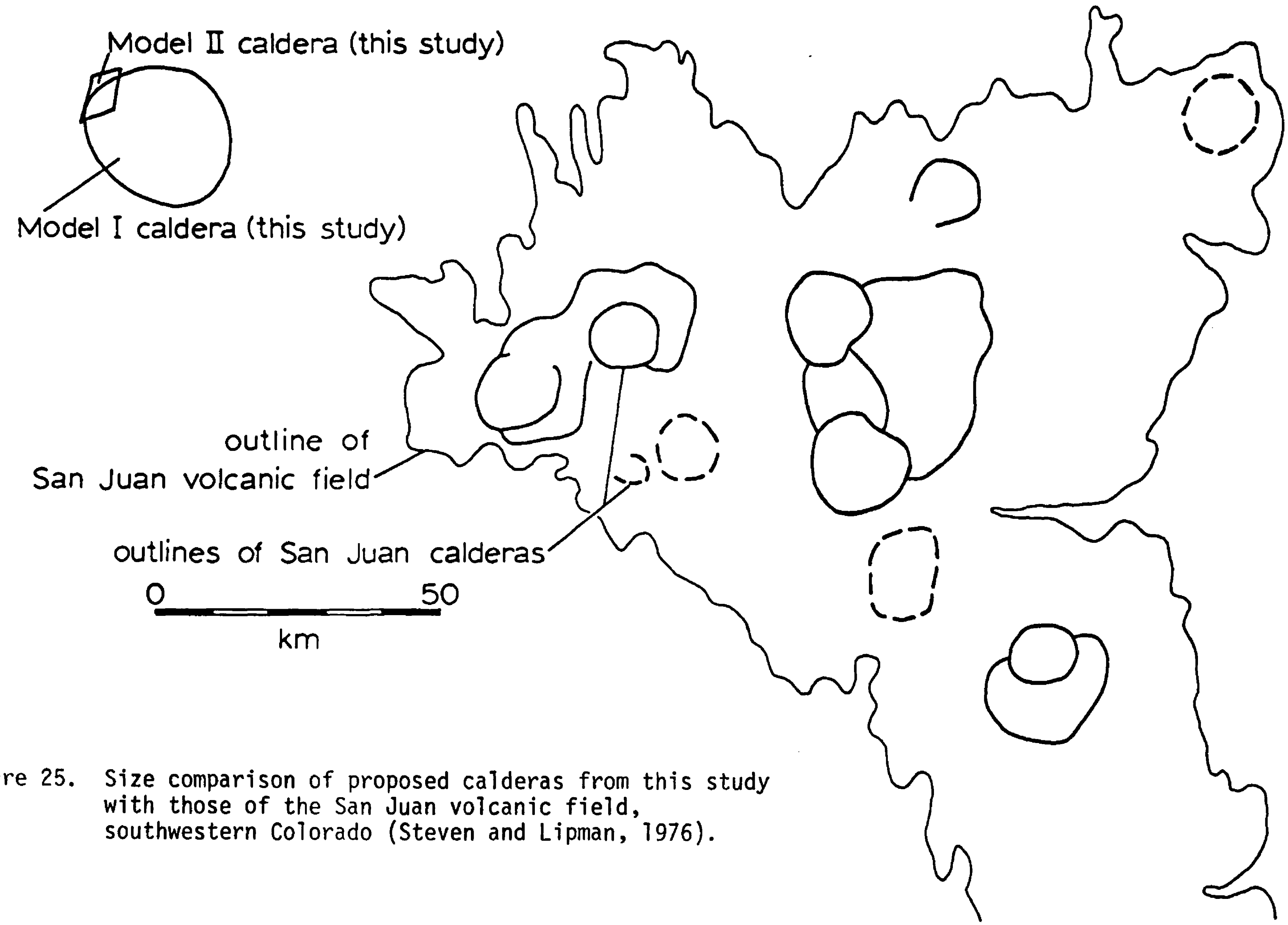

Figure 25. Size comparison of proposed calderas from this study with those of the San Juan volcanic field, southwestern Colorado (Steven and Lipman, 1976).

sequence; the eastern boundary of the Model I caldera would thus lie an unknown distance farther to the east. The larger the postulated diameter of the Model I caldera, the greater the likelihood that its collapse structures should be visible today.

The sequence of events in Model I can be stated in terms of Smith and Bailey's (1968) seven-stage caldera cycle (Figure 26):

(I) regional tumescence (recognition of this stage requires regional investigations beyond the scope of this study).

(II) explosive pyroclastic eruption, centered east of the study area around Painted Rocks Lake.

(III) collapse, also centered east of the study area.

(IV) post-collapse caldera-margin volcanism to give the flows and lesser pyroclastic rocks of the Tlf, Tmf, Tt, and Tvc units; interbedded with the upper part of the latter are the sedimentary rocks of the Ttc unit.

(V) resurgent doming would not be expected in a caldera of this size (but see VI, below).

(VI) ring-fracture volcanism, represented by intrusion of the rhyolite of Castle Rock and possibly the rhyolite of Steep Hill. At about the same time, the subvolcanic pluton rose into the roots of the volcanic sequence, stoping several blocks of its volcanic and quartzite roof in the process. The trend of the Castle Rock plug and dikes is transverse to that expected for a fracture system concentric about the Painted Rocks Lake region. Very slight doming accompanying the granite

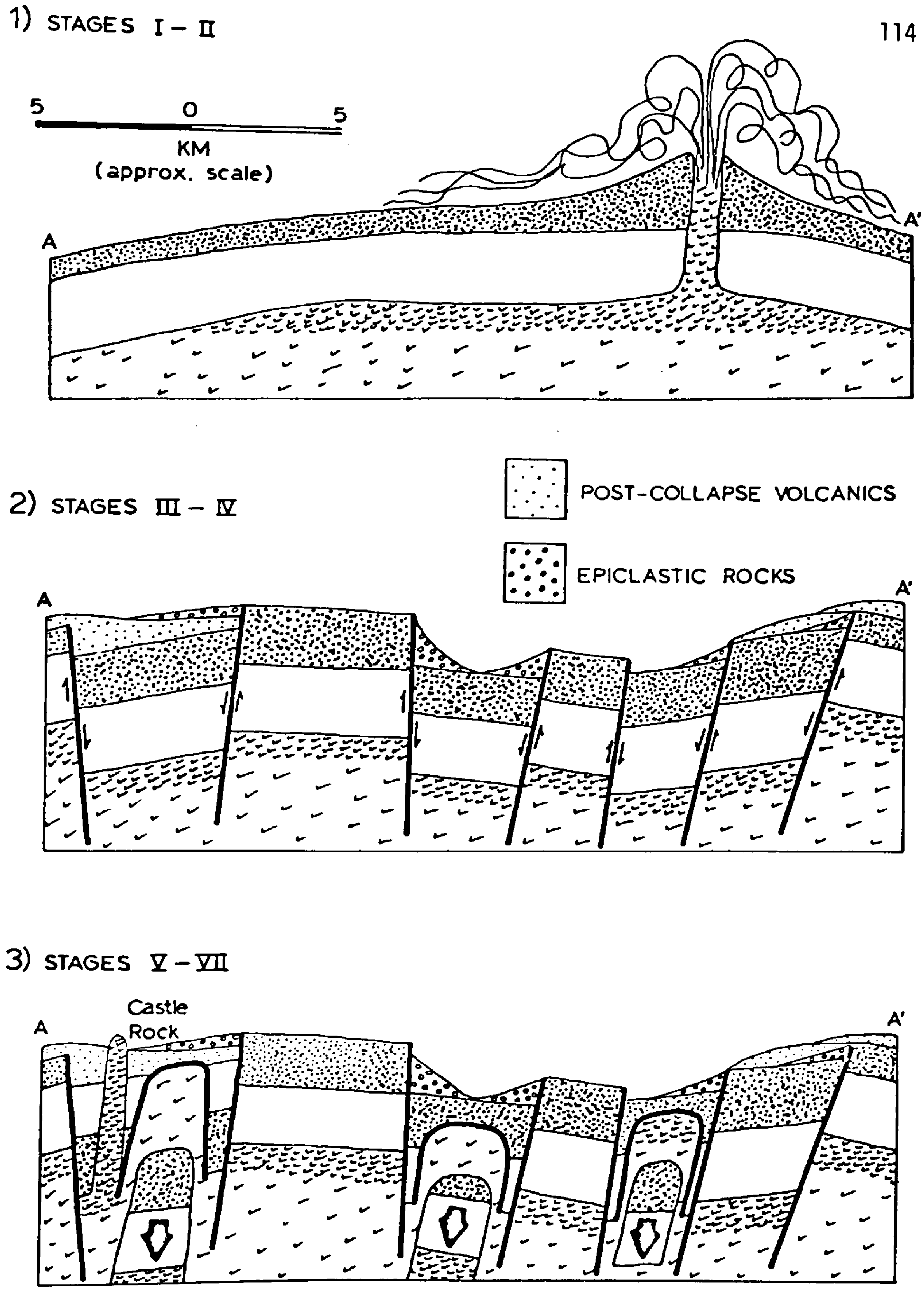

Figure 26. Stages in the evolution of Model I caldera, seen in cross section along line A—A'; lithology symbols same as in Figure 24.

intrusion might have produced fractures roughly perpendicular to the caldera margin (Smith and Bailey, 1968; Steven and Lipman, 1976) through which the magma penetrated.

(VII) terminal hot springs activity is indicated by two outcrops in the area; widespread hydrogen metasomatism probably began during stage VI.

Model II--Small caldera. The study area measures approximately 5 by 10 km. This area is several orders of magnitude smaller than that encompassed by the source calderas for most major ash-flow eruptions (Smith, 1979). On the other hand, several of the smaller San Juan calderas are only 5-15 km in diameter (Figure 25; Steven and Lipman, 1976) and the Red Hill caldera in southwestern Utah measures only 1,200m across (Cunningham and Steven, 1979). As noted above, such smaller calderas tend to exhibit a one-sided "trapdoor" style of subsidence; they are fault-bounded on three sides, but have only a monoclinal flexure on the fourth (Steven and Lipman, 1976). Formation of ring-dikes appears to be incomplete at best in these smaller calderas--intrusive plugs or dikes are present at only a few places along the structural margins of both the Ute Creek and Silverton calderas (Steven and Lipman, 1976) and appear to be entirely absent from the Cochetopa Park and Red Hill calderas (Steven and Lipman, 1976; Cunningham and Steven, 1979). If the study area is itself a small caldera, it should exhibit similar characteristics.

According to this model, the high-angle north-south-trending fault which marks the eastern extent of the volcanic rocks could also mark the eastern margin of a down-dropped intracaldera block (Figure 27). This zone of weakness was then later utilized during emplacement of the subvolcanic pluton, as discussed in Chapter IV. The northern margin of the subsided block could be represented by the postulated fault along Nez Perce Creek. Another possible location for the northern margin is the east-west line delineated by Castle Rock and its related dikes; similar quartz porphyry stocks and plugs mark the ring-fracture zone in the Silverton caldera (Smith and Bailey, 1968). However, there is no evidence for fault displacement of the volcanic rocks north of Castle Rock Ridge relative to those south of the ridge. The southern boundary of the subsided block could be placed along the postulated Blue Joint Creek fault. The hingeline would therefore be located along a more-or-less north-south line approximately coincident with the Montana-Idaho divide and the western limit of volcanic rocks. Steep Hill, located on the divide approximately 3.5 km southwest of the study area, consists of andesitic flows and breccias cut by an intrusive porphyritic rhyolite. Apparent dikes of this rhyolite underlie the state divide ridge for 2.5 km north and 3 km southwest of Steep Hill itself, and could represent ring dikes intruded along a bounding fracture. According to this model, the postulated faults along Nez Perce and Blue Joint creeks would be Eocene structures. Possible syn-eruptive

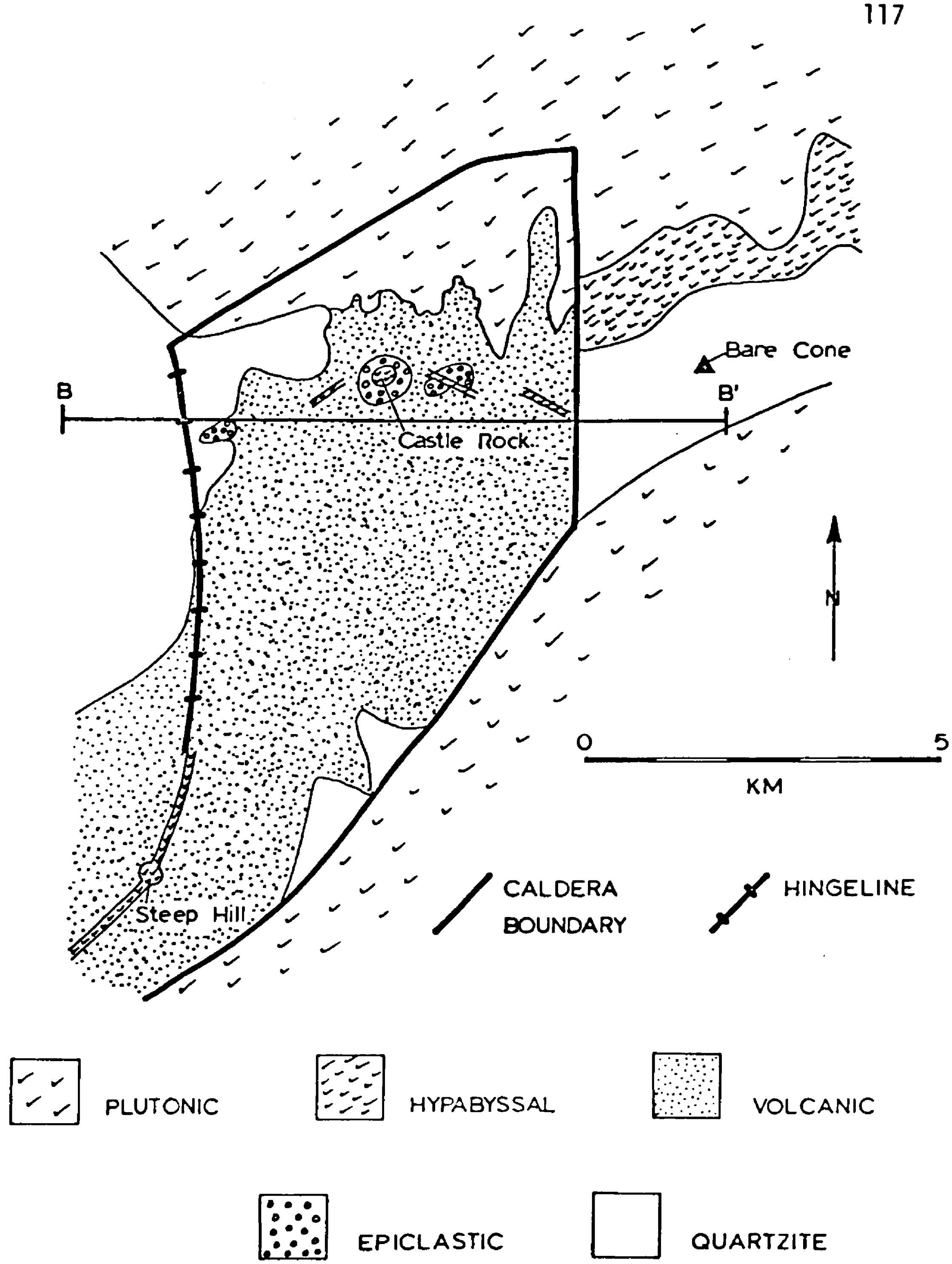

Figure 27. Sketch map of Model II caldera.

subsidence along these and the east-boundary fault would have resulted in a greater thickness of volcanic rocks within the central block. Extensive post-Eocene erosion would have stripped away the quartzite and volcanic rock cover in most places, exposing the granite pluton.

The sequence of events in Model II can be stated in terms of Smith and Bailey's (1968) seven-stage caldera cycle (Figure 28):

(I) regional tumescence.

(II) emplacement of volcanic rocks of the Tlf, Tmf, Tt, and lower part of the Tvc unit; the source of the lava flows and ash-flow tuffs could be the vents and fissures now occupied by the rhyolite of Castle Rock, or other fractures now buried beneath the volcanic rocks.

(III) trapdoor-style collapse of the intracaldera block.

(IV) post-collapse sedimentation represented by the epiclastic deposits of the Ttc unit, accompanied by minor volcanism to form the upper part of the Tvc unit.

(V) resurgent doming would not be expected in a caldera of this size (Smith and Bailey, 1968; Steven and Lipman, 1976).

(VI) ring-fracture volcanism is represented by intrusion of the rhyolite of Castle Rock and possibly the rhyolite of Steep Hill. At about the same time, the subvolcanic pluton rose into the roots of the volcanic sequence, stoping several blocksof volcanic and quartzite roof in the process.

(VII) terminal hot springs activity is indicated by two outcrops in the area; widespread hydrogen metasomatism probably began during stage VI.

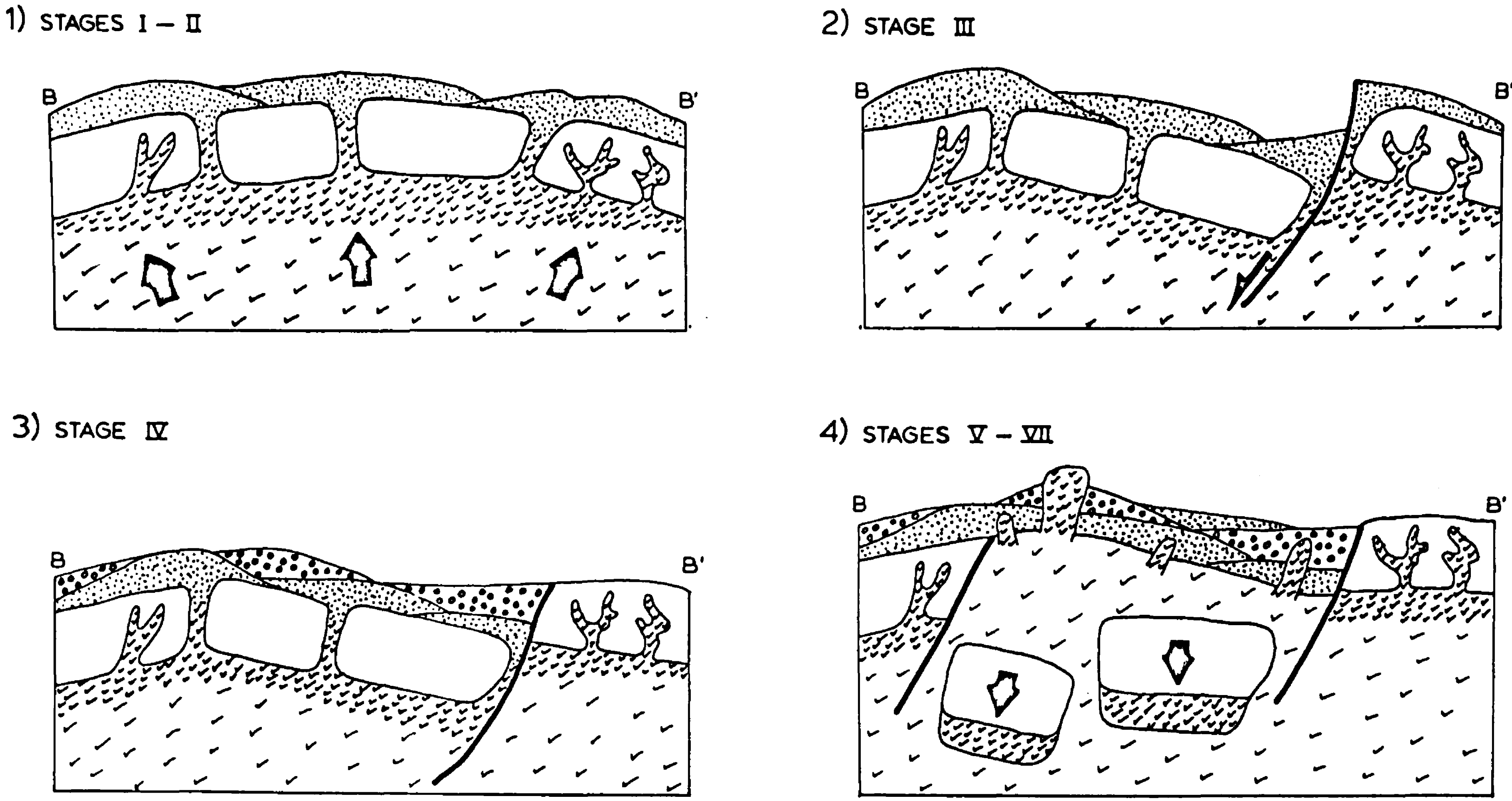

Figure 28. Stages in the evolution of Model II caldera, seen in cross section along line B—B'; scale and lithology symbols same as in Figure 27.

There are three main problems with this model. The first is the apparent absence of a monoclinal hinge structure on the western margin of the proposed caldera. Bedding attitudes within the study area as a whole are variable (Plate 1) and show no general eastward tilt, as would be expected if subsidence and tilting of the central block had occurred after volcanism. However, if subsidence and volcanism had been concurrent, the evidence of tilting would be considerably obscured.

The second problem concerns the nature of the volcanic lithologies themselves. Caldera collapse, on whatever scale, is almost always accompanied by eruptions of pyroclastic material (Steven and Lipman, 1976; Smith and Bailey, 1968; Chapin and Elston, 1979). In contrast, the volcanic rocks within the study area are primarily lava flows, with only subordinate pyroclastic deposits (Chapter II). Such a balance might be achieved in a relatively low-volatile eruption, perhaps one occurring early in a regional volcanic episode (Smith, 1979; Cunningham and Steven, 1979). Within the study area, most pumice fragments are found in epiclastic units which occur high in the section; these could have been carried in from outlying areas which were undergoing more explosive volcanic activity.

The third problem with this model is the absence of recognizable caldera-collapse breccias (c.f.: Lipman, 1976). In the study area these breccias would consist almost entirely of blocks of the quartzite country rocks, plus any volcanic rocks erupted prior to caldera collapse.

Their apparent absence might simply be due to inadequate outcrop exposure. North of Castle Rock Ridge, the rising granite body may have stoped the lower part of the volcanic sequence, including megabreccias, if present.

A possible compromise of sorts between models I and II might also be suggested. The Red Hill caldera of southwestern Utah appears to have formed above one of a number of small cupolas situated above a shallow granitic pluton (Cunningham and Steven, 1979). For the most part, magma was released episodically as lava flows and ash-flow tuffs issuing from a number of vents; only in the case of the Red Hill caldera did pressures in the magma build sufficiently to produce an explosive eruption. Perhaps the area between the Montana-Idaho divide and the east side of Painted Rocks Lake presents a similar situation. Repeated escape of magma through fractures in a thin quartzite roof could result in the types of lithologies and structures observed. Caldera-collapse would thus be due more to passive foundering of a number of individual roof-zone blocks, rather than to a single catastrophic explosion.

Summary

This study has described the petrography, whole-rock chemistry, and structural relationships of an Eocene volcano-plutonic assemblage. I have used these basic data to suggest models for the evolution of this sequence, using as a framework the seven-stage caldera cycle of

Smith and Bailey (1968). The present study is in many ways a reconnaissance one, and leaves ample room for further related investigations. These might include: (1) searching for the remains of a structural caldera margin, and for breccias produced by caldera-collapse; (2) additional radiometric dating of the extrusive and intrusive rocks; (3) studies of the alteration mineralogy, including isotopic studies of the hydrothermal fluids; (4) detailed regional mapping of the volcanic rocks east of the study area with the idea of identifying an intra-caldera facies; (5) detailed stratigraphic studies, both chemical (c.f.: Hildreth, 1979) and lithologic, to elucidate the variations with time of the erupted material; and (6) trace-element studies of the volcanic and intrusive lithologies to substantiate or refute the claim of their comagmicity.

REFERENCES CITED

Armstrong, R.L., 1974, Geochronometry of the Eocene volcanic-plutonic episode in Idaho: Northwest Geology, v. 3, p. 1-15.

_____, 1975, Precambrian (1500 m.y. old) rocks of central Idaho -- the Salmon River arch and its role in Cordilleran sedimentation and tectonics: Am. J. Sci., v. 275-A, p. 437-467.

_____, 1978, Cenozoic igneous history of the U.S. Cordillera from lat 42° to 49°N: Geol. Soc. America Mem. 152, p. 265-282.

_____; Taubeneck, William H.; and Hales, Peter O., 1977, Rb-Sr and K-Ar geochronometry of Mesozoic granitic rocks and their Sr isotopic composition, Oregon, Washington, and Idaho: Geol. Soc. America Bull., v. 88, p. 397-411.

Atwater, Tanya, 1970, Implications of plate tectonics for the Cenozoic tectonic evolution of western North America: Geol. Soc. America Bull., v. 81, pp. 3513-3536.

Badley, Ruth H., 1978, Petrography and chemistry of the East Fork dike swarm, Ravalli County, Montana: unpub. M.S. thesis, University of Montana, 54 p.

Barker, Daniel S., 1970, Compositions of granophyre, myrmekite, and graphic granite: Geol. Soc. America Bull., v. 81, p. 3339-3350.

Berg, Richard B., 1973, Geology of southernmost Ravalli County, Montana: Northwest Geology, v. 2, p. 1-5.

_____, 1977, Reconnaissance geology of southernmost Ravalli County, Montana: Montana Bur. Mines and Geology Mem. 44, 39 p.

_____ and Goldberg, W.C., 1973, Preliminary geologic map, northwestern part of Painted Rocks Lake Quadrangle, Ravalli County, Montana: Montana Bur. Mines & Geology open file map.

Blatt, Harvey; MIddleton, Gerard; and Murray, Raymond, 1972, Origin of sedimentary rocks: Prentice-Hall, Englewood Cliffs, New Jersey, 634 p.

Bond, J.G., compiler, 1978, Geologic map of Idaho: Idaho Bur. Mines and Geology, scale 1:500,000.

Branch, C.D., 1967, Genesis of magma for acid calc-alkaline volcano-plutonic formations: Tectonophysics, v. 4, n. 1, p. 83-100.

Byers, F.M., Jr.; Carr, W.J.; Orkild, Paul P.; Quinlivan, W.D.; and Sargent, K.A., 1976, Volcanic suites and related cauldrons of Timber Mountain - Oasis Valley caldera complex, southern Nevada: U.S. Geol. Survey Prof. Paper 919, 70 p.

Cater, F.W.; Pinckney, D.M.; Hamilton, W.B.; Parker, R.L.; Weldin, R.D.; Close, T.J.; and Zilka, N.T., 1973, Mineral resources of the Idaho Primitive Area and vicinity, Idaho: U.S. Geol. Survey Bull. 1304, 431 p.

Chadwick, R.A., 1977, Overview of early Tertiary volcanism in the northern Rockies region: Geol. Soc. America Abstracts with Programs, v. 9, n. 6, p. 715-716.

Chapin, Charles E. and Elston, Wolfgang E., 1979, Ash-flow tuffs: Geol. Soc. America Spec. Pap. 180, 211 p.

Church, B.N., 1975, Quantitative classification and chemical comparison of common volcanic rocks: Geol. Soc. America Bull., v. 86, p. 257-263.

Cohee, George V., 1974, Stratigraphic nomenclature in reports of the U.S. Geological Survey: for official use within the geological survey, 45 p.

Cunningham, C.G. and Steven, T.A., 1979, Mount Belknap and Red Hills calderas and associated rocks, Marysvale volcanic field, west-central Utah: U.S. Geol. Survey Bull. 1468, 34 p.

Deer, W.A.; Howie, R.A.; and Zussman, J., 1966, An introduction to the rock-forming minerals: Longman, London, 528 p.

Elston, Wolfgang E.; Rhodes, Rodney C.; Coney, Peter J.; and Deal, Edmond G., 1976, Progress report on the Mogollon Plateau volcanic field, southwestern New Mexico, no. 3 -- surface expression of a pluton: New Mexico Geol. Soc. Spec. Pub. n. 5, p. 3-151.

Fisk, H.G., 1969, Painted Rocks Lake area, Southern Ravalli County, Montana: Montana Bur. Mines and Geology Spec. Pub. 47.

Fiske, Richard S.; Hopson, Clifford A.; and Waters, Aaron C., 1963, Geology of Mount Rainier National Park, Washington: U.S. Geol. Survey Prof. Paper 444, 93 p.

Gilbert, Charles M., 1938, Welded tuff in eastern California: Geol. Soc. America Bull., v. 49, p. 1829-1862.

Greenwood, W.R. and Morrison, D.A., 1973, Reconnaissance geology of the Selway-Bitterroot Wilderness Area: Idaho Bur. Mines and Geology Pamphlet 154, 30 p.

Hamilton, Warren and Myers, W. Bradley, 1967, The nature of batholiths: U.S. Geol. Survey Prof. Pap. 554-C, 30 p.

Hemley, J.J. and Jones, W.R., 1964, Chemical aspects of hydrothermal alteration with emphasis on hydrogen metasomatism: Econ. Geol., v. 59, p. 538-569.

Hildreth, Wes, 1979, The Bishop Tuff: evidence for the origin of compositional zonation in silicic magma chambers, in Chapin, Charles E. and Elston, Wolfgang E., eds., Ash-flow tuffs: Geol. Soc. America Spec. Pap. 180, p. 43-75.

Hills, E.S., 1959, Cauldron subsidences, granitic rocks and crustal fracturing in southeast Australia: Geol. Rdsch, v. 47, p. 543-561.

Hyndman, Donald W., 1972, Petrology of igneous and metamorphic rocks: McGraw-Hill, New York, 533 p.

_____, 1978, Major tectonic elements and tectonic problems along the line of section from northeastern Oregon to west-central Montana: Geol. Soc. America Map MC-28C, 12 p.

_____, ms, Petrology of igneous and metamorphic rocks, 2nd edition: McGraw-Hill, New York.

_____, Vitaliano, Charles J.; and Suttner, Lee J., 1980, Granite II--near-surface batholiths, related volcanism, tectonism, sedimentation, and mineral deposition (Penrose Conference Report): Geology, v. 8, p. 107-110.

_____, and Williams, Larry D., 1977, The Bitterroot Lobe of the Idaho batholith: Northwest Geology, v. 6-1, p. 1-17.

Jacobson, R.R.E.; MacLeod, W.N.; and Black, Russell, 1958, Ring-complexes in the Younger Granite province of northern Nigeria: Geol. Soc. London Mem. 1, 72 p.

Krauskopf, Konrad B., 1979, Introduction to geochemistry, 2nd ed.: McGraw-Hill, New York, 617 p.

Lipman, P.W., 1976, Caldera-collapse breccias in the western San Juan Mountains, Colorado: Geol. Soc. America Bull., v. 87, n. 10, p. 1397-1410.

Lipman, P.W.; Christiansen, Robert L.; and O'Connor, J.T.; 1966, A compositionally zoned ash-flow sheet in southern Nevada: U.S. Geol. Survey Prof. Paper 524-F, 47 p.

_____, Prostka, H.J.; and Christiansen, R.L., 1972, Cenozoic volcanism and plate tectonic evolution of the western United States. I. Early and Middle Cenozoic: Phil. Trans. R. Soc. Lond. A., v. 271, p. 217-248.

Lund, K.; Rehn, W.M.; and Holloway, C.D., ms, Geologic map of Blue Joint Study Area, Montana-Idaho: U.S. Geol. Survey MF map ____

Marshall, P., 1935, Acid rocks of Taupo-Rotorua volcanic district: Royal Soc. New Zealand Trans., v. 64, pt. 3, p. 323-366.

Meyer, Charles and Hemley, J. Julian, 1967, Wall rock alteration, in Barnes, Hubert Lloyd, ed., Geochemistry of hydrothermal ore deposits: Holt, Rinehart and Winston, New York, p. 166-235.

Mutschler, F.E.; Pawlowski, M.; Bruce, R.; and Hall, B., ms, Geologic map of Magruder RARE II Area, Idaho: U.S. Geol. Survey MF map ____

Myers, John S., 1975, Cauldron subsidence and fluidization: mechanisms of intrusion of the Coastal Batholith of Peru into its own volcanic ejecta: Geol. Soc. America Bull., v. 86, p. 1209-1220.

Nockolds, S.R., 1954, Average chemical compositions of some igneous rocks: Geol. Soc. America Bull., v. 65, p. 1007-1032.

Nold, J.L., 1974, Geology of the northeastern border zone of the Idaho batholith: Northwest Geology, v. 3, p. 47-52.

Peacock, M.A., 1931, Classification of igneous rock series: J. Geol., v. 39, p. 54-67.

Peterson, Donald W., 1961, AGI data sheet 23: Geotimes, v. V, n. 6, p. 30-36.

Pitcher, W.S., 1978, The anatomy of a batholith: Geol. Soc. Lond. Jour., v. 135, pt. 2, p. 157-182.

_____, 1979, The nature, ascent and emplacement of granitic magmas: Geol. Soc. Lond. Jour., v. 136, p. 627-662.

Plouff, Donald and Pakiser, L.C., 1972, Gravity study of the San Juan Mountains, Colorado, in Geological Survey research 1972: U.S. Geol. Survey Prof. Paper 800-B, p. B183-B190.

Prostka, H.J.; McIntyre, D.H.; and Skipp, Betty, 1977, Interrelations of lower Tertiary volcanic fields in northwestern interior United States: Geol. Soc. America Abstracts with Programs, v. 9, n. 6, p. 755-756.

Reineck, H-E. and Singh, I.B., 1975, Depositional sedimentary environments: Springer-Verlag, New York, 439 p.

Ross, Clarence S. and Smith, Robert, L., 1961, Ash-flow tuffs: their origin, geologic relations, and identification: U.S. Geol. Survey Prof. Pap. 366, 81 p.

Ross, C.P., 1934, Geology and ore deposits of the Casto quadrangle, Idaho: U.S. Geol. Survey Bull. 854, 135 p.

_____, 1937, Geology and ore deposits of the Bayhorse region, Custer County, Idaho: U.S. Geol. Survey Bull. 877, 161 p.

_____, 1961, A redefinition and restriction of the term Challis volcanics: U.S. Geol. Survey Prof. Paper 424-C, p. C177-C180.

_____; Andrews, D.S.; and Witkind, I., 1955, Geologic map of Montana: U.S. Geol. Survey in cooperation with Montana Bur. Mines and Geology, scale 1:500,000.

_____ and Forrester, J. Donald, 1958, Outline of the geology of Idaho: Idaho Bur. Mines and Geology Bull. 15, 75 p.

Siems, Peter L. and Jones, Robert W., 1977, The Challis volcanic field: a review: Geol. Soc. America Abstracts with Programs, v. 9, n. 6, p. 762-763.

Smith, Eugene I. and Rhodes, Rodney C., 1972, Flow direction determination of lava flows: Geol. Soc. America Bull., v. 83, p. 1869-1874.

Smith, Robert L., 1960, Zones and zonal variations in welded ash flows: U.S. Geol. Survey Prof. Pap. 354-F, p. 149-159.

_____, 1979, Ash-flow magmatism, in Chapin, Charles E. and Elston, Wolfgang E., eds., Ash-flow tuffs: Geol. Soc. America Spec. Pap. 180, p. 5-27.

_____ and Bailey, Roy A., 1968, Resurgent cauldrons: Geol. Soc. America Mem. 116, p. 613-662.

Smith, R.L.; Bailey, R.A.; and Ross, C.S., 1961, Structural evolution of the Valles caldera, New Mexico, and its bearing on the emplacement of ring dikes, in Short papers in the geologic and hyrdologic sciences: U.S. Geol. Survey Prof. Paper 424-D, p. D145-D149.

Snyder, W.S.; Dickinson, W.R.; and Silberman, M.L., 1976, Tectonic implications of space-time patterns of Cenozoic magmatism in the western United States: Earth and Plan. Sci. Let., v. 32, p. 91-106.

Spry, Alan, 1969, Metamorphic textures: Pergamon Press Ltd., Oxford, 350 p.

Steven, Thomas A. and Lipman, Peter W., 1976, Calderas of the San Juan volcanic field, southwestern Colorado: U.S.G.S. Prof. Paper 958, 35 p.

Stewart, J.H. and Carlson, J.E., 1978, Generalized maps showing distribution, lithology, and age of Cenozoic igneous rocks in the western United States: Geol. Soc. America Mem. 152, p. 263-264.

Streckeisen, Albert, 1967, Classification and nomenclature of igneous rocks: N. Jb. Miner. Abh., v. 107, p. 144-240.

_____, 1979, Classification and nomenclature of volcanic rocks, lamprophyres, carbonatites, and melititic rocks: recommendations and suggestions of the IUGS Subcommission on the systematics of igneous rocks: Geology, v. 7, p. 331-335.

Tröger, W.E., 1958, Optische Bestimmung der gesteinsbildenden Minerale, Teil 1, Bestimmungstabellen, 3. Auflage: Stuttgart, E. Schweizerbart'sche Verlagsbuchhandlung, p. 101.

Vance, Joseph A., 1969, On synnensis: Contrib. Min. Petrol., v. 24, p. 7-29.

Whitney, James A., 1975, The effects of pressure, temperature, and X_{H_2O} on phase assemblage in four synthetic rock compositions: J. Geol., v. 83, p. 1-31.

Wilcox, Ray E., 1979, The liquid line of descent and variation diagrams, in Yoder, H.S., Jr., ed.: The evolution of the igneous rocks, fiftieth anniversary perspectives, p. 205-232.

Williams, Howel, 1932, The history and character of volcanic domes: University of California Publ. Geol. Sciences, v. 21, p. 51-146.

_____, 1941, Calderas and their origin: University of California Publ. Geol. Sciences, v. 25, n. 6, p. 239-346.

Williams, Howel and McBirney, Alexander R., 1979, Volcanology: Freeman, Cooper and Co., San Francisco, 397 p.

_____; Turner, Francis J.; and Gilbert, Charles M., 1954, Petrography: W. H. Freeman, San Francisco, 406 p.

Williams, Larry D., 1977, Petrology and petrography of a section across the Bitterroot Lobe of the Idaho batholith: unpubl Ph.D. diss., University of Montana, 221 p.

Winegar, Robert C., 1973, Geologic survey of the southern Bitterroot National Forest: Bitterroot National Forest Headquarters - Hamilton, Montana, contract no. 26-2914, 112 p. (Bitterroot Survey I).

_____, 1974, Bitterroot II Geologic Survey: Bitterroot National Forest Headquarters - Hamilton, Montana, contract no. 26-3214, 161 p.